THE EFFECT OF CYSTIC FIBROSIS TRANSMEMBRANE CONDUCTANCE REGULATOR ON THE FUNCTION OF ACID/BASE TRANSPORTERS OF HUMAN PANCREATIC DUCT CELLS

Ph.D. Thesis

Imre Ignáth, M.Sc.

First Department of Medicine
University of Szeged

2010

LIST OF FULL PAPERS DIRECTLY RELATED TO THE SUBJECT OF THE THESIS

I.

Ignáth I, Hegyi P, Venglovecz V, Székely C, Carr G, Hasewaga M, Inoue M, Takács T, Argent BA, Gray MA, Rakonczay Z Jr. CFTR expression but not Cl^- transport is involved in the stimulatory effect of bile acids on apical Cl^-/HCO_3^- exchange activity in human pancreatic duct cells. *Pancreas,* 2009, 38:921-9.

IF: 2.708

II.

Rakonczay Z Jr, Hegyi P, Hasegawa M, Inoue M, You J, Iida A, **Ignáth I**, Alton EW, Griesenbach U, Óvári G, Vág J, Da Paula AC, Crawford RM, Varga G, Amaral MD, Mehta A, Lonovics J, Argent BE, Gray MA. CFTR gene transfer to human cystic fibrosis pancreatic duct cells using a Sendai virus vector. *J Cell Physiol*, 2008, 214: 442-55.

IF: 4.313

LIST OF FULL PAPERS RELATED TO THE SUBJECT OF THE THESIS

Tóth-Molnár E, Venglovecz V, Ózsvári B, Rakonczay Z Jr, Varró A, Tóth A, Lonovics J, Takács T, **Ignáth I**, Iványi B, Hegyi P. A new experimental method to study the acid/base transporters and their regulation in lacrimal gland ductal epithelia. *Invest Ophthal Vis Sci,* 2007, 48: 3746-55.

IF : 3.528

TABLE OF CONTENTS

LIST OF ABBREVIATIONS

β:	buffering capacity
$ß_{HCO3}^-$:	buffering capacity of HCO_3^-/CO_2 system
$ß_{total}$:	total buffering capacity
BCECF-AM ester	2′,7′-bis-(2-carboxyethyl)-5(6)-carboxyfluorescein-acetoxymethyl
BHK:	baby hamster kidney
CA:	carbonic anhydrase
CDC:	chenodeoxycholate
CF:	cystic fibrosis
CFTR:	cystic fibrosis transmembrane conductance regulator
dbcAMP:	2′-O-dibutyryladenosine 3′,5′-cyclic monophosphate
DMP:	dimethyl pimelimidate
DRA:	down-regulated in adenoma
EDTA:	ethylenediaminetetraacetic acid
EGTA:	ethylene glycol tetraacetic acid
FURA-2-AM:	2-(6-(bis-(carboxymetil)-amino)-5-(2-(2-(bis-(carboxymetil)-amino)-5-metilfenoxi)-etoxi)-2-benzofuranyl)-5-5-oxazolcarboxil-acetoxymethyl ester
H_2-DIDS:	dihydro-4,4′-diisothiocyanostilbene-2,2′-disulfonic acid
IBMX:	3-isobutyl-1-methylxanthine
J(B):	base flux
-*J*(B):	base efflux
LacZ:	β-galactosidase
MOI:	multiplicity of infection
NBC:	Na^+/HCO_3^- cotransporter
NHE:	Na^+/H^+ exchanger
PAT-1:	putative anion transporter-1
PBS:	phosphate-buffered saline
pH_i:	intracellular pH
PKA:	protein kinase A
R_s:	serial resistance

R_T:	transepithelial resistance
SeV:	Sendai virus
SLC:	solute carrier family
V_m:	membrane potential
V_p:	potencial of pipette
Wt:	wild-type
ZO-1:	zonula occludens-1

SUMMARY

Background. The main function of the pancreatic ductal epithelium is to secrete HCO_3^-/ HCO_3^- secretion across the apical membrane of duct cells is thought to occur via cystic fibrosis transmembrane conductance regulator (CFTR), a cAMP/protein kinase A (PKA) regulated Cl^- channel, and the SLC26 anion exchangers SLC26A3 (DRA, downregulated in adenoma) and SLC26A6 (PAT-1, putative anion transporter-1). The central role of CFTR in the secretory process can't be questioned. Pancreatic HCO_3^- secretion is markedly reduced in patients with cystic fibrosis (CF), a fatal inherited autosomal recessive disease which is caused by the absence or dysfunction of CFTR. The availability of gene therapy would offer the best hope for a cure of CF.

Pathophysiological factors have been shown to modulate HCO_3^- secretion. Luminal administration of a low dose (0.1 mM) of the unconjugated bile salt, chenodeoxycholate (CDC), significantly elevates apical Cl^-/HCO_3^- exchange activity and HCO_3^- secretion in guinea pig pancreatic ducts, and these effects were Ca^{2+}-dependent. It remains to be investigated whether the effects of CDC are dependent on CFTR expression and Cl^- channel activity.

Aims. The main aims of my work were to investigate the potential of a recombinant Sendai virus (SeV) vector to introduce wild-type (wt) CFTR into human CF pancreatic duct (CFPAC-1) cells, and to assess the effect of CFTR gene transfer on the key transporters involved in HCO_3^- transport. The other important objectives of my work were to examine the effects of CDC on intracellular pH (pH_i), intracellular Ca^{2+} concentration ($[Ca^{2+}]_i$) and apical Cl^-/HCO_3^- exchange activity in human pancreatic duct cells lacking or expressing wt CFTR, and to determine whether any effects were dependent on CFTR expression and Cl^- channel activity.

Methods. We performed the majority of our experiments on polarized cultures of homozygous F508del CFPAC-1 cells as a model for the human CF pancreatic ductal epithelium. CFPAC-1 cells were transduced with SeV constructs containing cDNAs for either wt CFTR or β-galactosidase (LacZ). We detected the expression of CFTR by Western blot analysis and immunocytochemistry. The presence of functional CFTR was confirmed using iodide efflux assay. mRNA expression of pNBC, AE2, NHE2, NHE3, DRA, and PAT-1 was determined using real-time RT-PCR. The activities of acid/base

transporters were investigated using a fluorescent dye BCECF to monitor pH_i by microfluorometry. Ca^{+}_i was measured by FURA-2. Patch clamp experiments were performed on isolated guinea pig duct cells to examine whether CDC could directly activate CFTR Cl^- conductance.

Results. SeV-LacZ transduced CFPAC-1 cells showed a strong, homogeneous LacZ activity 48-96 h after the infection. In the SeV-CFTR cells we observed significant elevation of CFTR expression and activity. Wt CFTR expression had no effect on cell growth, monolayer integrity, and mRNA levels for key transporters in the duct cell (pNBC, AE2, NHE2, NHE3, DRA, and PAT-1), but did upregulate the activity of apical Cl^-/HCO_3^- and Na^+/H^+ exchangers (NHEs). In CFTR-corrected cells, apical Cl^-/HCO_3^- exchange activity was further enhanced by cAMP, a key feature exhibited by normal pancreatic duct cells. The cAMP stimulated Cl^-/HCO_3^- exchange was inhibited by dihydro-4,4′-diisothiocyanostilbene-2,2′-disulfonic acid (H_2-DIDS), but not by a specific CFTR inhibitor, $CFTR_{inh}$-172. Basolateral Cl^-/HCO_3^- exchange and Na^+/HCO_3^- co-transport activities were significantly reduced in SeV-CFTR transduced CFPAC-1 cells.

CDC caused a dose-dependent increase in $[Ca^{2+}]_i$ in CFPAC-1 human pancreatic duct cells. Apical administration of CDC to CFPAC-1 cells resulted in a greater elevation of $[Ca^{2+}]_i$ compared to basolateral application. These bile acid-induced Ca^{2+} signals were not dependent on the expression of CFTR. CDC dose-dependently decreased pH_i, of CFPAC-1 cells, the effect of CDC on the pH_i was greater when the bile acid was given from the apical side. Interestingly, CDC-induced acidosis was somewhat higher in CFTR-deficient pancreatic duct cells. Luminal administration of 0.1mM CDC significantly elevated apical Cl^-/HCO_3^- exchange activity, but only in cells that expressed wt CFTR. 0.1 mM CDC did not activate CFTR Cl^- conductance in duct cells isolated from guinea pig.

Conclusions. Our data show that SeV vector is a potential cftr gene transfer agent for human pancreatic duct cells and that expression of CFTR in CF cells is associated with a restoration of Cl^- and HCO_3^- transport at the apical membrane. Apical Cl^-/HCO_3^- exchange activity could be stimulated by cAMP or low doses of CDC. This increase in anion exchange activity was independent of the Cl^- conductance of CFTR. Taken together, this work lead to an improved understanding of the regulation of acid/base transporters in the diseased CF and corrected (with wt CFTR) pancreatic ductal epithelium. Cftr gene transfer may be beneficial in patients with CF.

1. Introduction

The pancreas is part of the digestive tract and has both endocrine and exocrine functions. The exocrine pancreas includes two main types of cells: acinar and duct cells. In general, the physiology and pathophysiology of acinar cells have been more widely investigated. However, it is well known that numerous pancreatic diseases (such as adenocarcinoma and cystic fibrosis, CF) are associated with abnormal ductal cell morphology and function. Therefore, my research was focused on studying the molecular and cellular regulation of pancreatic duct cell function.

1.1. Pancreatic ductal HCO_3^- absorption and secretion

The pancreatic ductal cells both absorb (salvage) and secrete HCO_3^- ions (Argent et al., 2006; Steward et al., 2005). In the resting state, pancreatic ducts absorb HCO_3^- across the apical membrane. A luminal Na^+/H^+ exchanger (NHE3), a Na^+-dependent mechanism that is different from any known NHE isoform and an electroneutral Na^+/HCO_3^- cotransporter (SLC4A7, NBCn1, NBC3) have been identified in the main duct of the mouse pancreas and probably explains HCO_3^- absorption (Ahn et al., 2001; Lee et al., 2000; Park et al., 2002). The absorbed HCO_3^- is probably exported to the extracellular space from the duct cell via a basolateral AE2 Cl^-/HCO_3^- exchanger. The activity of these luminal HCO_3^- salvage transporters is down-regulated following stimulation of HCO_3^- secretion by a rise in intracellular cAMP (Ahn et al., 2001; Lee et al., 2000; Park et al., 2002).

The pancreatic duct secretes a HCO_3^--rich, alkaline fluid that flushes digestive enzymes (secreted by acinar cells) down the ductal tree and into the duodenum and also helps to neutralize acid chyme entering the duodenum from the stomach (Ahn et al., 2001; Hegyi & Rakonczay, 2007). The initial step of HCO_3^- secretion is uptake of HCO_3^- into the duct cells from the extracellular space (Figure 1). HCO_3^- can enter the epithelium either by the forward transport of HCO_3^-, via a basolateral Na^+/HCO_3^- co-transporter (NBC), or by the diffusion of CO_2 into the cells, subsequent hydration to H_2CO_3 by carbonic anhydrase (CA) and backward transport of protons via Na^+/H^+ exchangers (NHEs) and/or H^+ pumps. HCO_3^- secretion across the apical membrane is thought to occur via cystic fibrosis transmembrane conductance regulator (CFTR), a cAMP/protein kinase A (PKA) regulated Cl^- channel and the SLC26 anion exchangers SLC26A3 (DRA, downregulated in adenoma)

and SLC26A6 (PAT-1, putative anion transporter-1). However, the relative importance of each of these apical transporters in HCO_3^- secretion is a controversial issue (Argent et al., 2006; Hegyi et al., 2008; Steward et al., 2005). Rats and mice are capable of secreting a Cl^--rich pancreatic fluid in the absence of HCO_3^-. This is likely to be driven by a Na^+-K^+-$2Cl^-$ cotransporter, probably NKCC1 (Dehaye et al., 2003; Nagy et al., 2007).

1.2. Cystic fibrosis and the role of cystic fibrosis transmembrane conductance regulator in HCO_3^- transport

CF is the most common fatal autosomal recessive disease in the Caucasian ethnic group and is caused by the absence or the dysfunction of CFTR. On average, individuals with CF have a lifespan of about 30 years. The disease affects the pancreas, the liver, the respiratory organs, the bile and the urinary and reproductive organs. The disturbed function of CFTR plays an important role in decreased epithelial HCO_3^- secretion. CFTR itself has been shown to transport HCO_3^-, albeit at a slower rate than Cl^- (Gray et al., 1990; Linsdell et al., 1997). However, it is still unclear whether CFTR's main role in HCO_3^- secretion is to secrete HCO_3^- directly, to provide a source of luminal Cl^- to support apical Cl^-/HCO_3^- exchange or to directly activate the apical Cl^-/HCO_3^- exchangers (Choi et al., 2001; Ko et al., 2004; Lee et al., 1999a, 1999b; Shcheynikov et al., 2006). It remains possible that all three mechanisms could be present.

1.3. Effect of bile acids on HCO_3^- secretion

Obstruction of the Ampulla of Vater by gallstones that have migrated down the common bile duct is a major risk factor for acute pancreatitis (Pandol et al., 2007). The consequent obstruction of bile and pancreatic juice outflow into the duodenum might cause bile reflux into the pancreas. In pancreatic acinar cells, bile acids cause a global elevation of intracellular calcium concentration $[Ca^{2+}]_i$ which leads to trypsinogen activation and, subsequently, cell death (Criddle et al., 2007).

Venglovecz et al. (2008) have shown that luminal administration of a low dose (0.1 mM) of the unconjugated bile acid, chenodeoxycholate (CDC), significantly elevated apical Cl^-/HCO_3^- exchange activity and HCO_3^- secretion in guinea pig pancreatic ducts, and that these effects were Ca^{2+}-dependent. In contrast, a higher dose of CDC (1 mM) strongly inhibited ductal HCO_3^- transport. Recently our work group has demonstrated that the inhibition of HCO_3^- secretion by 1 mM CDC is caused by mitochondrial damage and

consequently depletion of intracellular ATP level (Maléth et al., 2009). The stimulatory effect of 0.1 mM CDC on apical Cl^-/HCO_3^- exchange activity in intact ducts is most likely mediated by upregulation of SLC26A6 (PAT-1), since it was blocked by a competitive inhibitor of anion exchangers dihydro-4,4′-diisothiocyanostilbene-2,2′-disulfonic acid (H_2-DIDS) (Venglovecz et al., 2008). Under physiological conditions, ductal HCO_3^- secretion is regulated by a direct interaction between SLC26 family Cl^-/HCO_3^- exchangers and CFTR (Alper et al., 2006; Alvarez et al., 2005). Therefore, assessing whether the stimulatory effects of CDC on anion exchange activity and HCO_3^- secretion are dependent on CFTR expression and functional Cl^- channel activity should help to clarify the underlying mechanism.

1.4. The investigation of HCO_3^- transport in CFPAC-1 cell line

Due to the limited availability of human pancreatic tissue, most studies on HCO_3^- transport have been performed on mice and guinea pigs (Ahn et al., 2001; Hegyi et al., 2003, 2005). On the other hand, human ductal cell lines have also been widely used for investigation of HCO_3^- transport Demeter et al., 2009; Greeley et al., 2001; Rakonczay et al., 2006; Szűcs et al., 2006). The CFPAC-1 is a human pancreatic ductal adenocarcinoma cell line isolated first from a 26-year-old male CF patient (Schoumacher et al., 1990). The CFPAC-1 cells are homozygous for the most frequent CFTR mutation, which is characterized by deletion of three nucleotides leading to the deficiency of phenylalanine in position 508 (F508del). The greater proportion of this mutant protein remains in the endoplasmatic reticulum and is decayed (Cheng et al., 1990). The smaller proportion of the damaged protein, which reaches the plasma membrane (Zsembery et al., 2000), does not respond adequately to the cAMP stimulation (Wang et al., 2006). cAMP-analogues, phosphodiesterase-inhibitors and forskolin are not able to activate the impaired CFTR (Schoumacher et al., 1990; Park et al., 2002). Ca^{2+}-activated Cl^- channels expressed by CFPAC-1 cells can be stimulated by Ca^{2+} ionophore and extracellular nucleotides, for instance with ATP (Namkung et al., 2003; Park et al., 2002). All these characteristics have been stable through more than 80 passages. This fact proves that the CFPAC-1 cells are maintainable as a cell line that they keep their CFTR defect. CFPAC-1 cells are suitable to use for *in vitro* ductal model of CF. The H^+ and HCO_3^- transport mechanisms of the cell line have already been well characterized previously (Greeley et al., 2001; Rakonczay et al., 2006). The transfection of CFPAC-1 cells with wild-type (wt) CFTR increased the HCO_3^- uptake through the basolateral NBC. The activation of CFTR induced a membrane

depolarisation and it caused an increase in the NBC electric conductivity. Later Greely et al. (2001) demonstrated increased Cl^-/HCO_3^- exchange activity, *dra* and *pat-1* mRNA expression in CFPAC-1 cells, which steadily expressed wt CFTR. On the basis of these results CFTR expression was suggested to modify the synthesis of SLC26 anion changers. Although Greeley and his collaborators made their experiments primarily on unpolarized CFPAC-1 cells, it is not possible to establish, whether the anion changer activity occurred on the apical or on the basolateral membrane. Furthermore, they did not examine the effect of the cAMP mediated CFTR activation on the Cl^-/HCO_3^- exchange activity. Namkung et al. (2003) demonstrated, that CFPAC-1 cells transfected with CFTR containing adenovirus, will be able again to increase the luminal Cl^-/HCO_3^- exchange activity by Ca^{2+}-mobilisation. In contrast, Cheung et al. (1998) and Zsembery et al. (2000) found that increased $[Ca^{2+}]_i$ stimulated HCO_3^- secretion, but it was independent from functional CFTR.

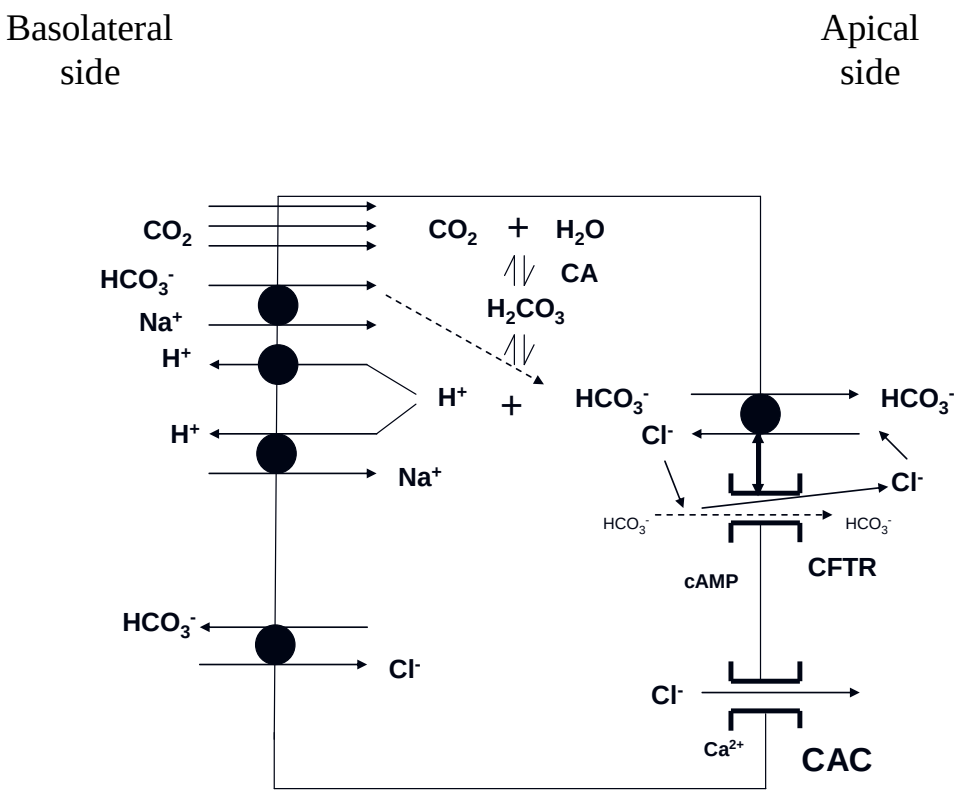

Figure 1. Schematic representation of the ion transport systems in the pancreatic duct cell. The model is based on data derived from experiments on rat and guinea pig duct cells. **CAC**: calcium activated Cl^- channel; **CA**: carbonic anhydrase; **CFTR**: cystic fibrosis transmembrane conductance regulator.

Aims

The main aims of this work were to investigate the potential of a recombinant Sendai virus (SeV) vector to introduce wt CFTR into human CF pancreatic (CFPAC-1) duct cells and to examine the effects of (1) wt CFTR expression on the H^+ and HCO_3^- transport mechanisms of impaired CF pancreatic ducts cells and (2) CDC on intracellular pH (pH_i), $[Ca^{2+}]_i$ and apical Cl^-/HCO_3^- exchange activity in pancreatic duct cells lacking or expressing wt CFTR. Finally, we wanted to test whether low doses of CDC increased CFTR Cl^- channel activity and for these experiments we used guinea pig pancreatic duct cells in which CFTR activity and its regulation have been well characterized (Gray et al., 1993).

2. Materials and Methods

2.1. Materials

CFPAC-1 cells (passage number 50-60) were obtained from Prof. R. A. Frizzell (University of Pittsburgh, Pittsburgh, PA, USA). Laboratory chemicals were purchased from Sigma-Aldrich (Poole, Dorset, UK) unless indicated otherwise. 2',7'-bis-(2-carboxyethyl)-5(6)-carboxyfluorescein-acetoxymethyl ester (BCECF-AM), 2-(6-(bis-(carboxymetil)-amino)-5-(2-(2-(bis-(carboxymetil)-amino)-5-metilfenoxi)-etoxi)-2-benzofuranyl)-5-5-oxazolcarboxil-acetoxy-methyl ester (FURA-2-AM) and H_2-DIDS were from Molecular Probes Inc. (Eugene, OR, USA). The selective CFTR inhibitor $CFTR_{inh}$-172 (Ma et al., 2002) was kindly provided by Prof. A. S. Verkman (University of California, San Francisco, CA, USA). Stock solutions of BCECF-AM (2 mM) and $CFTR_{inh}$-172 inhibitor (10 mM) were prepared in dimethyl sulphoxide. 5-bromo-4-chloro-3-indolyl-β-D-galactopyranoside (50 mg/ml) was dissolved in dimethylformamide. Nigericin (10 mM) and forskolin (50 mM) were dissolved in ethanol and stored at -20°C. Polyester Transwells were supplied by Corning-Costar (Buckinghamshire, UK). The anti-PKAcat (C20) antibody was from Santa Cruz (sc-903, Santa Cruz, CA, USA). Mouse anti-ZO-1 antibody was supplied by Zymed Laboratories (33-9100, San Francisco, CA, USA) anti-CFTR antibody was supplied by Chemicon (MAB3480, Temecula, CA, USA). Vectashield mounting medium was from Vector Laboratories Ltd. (Peterborough, UK) Enhanced chemiluminescent reagent was from Amersham (Little Chalfont, UK). SeV vectors were supplied by DNAVEC Corporation (Tsukuba Ibaraki, Japan). Propidium iodide and goat anti-mouse-FITC secondary antibody (Alexa Fluor 488) were supplied by Invitrogen Corporation (Carlsbad, CA, USA).

2.2. Solutions

The standard HEPES-buffered solution contained (mM): 130 NaCl, 5 KCl, 1 $MgCl_2$, 1 $CaCl_2$, 10 Na-HEPES, 10 D-glucose (pH 7.4 with HCl). In the Na^+-free HEPES solution NaCl was replaced by 140 mM N-methyl-D-glucamine-Cl and the Na-HEPES was replaced by equimolar HEPES-acid. In the Na^+-free HEPES solution containing 20 mM NH_4Cl, the concentration of N-methyl-D-glucamine-Cl was reduced to maintain osmolarity. The standard HCO_3^--buffered solution contained (mM): 115 NaCl, 5 KCl, 1 $MgCl_2$, 1 $CaCl_2$, 25 Na-HCO_3, 10 D-glucose. In the K^+-free HCO_3^--buffered solution KCl was replaced by equimolar NaCl. The high-K^+ HCO_3^--buffered solution contained (mM): 5

NaCl, 115 KCl, 1 $MgCl_2$, 1 $CaCl_2$, 25 Na-HCO_3, 10 D-glucose. The Cl^--free HCO_3^- solution contained (mM): 115 Na-gluconate, 2.5 K_2SO_4, 6 Ca-gluconate, 1 Mg-gluconate, 25 Na-HCO_3, 10 D-glucose. All solutions containing HCO_3^- were continuously equilibrated with 5% CO_2 - 95% O_2 to maintain pH at 7.4.

2.3. Culturing of CFPAC-1 cells

CFPAC-1 cells were grown in Iscove's modified Dulbecco's medium supplemented with 10% foetal calf serum, 2 mM glutamine, 100 units/ml penicillin, and 0.1 mg/ml streptomycin and were cultured as described previously (Schoumacher et al., 1990). The medium was changed every 1-2 days. Cells were maintained at 37 °C in a humidified atmosphere containing 5% CO_2. Cell monolayers were prepared by seeding at high density (300,000-350,000 cells/cm^2) onto polyester permeable supports (12 mm diameter, 0.4 μm pore size Transwells). Cell confluence was checked by microscopy and determination of transepithelial electrical resistance (R_T) using an EVOM-G voltohmmeter (World Precision Instruments, Sarasota, FL, USA).

2.4. Isolation of guinea pig pancreatic duct cells

For patch clamp experiments small intra- and interlobular ducts were isolated from guinea pig (weighing 150-250g) pancreas, cultured overnight, and dissociated into single cells as described previously (Gray et al., 1994).

2.5. Construction of recombinant Sendai virus vectors

SeV vectors were constructed by DNAVEC Corporation. The genome order of the full length SeV used in this study was as follows: a leader (ld) sequence at the 3'-end followed by the following viral genes; nucleocapsid (NP), phospho (P), matrix (M), fusion (F), hemagglutinin-neuraminidase (HN), and large proteins (L). Finally, a small trailer (tr) sequence was placed at the 5'-end. We utilized the wt SeV vector (SeV(+)MF) (Tokusumi et al., 2002), in which a NotI restriction site for insertion of the gene of interest is located between the M and F genes. SeV(+)MF carrying the human CFTR gene (SeV-CFTR) was constructed as previously described (Kato et al., 1996).

In brief, human CFTR (accession no. M28668) cDNA was amplified with a pair of NotI-tagged primers that contained SeV-specific transcriptional regulatory signal sequences,

5′-ACTTGCGGCCGCCAAAGTTCAATGCAGAGGTCGCCTCTGGAAAAGGCCAGC-3’ and 5’-ATCCGCGGCCGCGATGAACTTTCACCCTAAGTTTTTCTTACTACGGCTAAAGCCTTGTATCTTGCACCTCTTCTTC-3′. The amplified fragment was introduced into the NotI restriction site of the parental pSeV(+)MF, thereby incorporating the cDNA of SeV-CFTR. Note that a number of silent nucleotide changes were introduced into the CFTR cDNA to ensure efficient SeV vector-mediated CFTR expression (Ferrari et al., 2007). The cDNA of the wt SeV vector carrying the LacZ gene (SeV-LacZ) was constructed as previously described using the amplified fragment of LacZ (Shiotani et al., 2001). pSeV-CFTR and pSeV-LacZ were transfected into LLC-MK2 cells after infection of the cells with vaccinia virus vTF7-3 (Fuerst et al., 1986), which expresses T7 polymerase. The T7-driven recombinant SeV-CFTR and SeV-LacZ RNA genomes were encapsulated by NP, P, and L proteins, which were derived from their respective cotransfected plasmids. Forty hours later, the transfected cells were injected into 10-day-old embryonated chicken eggs to amplify the recovered virus (Kato et al., 1996). The SeV vector titer was determined by a hemagglutination assay using chicken red blood cells, and the virus was stored at -70°C until use.

2.6. Infection with recombinant Sendai virus

For pH_i and $[Ca^{2+}]_i$ measurements, LacZ staining and immunocytochemistry, confluent CFPAC-1 cells grown on Transwells were infected with SeV-CFTR or SeV-LacZ (nuclear localized) 3 days after seeding. Preliminary experiments showed that the cells were much more efficiently infected from the apical compared to the basolateral side. Therefore, after washing the cells with phosphate-buffered saline (PBS), 6×10^5 (0.6 µl) or 3×10^6 (3 µl) plaque forming units (multiplicity of infection, MOI = 3 or 15) of SeV vector was applied to the apical side of the cells in serum-free Iscove's modified Dulbecco's medium (30-32.4 µl) for 1 h. The basolateral side of the cells was incubated in serum-free Iscove's modified Dulbecco's medium (800 µl) only. Thereafter, serum containing Iscove's modified Dulbecco's medium was added to the upper (470 µl) and lower (700 µl) compartments of the Transwells. Twenty-four hours later the cells were rinsed with PBS and fed with fresh virus-free, serum-containing Iscove's modified Dulbecco's medium. Control (i.e., uninfected) CFPAC-1 cells were subjected to a similar protocol, but the virus aliquots were substituted with serum-free Iscove's modified Dulbecco's medium. Experiments were performed 48-96 h after infection.

To determine the expression of CFTR, H^+ and HCO_3^- transporters, or protein kinase A (PKA) analysis, confluent CFPAC-1 cells, grown in 25 cm^2 tissue culture flasks, were

washed with PBS and incubated with serum-free Iscove's modified Dulbecco's medium (825 µl, control), SeV-CFTR or SeV-LacZ in serum-free Iscove's modified Dulbecco's medium (MOI = 3 or 15) for 1 h. Thereafter, 9.2 ml of serum-containing Iscove's modified Dulbecco's medium was added to the flasks. Twenty-four hours later the cells were rinsed with PBS and were fed with fresh virus-free serum-containing Iscove's modified Dulbecco's medium. The cells were trypsinised, pelleted, and frozen on dry ice 48 h after infection.

2.7. β-Galactosidase staining

β-Galactosidase activity was detected by *in situ* staining (Yonemitsu et al., 2000). CFPAC-1 cells grown on Transwells or plastic were washed with PBS and fixed at 4°C in a PBS solution containing 2% formaldehyde, 0.2% glutaraldehyde, 2 mM $MgCl_2$, and 5 mM EGTA for 10 min. The cells were then rinsed with washing buffer (0.01% sodium deoxycholate, 0.02% NP-40 and 2 mM $MgCl_2$ in PBS) and incubated with a chromophore solution (0.1% 5-bromo-4-chloro-3-indolyl-β-D-galactopyranoside, 5 mM potassium ferrocyanide, and 5 mM potassium ferricyanide in washing buffer) at 37°C for 1-2 h. The number of infected (blue) and uninfected cells was counted microscopically and averaged in 5-6 randomly selected 400× viewing fields.

2.8. Western blot

2.8.1. CFTR

Total protein extracts from CFPAC-1 and CAPAN-1 cells, as well as from baby hamster kidney (BHK) cells stably expressing wt or F508del CFTR (Chang et al., 1993) (as controls) were analyzed for CFTR protein expression by Western blotting as described previously (Farinha et al., 2004a-b).

2.8.2. Protein kinase A catalytic subunit

The protein kinase A catalytic subunit (PKAcat) was detected from the immunoprecipitated pellet used for the PKA activity assay (see 2.14). Sodium dodecyl sulphate - polyacrylamide gel electrophoresis was performed using the Novex (Invitrogen Ltd., Paisley, UK) system on 4-12% Bis-Tris polyacrylamide gels and the proteins were transferred to nitrocellulose membranes. Following blocking in TBS-Tween (0.5% Tween-20) plus 5% milk powder for 30 min, membranes were incubated with anti-PKAcat antibody.

2.9. Immunocytochemistry

Two days after infection with SeV-LacZ or SeV-CFTR, CFPAC-1 monolayers were washed with PBS and then fixed and permeabilized with methanol on ice for 15 min. The monolayers were blocked in 3% horse serum for 1 h. The cells were then incubated overnight at 4 ^{o}C with mouse anti-ZO-1 or anti-CFTR antibody (1:100). Following 3 washes with PBS, the cells were incubated in 3% goat serum for 1 h and goat anti-mouse-FITC secondary antibody (1:100) for 1 h. The filters were washed in PBS and incubated in 1 μg/ml propidium iodide for 5-10 min (to stain the nuclei of cells) and were mounted in Vectashield mounting medium. Control experiments omitted the primary antibody (and were negative). Staining was visualized using confocal laser microscopy (TCS-NT, Leica with Kr-Ar laser) with appropriate excitation and emission filter sets. A gallery of 10-20 optical sections (0.5 μm thick) through the x-y and *z*-planes were obtained.

2.10. Iodide efflux assay

Iodide efflux was performed on CFPAC-1 cells grown on 6-well plastic culture plates using the protocol described for CFTR-transfected BHK cells (Hughes et al., 2004). After the iodide release had reached a steady state (6 min), the intracellular cAMP level was raised by agonists (10 μM forskolin, 100 μM 3-isobutyl-1-methylxanthine, IBMX, and 100 μM 2'-O-dibutyryladenosine 3',5'-cyclic monophosphate, dbcAMP) and collection of the efflux medium was resumed for an additional 10 min. In some experiments the cells were administered 10 μM $CFTR_{inh}$-172 or dimethyl sulphoxide after removing the iodide loading buffer. The amount of iodide in each sample was determined with an iodide-selective electrode (Thermo Electron Corporation, Fife, Scotland).

2.11. mRNA expression of DRA, PAT-1, AE2, pNBC1, NHE2, NHE3

2.11.1. Isolation of mRNA and reverse transcription

To study the expression of transporter mRNAs in uninfected, SeV-LacZ or SeV-CFTR infected CFPAC-1 cells grown in 25 cm^2 tissue culture flasks, total RNA was isolated using the GenElute^{TM} Mammalian Total RNA Miniprep Kit (Sigma). The RNA concentration was determined by measuring the optical density at 260 nm. RNA integrity was verified by electrophoresis on 1% agarose gel. Total RNA (1 μg) was used for cDNA synthesis by oligodT priming (M-MLV Reverse Transcriptase, RNase H Minus, Point Mutant, Promega, Madison, WI).

2.11.2. Semi-quantitative polymerase chain reaction (PCR)

First-strand cDNA was amplified with PCR primers designed, by Primer3 software (Whitehead Institute for Biomedical Research, Cambridge, MA, USA), to be specific for selected transporters. (Table 1.) PCR was performed using *Taq* polymerase (Promega). Following an initial denaturation at 95°C for 2 min and 30-35 cycles of amplification, samples were incubated at 72°C for a further 5 min. The PCR products were resolved on agarose gels. As an internal concentration reference for the PCR experiments, we performed 19 cycles of amplification with primers for the acidic ribosomal phosphoprotein (XS13) (Wallrapp et al., 1997). Total RNA extracts from normal human pancreas (Stratagene, La Jolla, CA, USA) and HPAF cells were used as positive control for selected primers of electrolyte transporters.

			Expected product size (bp)
AE2	Fwd:	5'-CCTCGGTGCAGTTCTTTCTC-3'	373
	Rev:	5'-TTCATGAGGTCTAGGTCGGC-3'	
DRA	Fwd:	5'-GTTCAGGAGAGCACAGGAGG-3'	281
	Rev	5'-TGAAATGCCACACTAGCTGC-3'	
PAT-1	Fwd:	5'-AGGTAGATGTCGTGGGCAAC-3'	264
	Rev:	5'-CCAGGCTCCGAGACATAGAG-3'	
pNBC1	Fwd:	5'-ACA CCT CTT CCA TGG CTC TG-3'	191
	Rev:	5'-ACC TCG GTT TGG ACT TGT TG-3'	
XS13	Fwd:	5'-CGT GCT AAG TTG GTT GCT TT-3'	500
	Rev:	5'-GCAGCTGATCAAGACTGGA-3'	

Table 1. Sequences of primers used for semi-quantitative RT-PCR.

2.11.3. Real-time PCR

For quantitative analysis of gene expression of DRA, PAT-1, AE2, NHE2, and NHE3, real-time PCR was performed. Real time PCR primers and FAM-labeled MGB target-specific fluorescence probe were purchased from Applied Biosystems (Foster City, CA, USA) for DRA (Hs00230798_m1), PAT-1 (Hs00370470_m1), AE2 (Hs00161738_m1), NHE2 (Hs00268166_m1), NHE3 (Hs00188200_m1), and human acidic ribosomal phosphoprotein P0 (RPLPO, Hs99999902_m1). RPLPO, was used as positive control. The template cDNAs was amplified by the Universal Mastermix (Applied Biosystems) containing AMP-erase. For detection of fluorescence signal during the PCR cycles, the ABI Prism Sequence Detection System 7700 (Applied Biosystems) was employed with the default setting (50°C for 2 min, 95°C for 10 min, 45 cycle: 95°C for

15 s, 60°C for 1 min). Each experiment was repeated two times with 2 replicates. Changes in levels of gene expression were estimated based on the real-time PCR data by calculating the relative expression values (reference/control sample) for the target RNA in each sample and normalizing them by dividing with the relative value of RPLPO from the same sample (Livak & Schmittgen, 2001).

2.12. Measurement of intracellular pH and intracellular Ca^{2+} concentration and determination of buffering capacity

The pH_i was estimated as described previously (Hegyi et al., 2004; Rakonczay et al., 2006; Thomas et al., 1979). Briefly, after loading the cells with 2 μM BCECF-AM, the Transwells were transferred to a perfusion chamber mounted on an inverted Olympus microscope (Olympus Hungary Ltd., Budapest, Hungary). 4-5 small areas (Regions of interests – ROIs) of 180-240 cells were excited with light at wavelengths of 440 and 495 nm, and the 440/495 fluorescence emission ratio was measured at 535 nm. Experiments were performed on 37°C. Apical and basal bath volumes were 0.5 and 1 ml and the perfusion rates were 3 and 6 ml/min, respectively. The intrinsic buffering capacity (β_i) of CFPAC-1 cells was estimated according to the NH_4^+ prepulse technique (Weintraub & Machen, 1989; Rakonczay et al., 2006). The total buffering capacity (β_{total}) was calculated as $\beta_{total} = \beta_i + \beta_{HCO3^-}$, where β_{HCO3^-} is the buffering capacity of the HCO_3^-/CO_2 system. $\beta_{HCO3^-} = 2.3 \times [HCO_3^-]_i$. $[HCO_3^-]_i$ is the intracellular concentration of HCO_3^-.

Measurement of $[Ca^{2+}]_i$ was performed using the same method except that the cells were loaded with the Ca^{2+}-sensitive fluorescent dye FURA 2-AM (5 μM) for 60 min. For excitation, 340 and 380 nm filters were used, and the changes in $[Ca^{2+}]_i$ were calculated from the fluorescence ratio (F_{340}/F_{380}) measured at 510 nm.

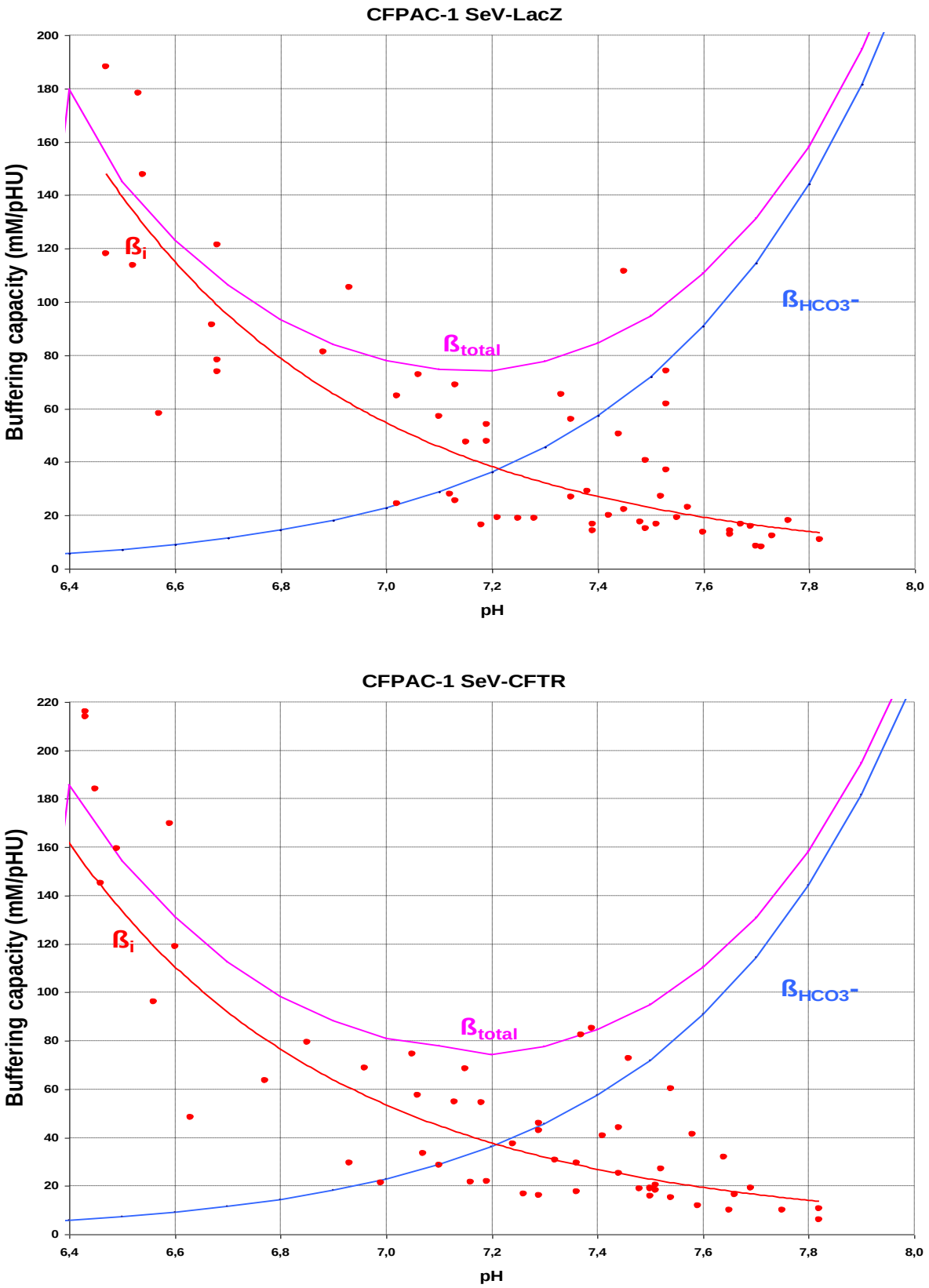

Figure 2. Buffering capacity of CFPAC-1 cells transduced with SeV-LacZ or SeV-CFTR at different pH_i.

2.13. Net change in pH_i and calculation of base flux

The net change in pH_i (ΔpH_i) was measured by determining the pH_i immediately before and at the peak level after the changes of solutions by averaging the values of 80 data points. The initial rates of change of pH_i (over 30-50 sec) resulting from solution changes were used to calculate transmembrane base flux (J_B). J_B = change of $pH_i/\Delta t \times \beta_{total}$. The β_{total} value used in the calculation of J_Bs was obtained by using the average pH_i value over a 30 sec period immediately before changing solutions. We denote base influx as J_B and base efflux as $-J_B$.

2.14. Protein kinase A activity assay

Homogenization of CFPAC-1 cells was achieved by mechanical lysis (Polytron) in three volumes of ice-cold buffer (10 mM Tris, 20 mM NaH_2PO_4, 1 mM EDTA, pH 7.8 containing a fresh protease inhibitor cocktail (Boehringer complete tablet)). Whole cell lysates were used as input material for immunoprecipitation. Prior to precipitation, dimethyl pimelimidate linking of PKAcat antibody to protein A sepharose beads was performed according to the method of Harlow & Lane (1988). A 7 µl slurry of antibody-crosslinked protein-A beads was added to 20 µg of whole cell lysate. Samples were then shake-incubated for 60 min at 4 °C. The samples were pelleted in a desktop centrifuge, followed by 3 × 1 ml washes with standard assay buffer (50 mM HEPES, pH 7.0, 50 mM NaF, 1.0 mM EGTA, 1.0 mM EDTA, 0.2% Tween-20, 10% glycerol) containing 1 M NaCl and 3 × 1ml washes into standard assay buffer. Precipitation pellets were re-suspended in 20 µl of assay buffer and assayed/probed as described. PKA activity was determined by measuring the incorporation of γ-^{32}P from [γ-^{32}P] ATP (Perkin-Elmer) into the S660 residue of a known amount of purified CFTR- nucleotide binding domain-1 fragment (bacterially expressed and purified to homogeneity). Assays were carried out at 30°C for 10 min and terminated by spotting a 15 µl aliquot onto a 1 cm^2 piece of P81 phosphocellulose paper and washing 3 × 5 min in 1% phosphoric acid. Incorporation of γ-^{32}P was quantified using a Packard Instant Imager (Muimo et al., 2000). PKA peptide inhibitor (Calbiochem, Nottingham, UK) was used at a working concentration of 100 nM to specify the phosphotransfer activity of PKA.

2.15. Electrophysiology

Patch pipettes were pulled from borosilicate and had resistances, after fire polishing, of between 3 and 5 MΩ. Seal resistances were typically between 5 and 10 GΩ.

An EPC-7 amplifier (List Electronic, Darmstadt, Germany) was used to record whole-cell currents from single duct cells at room temperature (Gray et al., 1993). Current/voltage (*I/V*) relationships were obtained by holding V_m at 0 mV and clamping to ± 100 mV in 20 mV increments for 500 ms with an 800 ms interval between each pulse. Data were filtered at 1 kHz, sampled at 2 kHz with a CED 1401 interface (Cambridge Electronic Design, Cambridge, England), and stored on computer hard disc. *I/V* plots were constructed using the average current measured over a 4 ms period starting 495 ms into the voltage pulse. Reversal potentials (E_{rev}) and current densities were determined from I/V plots after fitting a third order polynomial using regression analysis. Mean current amplitudes were calculated at E_{rev} ± 60 mV and normalized to cell capacitance (pF) measured using the EPC-7 amplifier. Series resistance (R_s) compensation was routinely used (50%–70%). V_m was corrected for current flow (I) across the uncompensated fraction of R_s using the relationship $V_m=V_p-I*R_s$, where V_p is the pipette potential. V_m was also corrected for liquid junction potentials using the program JPCalc and have been applied to V_m.

2.16. Statistical analysis

To avoid errors arising from the variation in the rate and magnitude of HCO_3^- uptake between different set of monolayers, we performed the respective measurements on the same day from one set of cell cultures in random order and where possible, internal control experiments were carried out. Statistical analyses were determined using either the Student's paired or unpaired *t*-test or the analysis of variance as appropriate. $P < 0.05$ was accepted as statistically significant.

3. Results

3.1 Efficiency of SeV vector-mediated gene transfer

To estimate the efficiency of gene transfer, SeV-LacZ was added to either the basolateral or apical membrane of polarized CFPAC-1 monolayers for 1 h. (n = 6). LacZ activity was measured between 48 and 96 h after infection. Initial experiments showed that very little gene transfer occurred following basolateral exposure to SeV-LacZ. However, following application of SeV-LacZ to the apical membrane at MOI = 3, strong, homogenous LacZ activity was observed in 32 ± 2% of cells. At the higher MOI = 15, 68 ± 3% of the cells were stained. Thus, transduction with SeV vector was more efficient via the apical membrane of CFPAC-1 cells and the proportion of cells infected was clearly dose-related.

3.2. Effect of SeV vector-mediated transduction on the expression of CFTR

Figure 3 shows that CFPAC-1 and SeV-LacZ infected cells exhibited very little CFTR protein expression as judged by Western blotting. In these cells only immature CFTR (i.e., core-glycosylated or band B) could be detected, as a very faint band. Similar results were obtained with BHK cells stably expressing F508del-CFTR, although band B staining was much stronger. However, both immature and mature (i.e., fully-glycosylated, processed, or band C) forms of CFTR were detected in SeV-CFTR transduced CFPAC-1 cells, and in the positive controls (CAPAN-1 cells and BHK cells stably expressing wt CFTR).

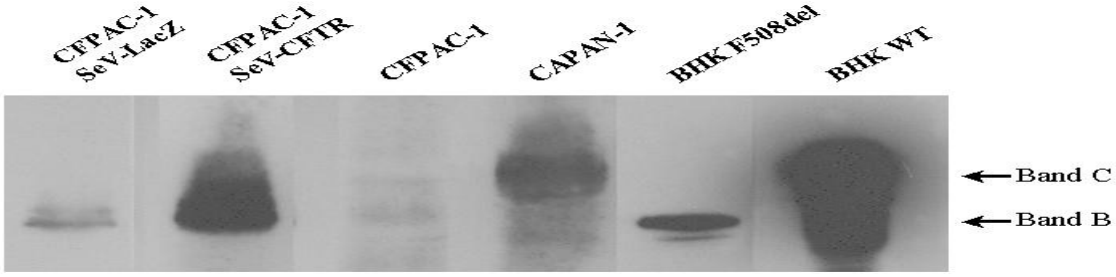

Figure 3. CFTR protein in SeV-infected CFPAC-1 cells (MOI = 15). Representative Western blots of total protein extracts from cells grown in 25 cm^2 flasks using anti-CFTR M3A7 antibody after Sodium dodecyl sulphate-polyacrylamide gel electrophoresis electrophoresis on a 7.5% (w/v) polyacrylamide gel. To prevent over exposure of the film different amounts of protein were loaded as follows: 30 µg for the BHK cells, 50 µg for the CFPAC-1 SeV-CFTR cells, and 100 µg for the remainder of the cell lines. Note the marked increase in CFTR protein expression in SeV-CFTR infected CFPAC-1 cells (50 µg protein per lane) compared to the untransduced and vector only cells (100 µg protein per lane). Both immature, core-glycosylated (band B, 160 kDa) and processed, that is, fully-glycosylated (band C, 170-180 kDa) forms of CFTR were detected in CAPAN-1 and CFPAC-1 SeV-CFTR cells, and in the control BHK wt cells. Uninfected and SeV-LacZ transduced cells exhibited very little CFTR expression (only band B).

CFTR overexpression has previously been shown to result in mislocalisation of the protein (Farmen et al., 2005). Therefore, we have used immunocytochemistry to clearly demonstrate apical localization of CFTR in SeV-CFTR (MOI=3) transduced CFPAC-1 cells. CFTR expression was only detected in the SeV-CFTR transduced CFPAC-1 cells (Fig. 4), and was localized solely to the apical plasma membrane.

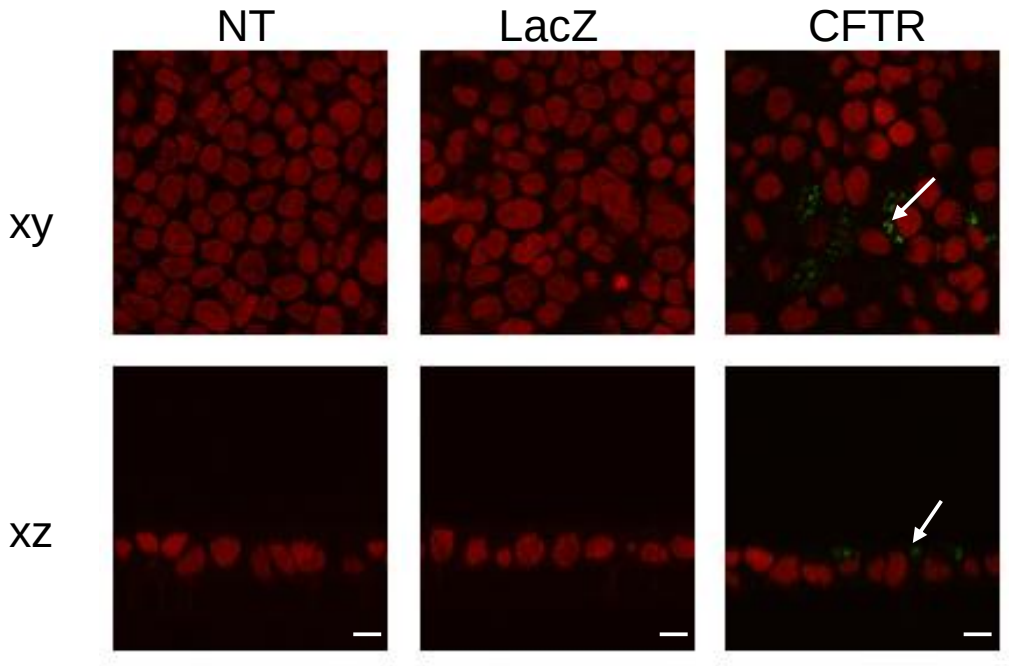

Figure 4. CFTR expression in untransduced and SeV-LacZ or SeV-CFTR (MOI: 3) CFPAC-1 pancreatic duct cells. CFPAC-1 monolayers were fixed and stained for CFTR expression 2 days after being transduced with SeV-LacZ or SeV-CFTR. CFTR expression could only be detected in the apical membrane of SeV-CFTR transduced CFPAC-1 cells (green staining in xy and xz sections). Nuclei of cells (red) were stained with propidium iodide. Scale bars = 10 μm.

Functional expression of CFTR was assessed by the iodide efflux assay (Fig. 5). Increases in intracellular cAMP had no effect on iodide efflux in SeV-LacZ (MOI = 3) (n = 8) (Fig. 5A) or in SeV-CFTR (MOI = 15) cells (n = 4, results not shown). In contrast, cAMP stimulated iodide efflux in four out of five experiments (80%) with SeV-CFTR (MOI = 3) cells (Fig. 5B). Finally, Figure 5B also shows that the effect of cAMP on iodide efflux was completely blocked by 10 μM $CFTR_{inh}$-172 (n = 4).

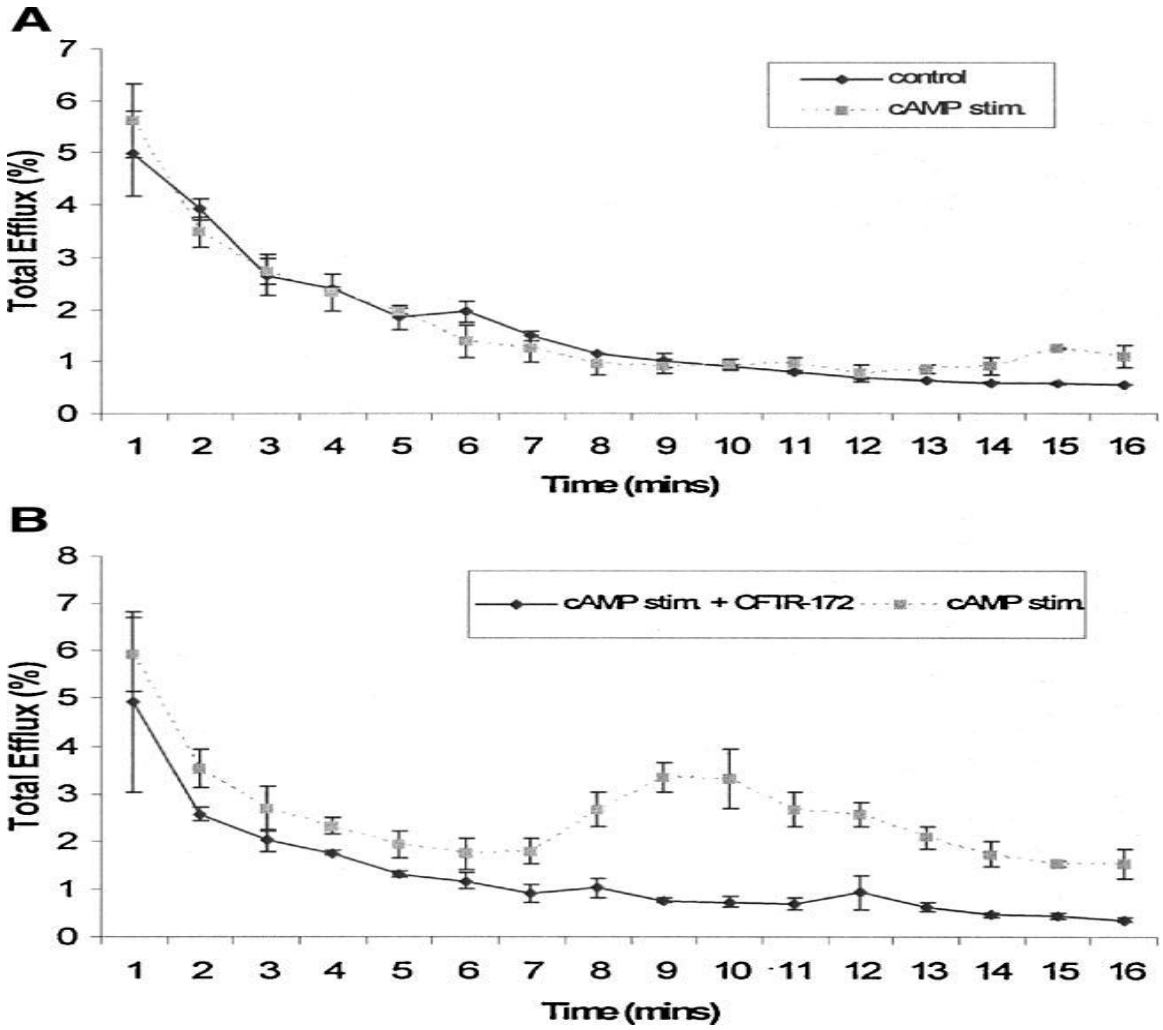

Figure 5. Functional expression of CFTR in CFPAC-1 cells determined using iodide efflux. **A**: Iodide efflux from SeV-LacZ cells was not increased by exposure to cAMP (n = 8 experiments). **B**: In contrast, cAMP-stimulated iodide efflux from SeV-CFTR (MOI = 3) in 4/5 experiments. Data shown are from the four positive experiments. CFTR-172 (10 μM) abolished the stimulatory effect of cAMP (n = 4 experiments). Cells were exposed to a cAMP cocktail (10 μM forskolin, 100 μM 3-isobutyl-1-methylxanthine, IBMX, and 100 μM 2′-O-dibutyryladenosine 3′,5′-cyclic monophosphate, dbcAMP) from the 7th till the 16th min. Data points are mean ± SE.

3.3. Expression of DRA, PAT-1, AE2, pNBC1, NHE2 and NHE3 mRNA in SeV vector transduced and untransduced CFPAC-1 cells

Figure 6A shows that PAT-1, AE2, and pNBC1 were constitutively expressed in uninfected and SeV vector transduced CFPAC-1 cells as determined by semi-quantitative PCR. However, we did not detect mRNA for DRA, NHE2, and NHE3 (results not shown). CFTR transduction had no obvious effect on the level of the mRNA's for PAT-1, AE2, pNBC1 (Fig. 6A), and NHE2 (data not shown). Again, mRNA for DRA and NHE3 was not detectable after CFTR expression. The control house-keeping gene XS13, which encodes a ribosomal phosphoprotein, showed similar expression levels in all the cell samples (Fig.

6A). Note that in the normal pancreas (lane P in Fig. 6A), PAT-1 and pNBC1 were expressed at relatively low levels, and AE2 was not detectable. However, duct cells form only ~10% by volume of the normal gland, so the extracted RNA will be largely derived from acinar cells (Argent et al., 2006).

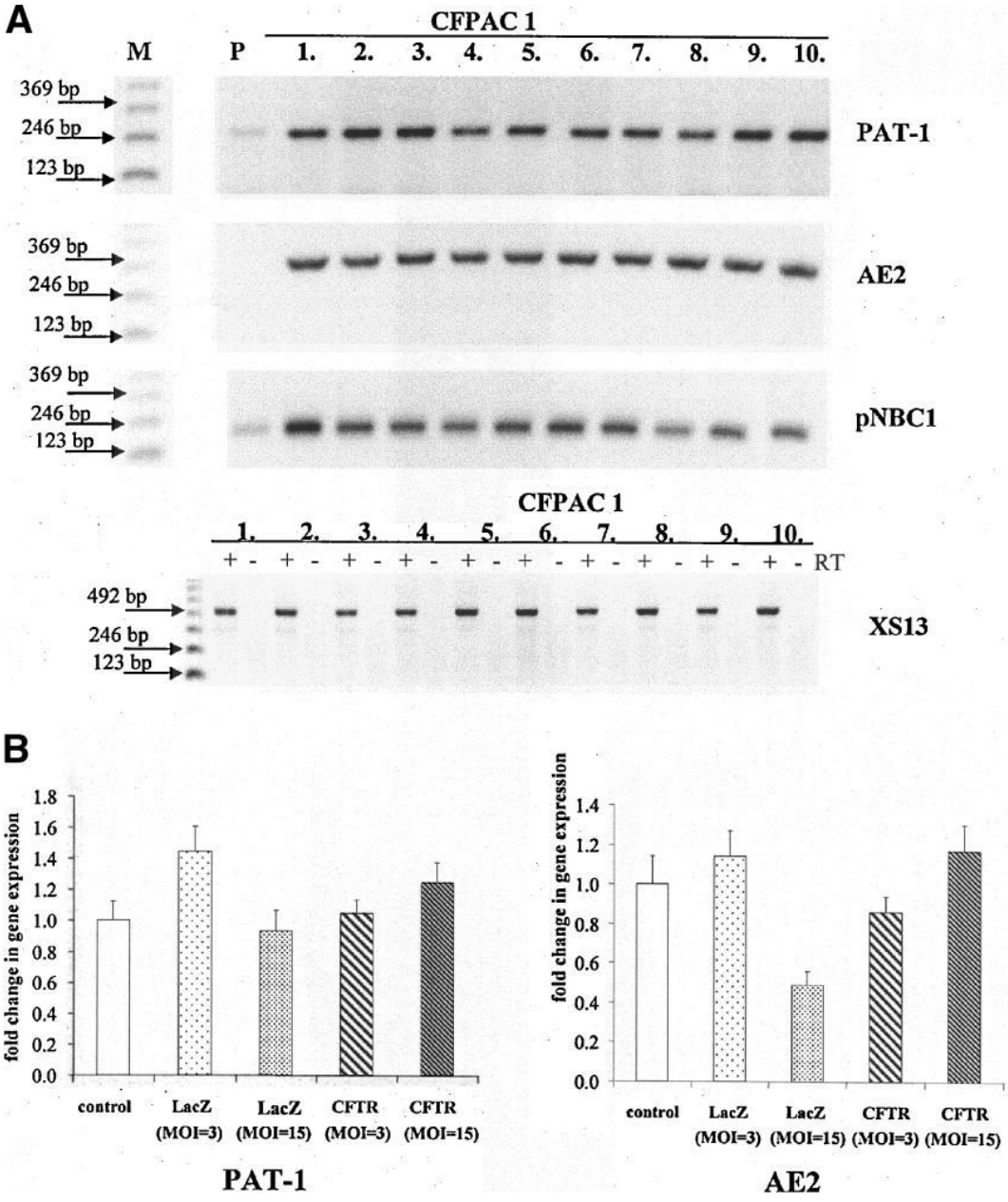

Figure 6. Expression of HCO_3^- transporters in CFPAC-1 cells. A: Semi-quantitative RT-PCR. Agarose gels stained with ethidium bromide show PCR products for PAT-1, AE2, pNBC1 (upper part) and the positive control ribosomal phosphoprotein gene, XS13 (lower part). Uninfected CFPAC-1 cells (lanes 1,2), Sev-LacZ cells (MOI = 3, lanes 3,4; MOI = 15, lanes 5,6) and SeV-CFTR cells (MOI = 3, lanes 7,8; MOI = 15, lanes 9,10). Lane M is the molecular weight ladder and lane P is normal human pancreas. RT ± indicates the presence/absence of reverse transcriptase in the XS13 experiment. **B**: Real-time RT-PCR data for PAT-1 and AE2 expression.

We also performed some experiments using real-time PCR (Fig. 6B). Again, no statistical difference was found in the expression levels of PAT-1 and AE2 amongst the different cell groups (Fig. 6B). As before, we were unable to detect DRA, NHE2, and NHE3 expression in any of the cells lines using real-time PCR. Taken together, these data indicate that with the exception of CFTR, CFPAC-1 cells express the key transporters required for HCO_3^- secretion, namely pNBC1 and PAT-1. Importantly, in terms of gene therapy, SeV vector infection at both MOI = 3 and MOI = 15 (either with or without CFTR expression), did not affect the expression of these key transporters.

3.4. Effect of SeV vector-mediated transduction on the integrity of CFPAC-1 cell monolayer

3.4.1 Transepithelial resistance

CFPAC-1 cells grown on polyester Transwells became confluent 2-3 days after seeding, as judged by visual observation. R_T can be used as an indicator of the structural integrity of an epithelial sheet, because electrical resistance is largely determined by the 'leakiness' of the tight junctions. CFPAC-1 cells grown on polyester Transwells became confluent 2-3 days after seeding, as judged by visual observation. R_T increased steadily over 4-5 days up to a maximum of $199 \pm 10\ \Omega\,cm^2$ in the untransduced cells. R_T was significantly higher in the SeV-LacZ (MOI = 3: $400 \pm 15\ \Omega\,cm^2$, MOI = 15: $314 \pm 13 \Omega\,cm^2$) and in the SeV-CFTR (MOI = 3: $243 \pm 5\ \Omega\,cm^2$, MOI = 15: $268 \pm 9\ \Omega\,cm^2$) infected groups compared to the untransduced cells (n = 9-69). These data show that transduction with SeV vector did not disrupt the structural integrity of the CFPAC-1 epithelium; if anything the epithelium became slightly 'tighter' after exposure to the virus.

3.4.2. Expression of ZO-1 in polarised cultures of untransduced and SeV-transduced CFPAC-1 cells

As shown in Figure 7, the tight junction protein ZO-1 was localized to the apical part of the cells and showed a characteristic 'chicken wire' pattern in both the control and SeV-transduced CFPAC-1 cells, consistent with its expression at the tight junctions. No difference was observed in ZO-1 expression between the different cell lines.

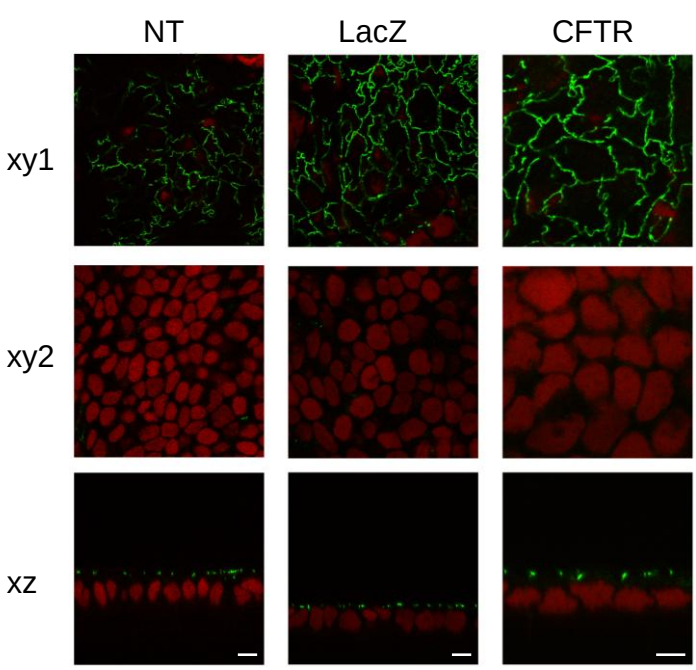

Figure 7. ZO-1 expression in untransduced and SeV-LacZ or SeV-CFTR transduced CFPAC-1 pancreatic duct cells. CFPAC-1 monolayers were fixed and stained for ZO-1 expression 2 days after being transduced with SeV-LacZ or SeV-CFTR. ZO-1 was localized to the apical part of the cells (see xy1, xz sections) and showed a characteristic 'chicken wire' pattern (green staining in xy1 section) in both the untransduced (NT) and transduced CFPAC-1 cells, consistent with its expression at the tight junctions. Xy2 and xz sections show the nuclei of cells stained (red) with propidium iodide. No difference was observed in ZO-1 expression between the different cell lines. Scale bars = 10 μm.

3.5. Resting pH_i and buffering capacity of CFPAC-1 cells

As HCO_3^- is a component of a buffer system, pH_i and β_i are crucial parameters in a HCO_3^--secreting epithelial cell. The resting pH_i of CFPAC-1 cells bathed in the standard HEPES solution was 7.11 ± 0.08 ($n = 6$) and was not significantly different in SeV-CFTR (MOI = 3) transduced cells (7.09 ± 0.10, $n = 6$). The resting pH_i value of SeV-LacZ cells (MOI = 15) was significantly increased (7.26 ± 0.01) compared to the SeV-CFTR cells (7.20 ± 0.02) in the standard HCO_3^-/CO_2 solution ($n = 12$). We have previously reported that the intrinsic β_i is quite variable in different CFPAC-1 monolayers (see Fig. 1 in Rakonczay et al., 2006). In a previous study, we found that uninfected CFPAC-1 cells had a β_i of 34 ± 8 mM/pH over the pH_i range 7.0-7.2. The respective β_i values for SeV-CFTR and SeV-LacZ (MOI = 15) transduced cells ($n = 9$-11) at this pH_i range were 46 ± 7 and 46 ± 6 mM/pH. These β_i values are not statistically different. Taken together, our results indicate that SeV vector infection has no obvious effect on pH_i regulatory mechanisms or β_i in CFPAC-1 cells.

3.6. Functional polarity of CFPAC-1 cells

Rakonczay et al. (2006) have previously shown that the apical and basolateral membranes of CFPAC-1 cell monolayers exhibit marked differences in their relative CO_2 and HCO_3^- permeabilities. Exposing the basolateral side of cells to a solution containing HCO_3^-/CO_2 causes pH_i to alkalinize rapidly, suggesting that HCO_3^- permeates the basolateral membrane rather faster than CO_2 (Rakonczay et al., 2006) consistent with

presence of base loaders (principally a NBC) on the basolateral membrane of the duct cell. In contrast, exposing the apical membrane to HCO_3^-/CO_2 causes pH_i to acidify rapidly, consistent with faster diffusion of CO_2 from lumen to cell compared with HCO_3^- (Rakonczay et al., 2006). That the apical membrane of pancreatic duct cells resists back diffusion of HCO_3^- from the lumen is likely to be of physiological importance, since it will favor retention of secreted HCO_3^- in the duct lumen. We therefore checked whether the functional polarity of CFPAC-1 cells was disrupted by SeV vector transduction by exposing the apical and basolateral membranes of SeV-LacZ and SeV-CFTR-transduced cells to HCO_3^-/CO_2.

Figure 8A shows a continuous pH_i recording from a SeV-LacZ (MOI = 15) infected monolayer (n = 12). Initially, the apical and basolateral membranes were perfused with the standard HEPES solution and then the apical solution was switched to HCO_3^-/CO_2 (Fig. 8A). This caused the expected rapid acidification of pH_i (Rakonczay et al., 2006), most likely due to CO_2 diffusion into the cells. In 24 similar experiments the ΔpH_i and $-J_B$ following apical HCO_3^-/CO_2 addition were -0.20 ± 0.01 and -23.7 ± 0.9 mM B/min, respectively. After the rapid acidification, pH_i remained stable at the new level (Fig. 8A). Finally, switching the basolateral solution to HCO_3^-/CO_2 caused a rapid alkalinization of pH_i (Fig. 8A), most likely due to rapid HCO_3^- uptake into the cells (Rakonczay et al., 2006). The associated ΔpH_i and J_B were 0.37 ± 0.01 and 17.14 ± 0.74 mM B/min, respectively. Figure 8B shows a similar experiment performed on SeV-CFTR (MOI = 15) transduced cells (n = 12). The fall in pH_i following apical HCO_3^-/CO_2 addition was not significantly different from that observed in the SeV-LacZ cells (compare Figs. 8A and B). However, after the rapid acidification, pH_i continued to rise slowly in about 50% of the experiments (by 0.034 ± 0.006 during 4 min, n = 8) with SeV-CFTR transduced cells (Fig. 8B). CFTR does exhibit a finite permeability to HCO_3^- (Gray et al., 1990; Linsdell et al., 1997), so this slow alkalinization might reflect back flux of HCO_3^- from the luminal compartment through CFTR. Switching the basolateral solution to HCO_3^-/CO_2 caused pH_i to alkalinize in the high titer SeV-CFTR (MOI = 15) cells (Fig. 8B). However, comparison of Fig. 8B with Fig. 8A, suggests that both the rate (J_B was 10.37 ± 0.69 mM B/min) and the degree of the alkalinization (ΔpH_i was 0.27 ± 0.01) of SeV-CFTR cells were significantly reduced compared to SeV-LacZ cells (see J_B and ΔpH_i values in the previous paragraph). In contrast, in the low titer SeV-CFTR (MOI = 3) cells, switching the basolateral solution to standard HCO_3^-/CO_2 caused pH_i changes similar to those observed in SeV-LacZ cells (data not shown).

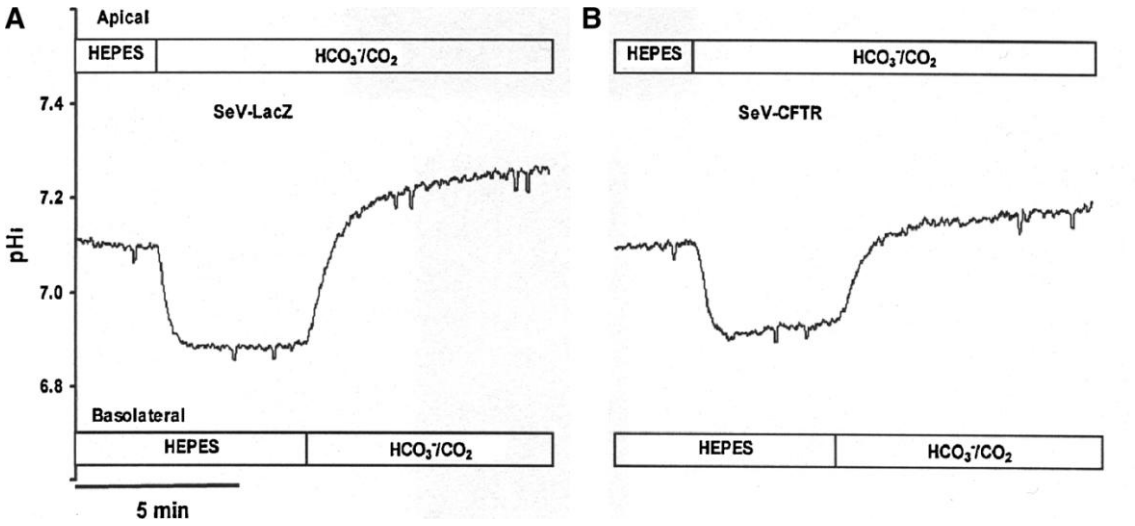

Figure 8. Functional polarity of CFPAC-1 monolayers. A: Continuous pH_i recording from a SeV-LacZ (MOI = 15) cell monolayer. Horizontal bars indicate the composition of the solutions bathing the apical and basolateral membranes. Both sides of the monolayer were initially perfused with a HCO_3^--free, HEPES-buffered solution and then the apical and basolateral solutions were sequentially changed to standard HCO_3^-/CO_2 as indicated by the horizontal bars. **B**: Similar experiment on a SeV-CFTR (MOI = 15) cell monolayer. Note that the alkalinization following basolateral addition of HCO_3^-/CO_2 is reduced in the CFTR expressing cells.

These data are consistent with hyperexpression of CFTR in the high titer MOI = 15 cells either decreasing the rate at which HCO_3^- enters across the basolateral membrane or increasing the rate of HCO_3^- efflux across the apical membrane. Nevertheless, cells transduced with SeV vector, even at a high vector concentration, clearly retain the typical differences in apical and basolateral CO_2 and HCO_3^- permeabilities that we have previously described in untransduced CFPAC-1 cells (Rakonczay et al., 2006).

3.7. Effect of SeV vector-mediated transduction and CFTR expression on Cl^-/HCO_3^- exchange activity

Anion exchange activity can be detected in both the basolateral and apical membranes of pancreatic duct cells (Argent et al., 2006; Steward et al., 2005). The physiological role of the basolateral anion exchangers (probably AE2) is uncertain, as with a normal transmembrane Cl^- gradient they would be expected to cause HCO_3^- efflux and to oppose secretion (Argent et al., 2006; Hegyi et al., 2008; Steward et al., 2005). In contrast, it is well established that secretion of HCO_3^- across the apical membrane of pancreatic duct cells involves both CFTR and SLC26 family Cl^-/HCO_3^- exchangers, although the quantitative importance of each pathway is controversial (Argent et al., 2006; Steward et al., 2005). Furthermore, it has been shown that phosphorylation of CFTR, as occurs during stimulation of HCO_3^- secretion, activates SLC26 anion exchangers (Lee et al., 1999b;

Shcheynikov et al., 2006). Our PCR data indicate that PAT-1 is the important SLC26 exchanger in CFPAC-1 cells. Given the role of anion exchangers in pancreatic duct cell function, we decided to investigate whether SeV vector transduction and CFTR expression had any effect on their activity.

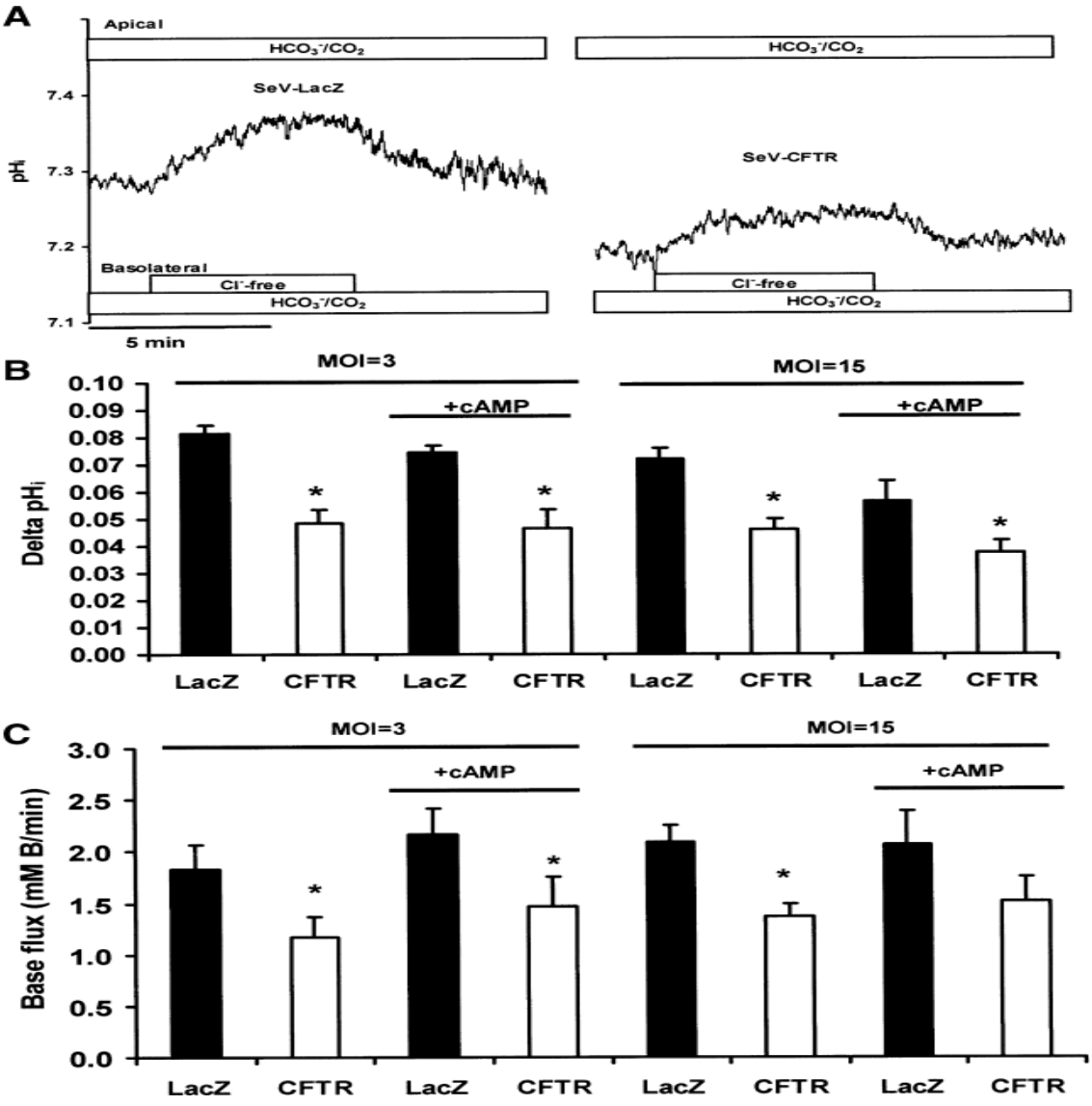

Figure 9. Basolateral Cl^-/HCO_3^- exchange in CFPAC-1 monolayers. A: Continuous pH_i recordings from SeV-LacZ (left part) and SeV-CFTR (MOI = 15) (right part) infected cells. Horizontal bars indicate the composition of the solutions bathing the apical and basolateral membranes. Removal of Cl^- from the basolateral solution caused pH_i to alkalinize in both cell types, but the effect is larger in the SeV-LacZ cells (left part). **B**: Summary data for ΔpH_i following basolateral Cl^- removal (n = 6-9) in SeV-LacZ (closed columns) and SeV-CFTR (open columns) transduced cells with and without cAMP stimulation. **C**: Summary data for the J_B changes following basolateral Cl^- removal. Column notation is the same as in **B**. * Indicates significant difference ($P < 0.05$) versus the respective control group.

3.7.1 Basolateral membrane

Figure 9A (left part) shows an experiment in which pH_i was continuously recorded from a SeV-LacZ infected CFPAC-1 monolayer. Removal of Cl^- from the basolateral HCO_3^-/CO_2 solution caused a clear increase in pH_i, indicating that the cells have an anion exchanger on their basolateral membrane. However, when the same experiment was performed on a SeV-CFTR infected monolayer; the alkalinization caused by Cl^- removal was much smaller (Fig. 9A right part).

Figures 9B and C show summary data for the increase in pH_i and J_B caused by basolateral Cl^- removal in SeV-LacZ and SeV-CFTR cells infected at MOI = 3 and 15. Note that in the SeV-CFTR cells (both MOI = 3 and 15) the effects of basolateral Cl^- removal on pH_i and J_B were significantly reduced (Fig. 9B,C). Also, increasing intracellular cAMP, by exposing the cells to a cocktail of forskolin (10 μM), IBMX (100 μM), and dbcAMP (100 μM), had no significant effect on the ΔpH_i and J_B observed after Cl^- removal in either the SeV-LacZ or the SeV-CFTR (MOI = 3 and 15) cell groups (Fig. 9B, C). These data indicate that transduction of CFPAC-1 cells with CFTR inhibits basolateral Cl^-/HCO_3^- exchange (probably mediated by AE2) and that cAMP has no effect on the activity of this exchanger. However, we cannot exclude the fact that the reduced pH_i change following Cl^- removal, in the absence or presence of cAMP stimulation could simply reflect faster exit of HCO_3^- across the apical membrane, either through the apical anion exchanger or CFTR. Nonetheless physiologically, inhibition of the basolateral AE2 by CFTR expression would tend to favor HCO_3^- secretion and would be beneficial to CF patients.

3.7.2. Apical membrane

In uninfected CFPAC-1 cells and in SeV-LacZ infected cells, removal of Cl^- from the apical membrane of the monolayers had no effect on pH_i, either in the absence or presence of cAMP (data not shown). Thus, Cl^-/HCO_3^- exchange activity was not detectable in the apical membrane of cells that did not express CFTR.

In contrast, Cl^- removal from the apical membrane of low titer SeV-CFTR MOI = 3 cells caused a clear alkalinization of pH_i (Fig. 10A). Thus, expression of CFTR revealed an anion exchange activity in the apical membrane of CFPAC-1 cells. Figure 10A also shows that stimulating the SeV-CFTR MOI = 3 monolayer with cAMP increased both the rate and magnitude of the pH_i alkalinization following Cl^- removal.

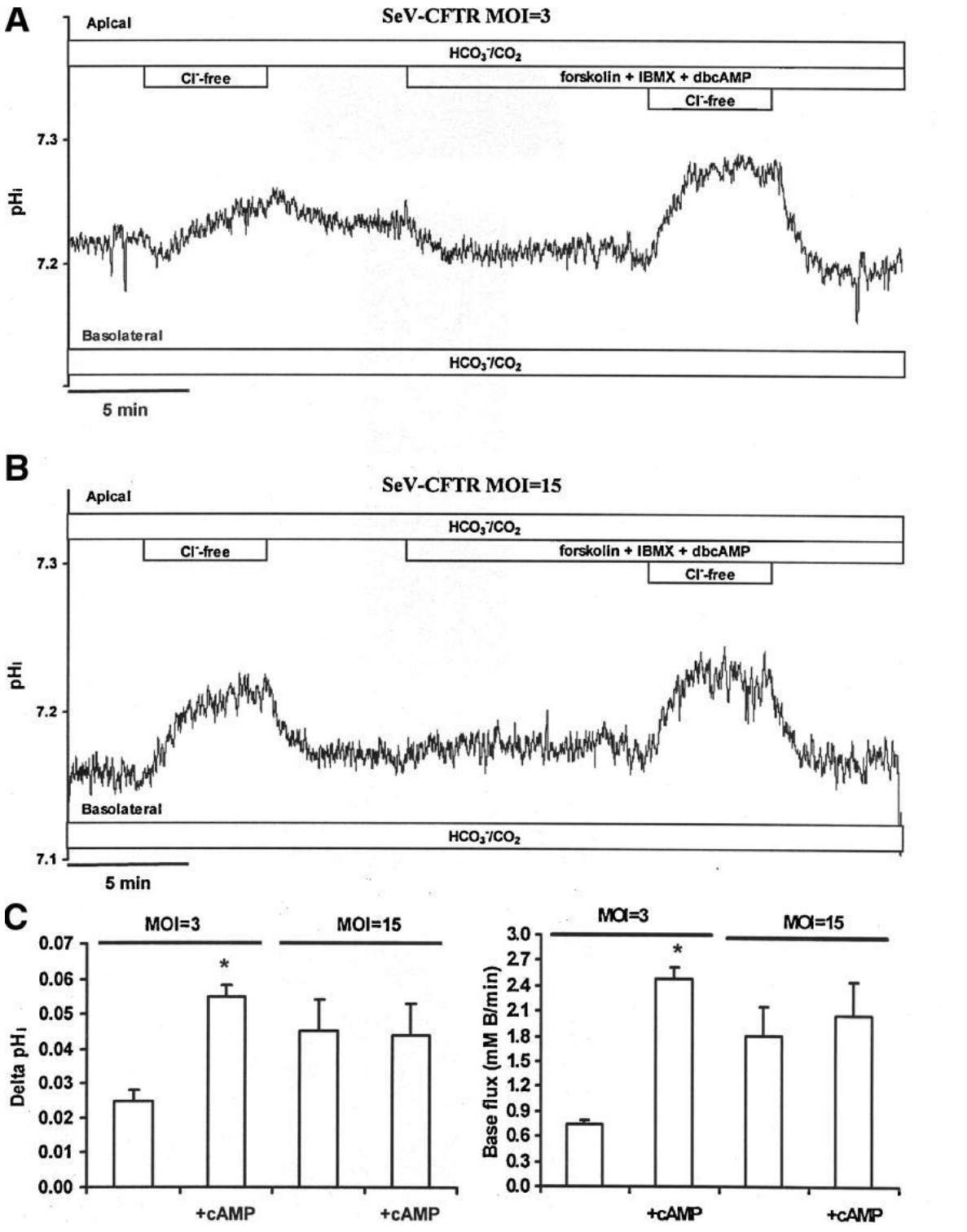

Figure 10. Apical Cl^-/HCO_3^- exchange activity in SeV-CFTR CFPAC-1 monolayers. A: Continuous pH_i recording from a low titer, SeV-CFTR (MOI = 3), monolayer. Horizontal bars indicate the composition of the solutions bathing the apical and basolateral membranes. Cl^-/HCO_3^- exchange activity was assessed by removing Cl^- from the apical solution, first in the absence and then in the presence of the cAMP cocktail. Note the clear stimulation of Cl^-/HCO_3^- exchange activity in the presence of cAMP. **B**: Similar experiment performed with a high titer, SeV-CFTR (MOI = 15) monolayer. Note that cAMP did not stimulate Cl^-/HCO_3^- exchange activity. **C**: Summary data showing the effects of Cl^- removal on pH_i and J_B; n = 31 for MOI = 3 cells and n = 6 for MOI = 15 cells. * Indicates significant difference ($P < 0.05$) versus the respective unstimulated control group.

Figure 10B shows a similar experiment performed on SeV-CFTR MOI = 15 cells. Removal of apical Cl^- caused a large alkalinization of pH_i. However, exposing the SeV-CFTR MOI = 15 cells to cAMP did not increase the degree of alkalinization in response to Cl^- withdrawal.

Figure 10C is a summary of the ΔpH_i and J_B values obtained in this series of experiments. Unstimulated CFTR MOI = 3 cells exhibited a low, but clearly detectable, level of apical anion exchange. Furthermore, in these cells cAMP significantly increased ΔpH_i and J_B after apical Cl^- removal by 2.2- and 3.4-fold, respectively ($P < 0.05$ for both parameters, n = 31). In contrast, unstimulated CFTR MOI = 15 cells exhibited a much higher level of anion exchange than the unstimulated MOI = 3 cells (Fig. 10C), and the ΔpH_i and J_B values were unaffected by cAMP (n = 6). We conclude that transducing CFPAC-1 cells with CFTR at MOI = 3 are consistent with an apical Cl^-/HCO_3^- exchange activity. In contrast, cells transduced with CFTR at the higher virus titer of MOI = 15 have a constitutively active apical Cl^-/HCO_3^- exchanger that cannot be further stimulated by cAMP.

cAMP-stimulated anion exchange activity in the MOI = 3 SeV-CFTR cells was completely blocked by 500 μM H_2-DIDS; J_B was -0.10 ± 0.26 mM B/min and ΔpH_i was -0.022 ± 0.011 when apical Cl^- was removed in the presence of the inhibitor (control values were 2.45 ± 0.40 mM B/min and 0.051 ± 0.007, respectively, n = 5). To test the electrogenicity of the cAMP stimulated anion exchange activity, SeV-CFTR cells were perfused with basolateral K^+-free or high-K^+ HCO_3^-/CO_2 solution 10 min before the removal of apical Cl^-. Apical Cl^- withdrawal in the absence of basolateral K^+ did not significantly alter J_B (1.48 ± 0.22 mM B/min) and ΔpH_i (0.066 ± 0.009) versus standard conditions (J_B: 1.54 ± 0.29 mM B/min, ΔpH_i: 0.05 ± 0.008, n = 7). In addition, apical Cl^- withdrawal in the presence of basolateral high-K^+ HCO_3^-/CO_2 solution resulted in no alteration of J_B (3.12 ± 0.49 mM B/min), but a significant increase of ΔpH_i (0.12 ± 0.01) compared to the control (2.24 ± 0.45 mM B/min and 0.06 ± 0.008, respectively, n = 9). Overall, it seems that the cAMP stimulated apical Cl^-/HCO_3^- exchange activity is electroneutral.

Finally, 10 μM $CFTR_{inh}$-172 had no effect on either the rate or magnitude of the pH_i alkalinization following activation of apical Cl^-/HCO_3^- exchange in cyclic AMP stimulated SeV-CFTR (MOI = 3) CFPAC-1 cells (n = 7, data not shown). Thus, Cl^- transport by CFTR is probably not required to maintain apical Cl^-/HCO_3^- exchange activity.

3.8. Effect of SeV vector-mediated CFTR expression on PKA activity and expression

Because apical Cl^-/HCO_3^- exchange in the MOI = 15 SeV-CFTR transduced cells was constitutively active and did not respond to cAMP (Fig. 10B,C), we were concerned that the higher virus titer may have affected the cAMP signaling system. We therefore measured PKA activity, and the amount of the 42 kDa PKAcat in the SeV-transduced CFPAC-1 cells. Figure 11A shows that PKA activity was similar in the uninfected, and in the SeV-LacZ and SeV-CFTR cells infected at MOI = 3. About the same level of PKA activity was also observed in SeV-LacZ cells infected at MOI = 15. However, in contrast, PKA activity was almost undetectable in SeV-CFTR cells infected at the higher titer.

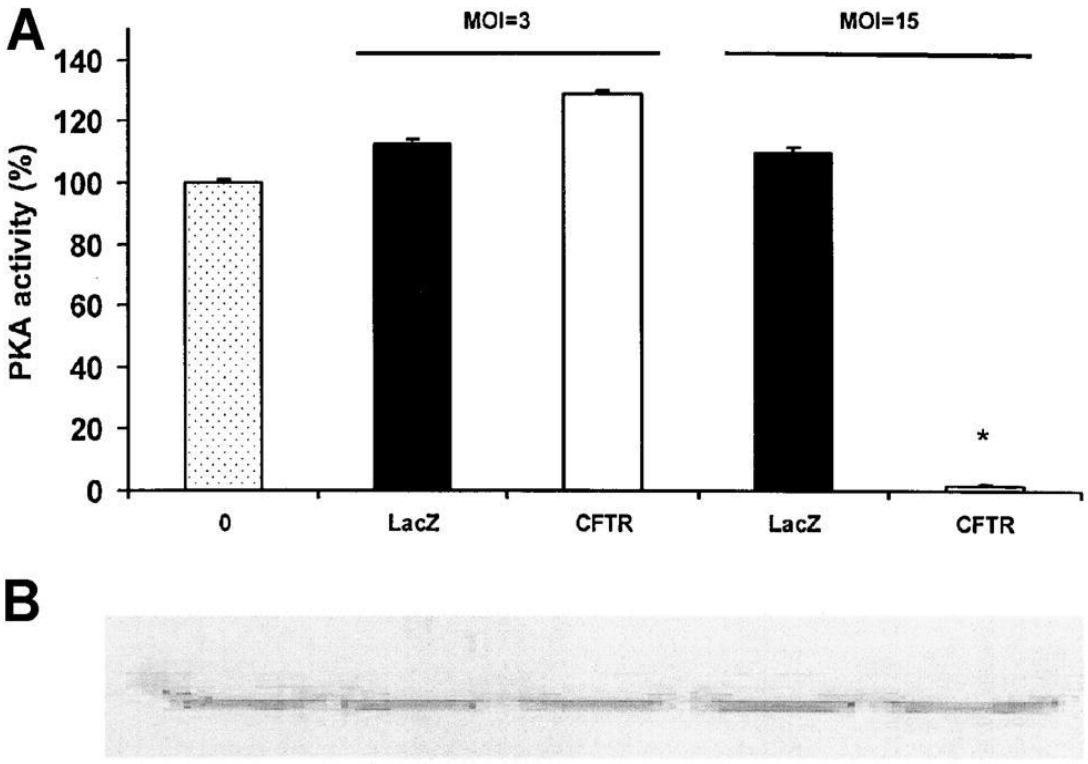

Figure 11. Protein kinase A activity and total catalytic subunit measured in CFPAC-1 cells. **A**: PKA activity was determined in uninfected (0), SeV-LacZ (LacZ) and SeV-CFTR (CFTR) transduced cells by measuring the incorporation of γ-^{32}P into purified CFTR-nucleotide binding domain-1 fragments. Data for low titer (MOI = 3) and high titer (MOI = 15) cells are shown. * Indicates significant difference ($P < 0.05$) versus the uninfected control group. **B**: Representative Western blots (20 µg protein) for the 42 kD catalytic subunit of PKA. Cell samples are as indicated in (A).

We used Western blotting to measure the amount of PKAcat expressed in the various cell types. The results indicated that all cell groups contained about the same amount of PKAcat (Fig. 11B). Taken together, these data suggest that hyperexpression of

CFTR inhibits PKA activity, thus, providing an explanation for our failure to detect cAMP stimulation of apical Cl^-/HCO_3^- exchange activity in SeV-CFTR MOI = 15 cells. Clearly, disabling the cAMP signaling pathway in this way would be a disadvantage in terms of gene therapy and predicts that over-expression of CFTR in pancreatic duct cells of CF patients will need to be avoided.

3.9. The effect of SeV vector-mediated CFTR expression on apical Na^+/H^+ exchange activity

Apical NHE activity has been detected in the main pancreatic duct and may be involved in HCO_3^- scavenging from the duct lumen (Argent et al., 2006; Marteau et al., 1995; Steward et al., 2005). HCO_3^- scavenging is probably a protective mechanism which acidifies the ductal contents, thereby reducing the chances of pro-enzyme activation when flow rates are low during interdigestive periods (Argent et al., 2006; Lee et al., 2000; Steward et al., 2005). Our work group has recently shown that CFPAC-1 cells express an apical NHE activity (Rakonczay et al., 2006). Figure 12A shows a continuous pH_i recording from a SeV-LacZ (MOI = 15) infected CFPAC-1 monolayer. Exposing the cells to a 20 mM NH_4Cl pulse, administered in the absence of Na^+ on both sides of the monolayer, reduced pH_i to about 6.7. In the continued absence of Na^+, pH_i stabilized at this new value, indicating the absence of any other Na^+-independent pH_i recovery mechanisms such as H^+ pumps (Fig. 12A). Re-addition of Na^+ to the apical membrane caused pH_i to increase, due to activation of the apical NHE. Similar results were obtained when the SeV-LacZ cells were exposed to the NH_4Cl pulse in the presence of the cAMP cocktail (Fig. 12A). Figure 12B shows a similar experiment performed on a SeV-CFTR (MOI = 15) transduced monolayer. Qualitatively, the results were similar to those obtained with the SeV-LacZ cells. However, the effect of re-adding Na^+ on pH_i and J_B was significantly greater in the SeV-CFTR cells as compared to the SeV-LacZ cells (MOI = 3: 1.71 ± 0.27-fold, n = 10; MOI = 15: 2.12 ± 0.44-fold, $P < 0.05$, n = 5) (compare Figs. 12A and B). Finally, exposure of the SeV-CFTR monolayer to the cAMP cocktail had no significant effect on the J_B observed in response to re-addition of Na^+ (Fig. 12B). Similar results were obtained in four other experiments. These data suggest that the NHE expressed in the apical membrane of CFPAC-1 cells is upregulated in the presence of CFTR, but is unaffected by cAMP stimulation.

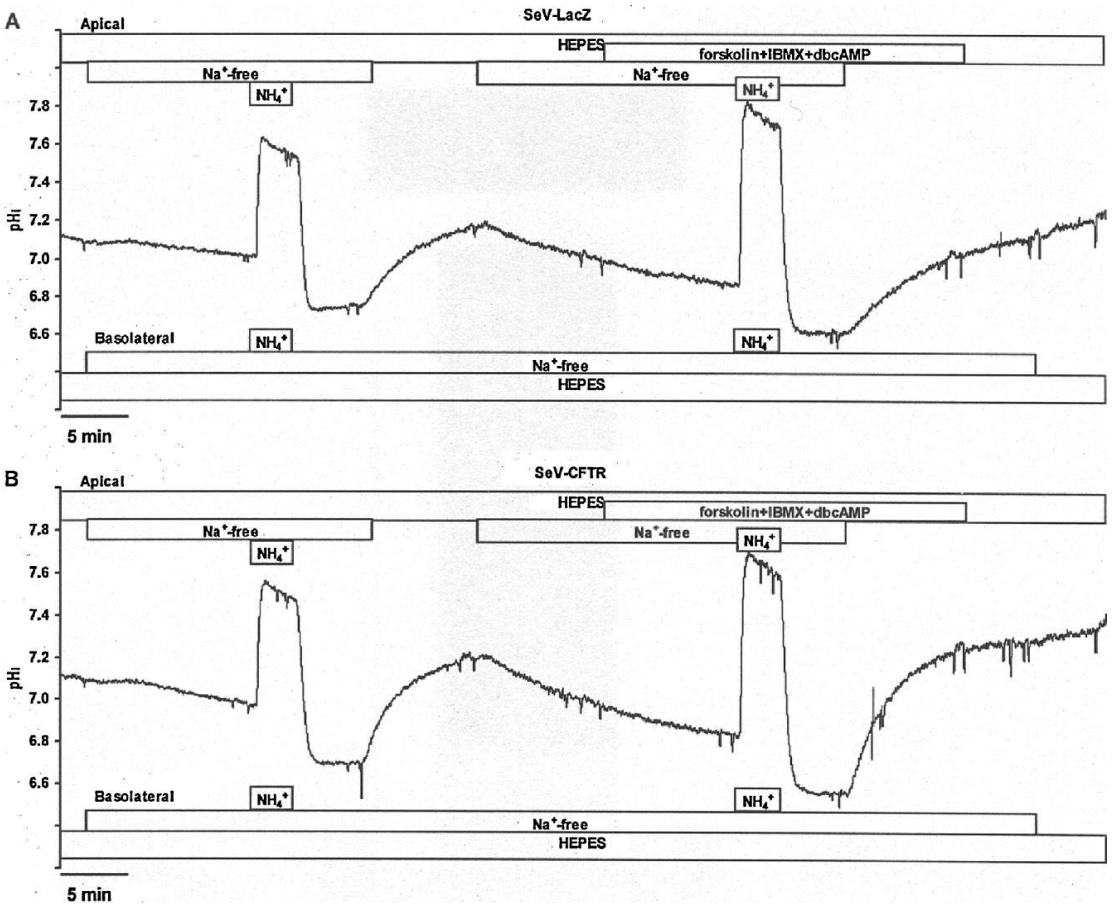

Figure 12. Apical Na^+/H^+ activity in SeV-transduced CFPAC-1 cells. A: Continuous pH_i recording from a SeV-LacZ (MOI = 15) monolayer. Horizontal bars indicate the composition of solutions bathing the apical and basolateral membranes. During bilateral perfusion with a Na^+-free solution, the cells were acidified by a pulse of NH_4Cl (20 mM). Subsequent re-introduction of Na^+ to the apical side caused pH_i and J_B to increase reflecting activation of the apical NHE. The same protocol was repeated in the second half of the experiment, but with the cells exposed to the cAMP cocktail. **B**: Continuous pHi recording from a SeV-CFTR (MOI = 15) transduced monolayer. Same protocol as in (**A**). Note that the effect of Na^+ re-addition on ΔpH_i and J_B was greater in the SeV-CFTR transduced cells (n=5).

3.10. Effect of chenodeoxycholate on pH_i

Please note that for all bile acid related experiments we used CFPAC-1 cells transduced with SeV-LacZ or SeV-CFTR at MOI=3. Administration of CDC (0.1 and 1.0 mM) in standard HEPES solution caused a dose-dependent decrease in the pH_i of CFPAC-1 cells (Fig. 13A-C). However, at both doses tested, apical administration of CDC resulted in a markedly higher rate of intracellular acidification as compared to basolateral administration (Figs. 13B and C). Moreover, the $-J_B$ response to 1 mM CDC was significantly lower in cells transduced with CFTR vs LacZ (Fig. 13B), probably indicating that CFTR expression had reduced the rate at which the bile acid entered the duct cells.

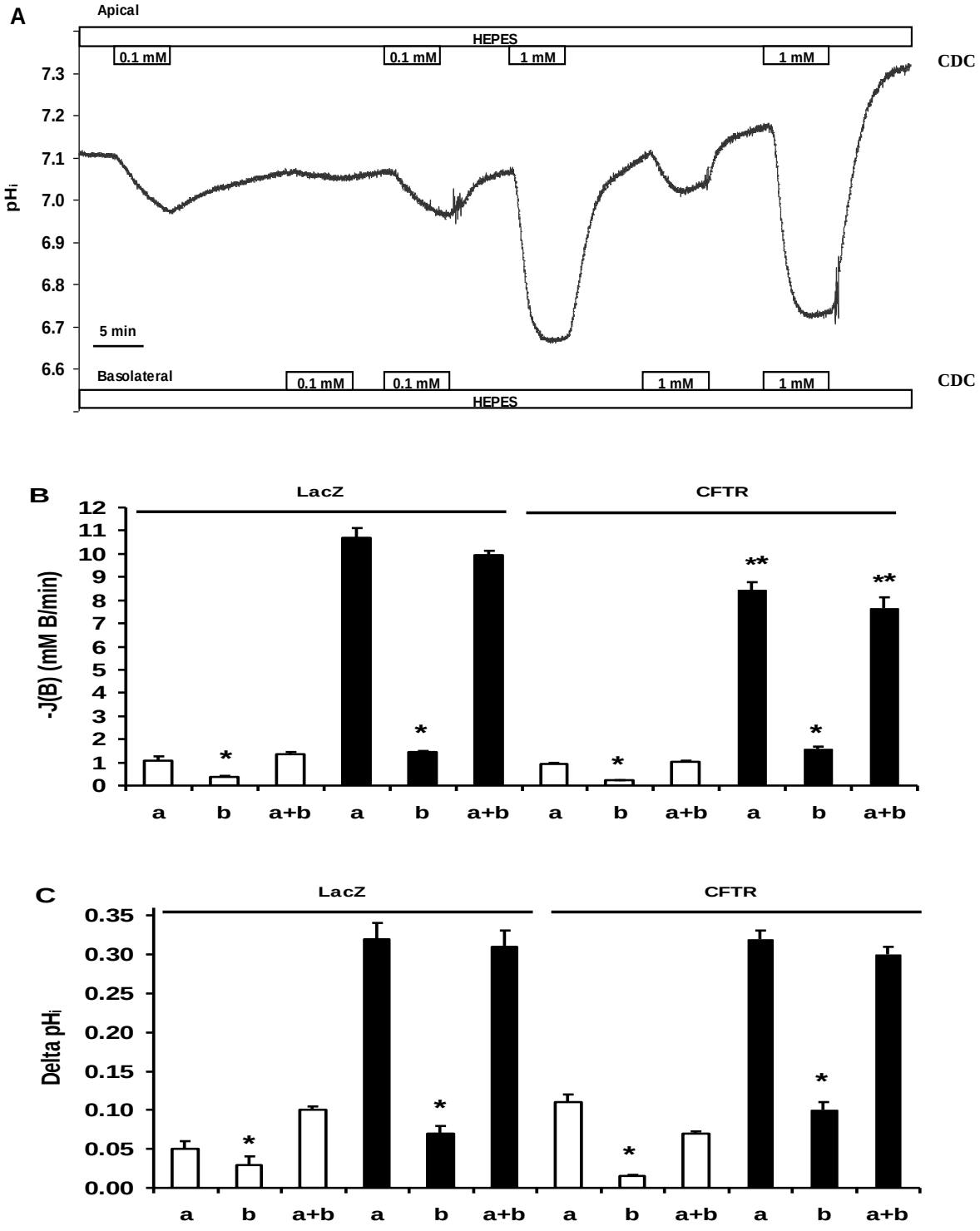

Figure 13. Differential effect of CDC on pH_i of CFPAC-1 cells. **A**: The figure shows a representative pH_i recording from SeV-CFTR transduced CFPAC-1 cells. Either 0.1 or 1 mM CDC was administered in standard HEPES solution from the apical (a) and/or the basolateral (b) membrane. **B**: Rate of intracellular acidification and C. net change in pH_i in response to 0.1 mM (open bars) or 1 mM (filled bars) CDC administration were measured in SeV-LacZ and SeV-CFTR transduced CFPAC-1 cells and depicted in the bar charts. Significant difference ($p<0.05$) *vs* * the apical administration or ** SeV-LacZ group.

3.11. Effect of CDC on intracellular Ca^{2+} concentration

Exposure of duct cells to CDC caused a dose-dependent increase in $[Ca^{2+}]_i$. Figure 14 shows that 0.1 mM CDC typically evoked a relatively slow rise in $[Ca^{2+}]_i$ to a peak value, which then declined slowly (Figs. 14B and C). In contrast, 1 mM CDC typically caused a fast rise in $[Ca^{2+}]_i$ to a peak that was followed by a maintained plateau phase (Figs. 14D and E). In accordance with our earlier findings in guinea pig ducts, apical 1 mM CDC caused a significantly larger Ca^{2+} signal when compared to the same dose applied from the basolateral membrane (compare Figs. 14D and E). Bilateral administration of CDC (at both 0.1 and 1.0 mM doses) elevated $[Ca^{2+}]_i$ to an even greater extent (Figs. 14C and E).

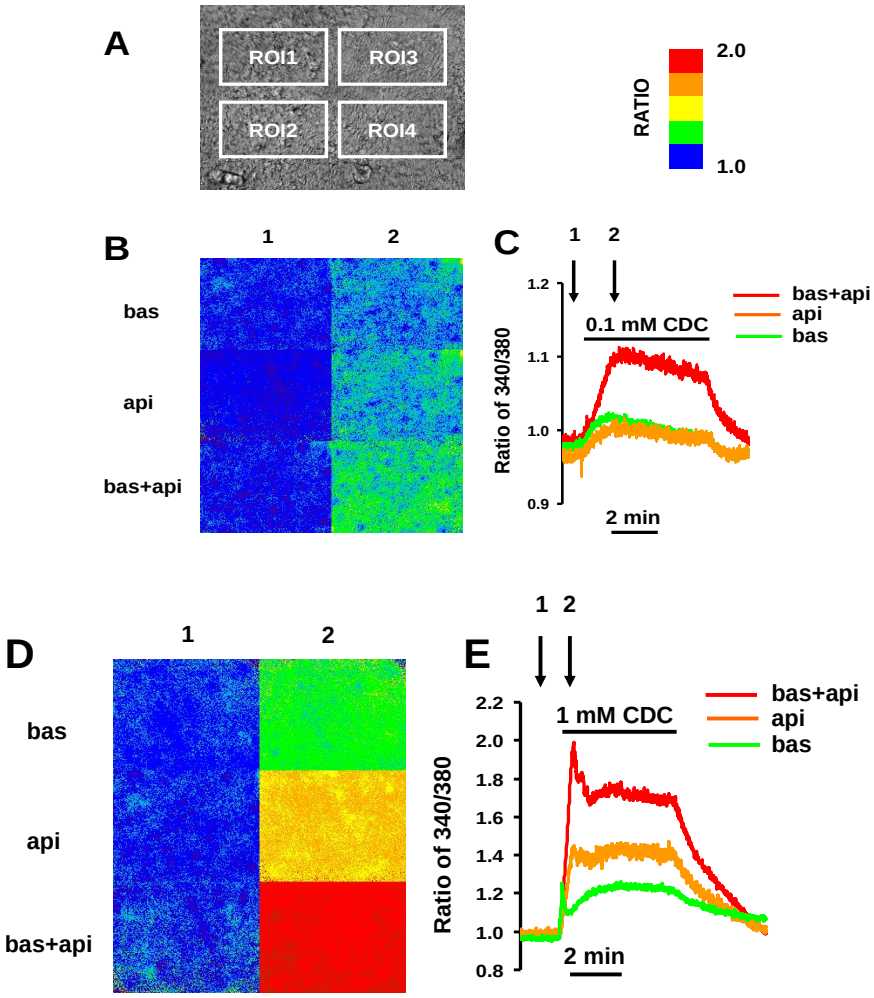

Figure 14. Effect of CDC on $[Ca^{2+}]_i$ in CFPAC-1 duct cells. CFPAC-1 cells were loaded with 5 μM FURA-2. **A.** 4-5 small areas (Regions of interests – ROIs) of 180-240 cells were excited with light at wavelengths of 340 and 380 nm, and the 340/380 fluorescence emission ratio was measured at 535 nm. The figure shows fluorescence ratio images (**B. and D.**) and representative 340/380 ratio traces (**C. and E.**) of CFPAC-1 cells perfused with 0.1 mM (**B. and C.**) or 1 mM CDC (**D. and E.**) from the basolateral (bas) and/or apical (api) side. In the fluorescent ratio images, an increase in $[Ca^{2+}]$i is denoted by a change from a ''cold'' color (blue) to a ''warmer'' color (yellow to red); see scale on top. Pictures were taken before (1) and soon after (2) exposure of CDC.

Figure 15 is a summary of the $[Ca^{2+}]_i$ data and shows that expression of wt CFTR had no effect on the $[Ca^{2+}]_i$ response to CDC administration, indicating that CFTR expression was not obligatory for CDC-induced Ca^{2+}-signaling.

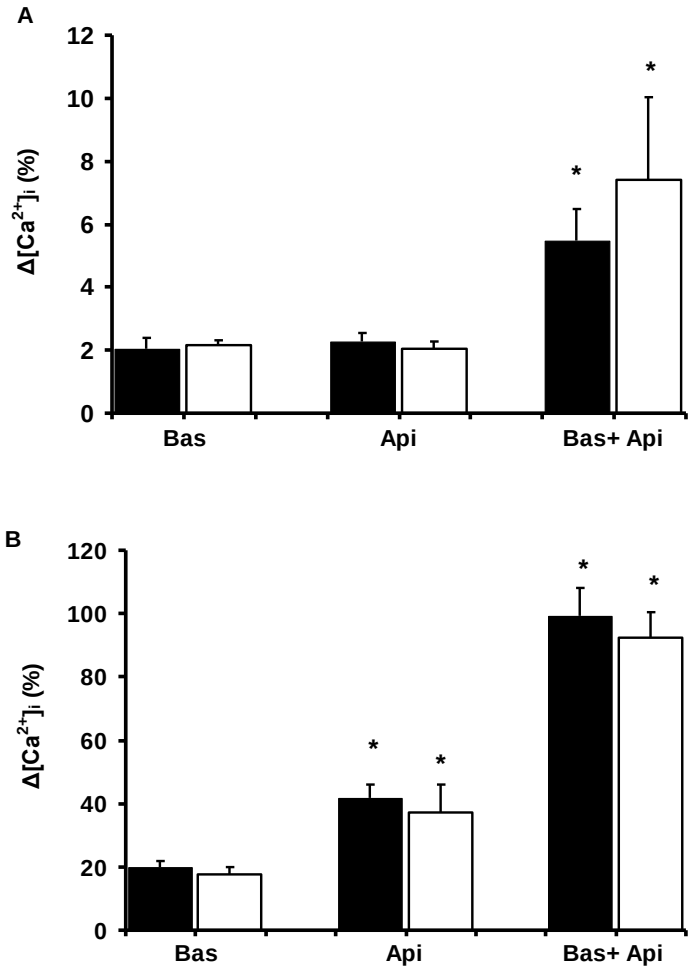

Figure 15. Summary of changes in $[Ca^{2+}]_i$ caused by CDC in SeV-LacZ and SeV-CFTR transduced CFPAC-1 cells. Addition of **A**: 0.1 mM or **B**: 1 mM CDC to SeV-LacZ (filled bars) or SeV-CFTR (open bars) transduced CFPAC-1 cells caused a significant increase in $[Ca^{2+}]_i$. 1 mM CDC caused a significantly higher Ca^{2+} signal from the apical (api) membrane vs from the basolateral (bas) membrane. Bilateral administration of CDC elevated $[Ca^{2+}]_i$ to an even greater extent. There was no significant difference in $[Ca^{2+}]_i$ in response to CDC between SeV-LacZ and SeV-CFTR transduced cells. The percent changes in F_{340}/F_{380} ratio were calculated using the 'peak' $[Ca^{2+}]_i$ responses (Fig. 3). * Significant difference ($p<0.05$) *vs* the basolateral administration.

3.12. CFTR expression is required for CDC-induced increase in apical Cl^-/HCO_3^- exchange activity

In SeV-LacZ transduced CFPAC-1 cells, removal of Cl^- from the standard HCO_3^-/CO_2 solution perfusing the apical membrane of the monolayers had no effect on pH_i, either in the absence or presence of 0.1 mM CDC (Fig. 16A). However, Cl^- removal from the

apical membrane of SeV-CFTR transduced cells (Fig. 16B) caused a clear alkalinization of pH_i (J_B, 0.61 ± 0.07 mM B/min and ΔpH_i, 0.018 ± 0.003), which was significantly increased by about three-fold (J_B 1.75 ± 0.08 mM B/min and ΔpH_i, 0.059 ± 0.006) in the presence of 0.1 mM CDC (Fig. 16C, D).

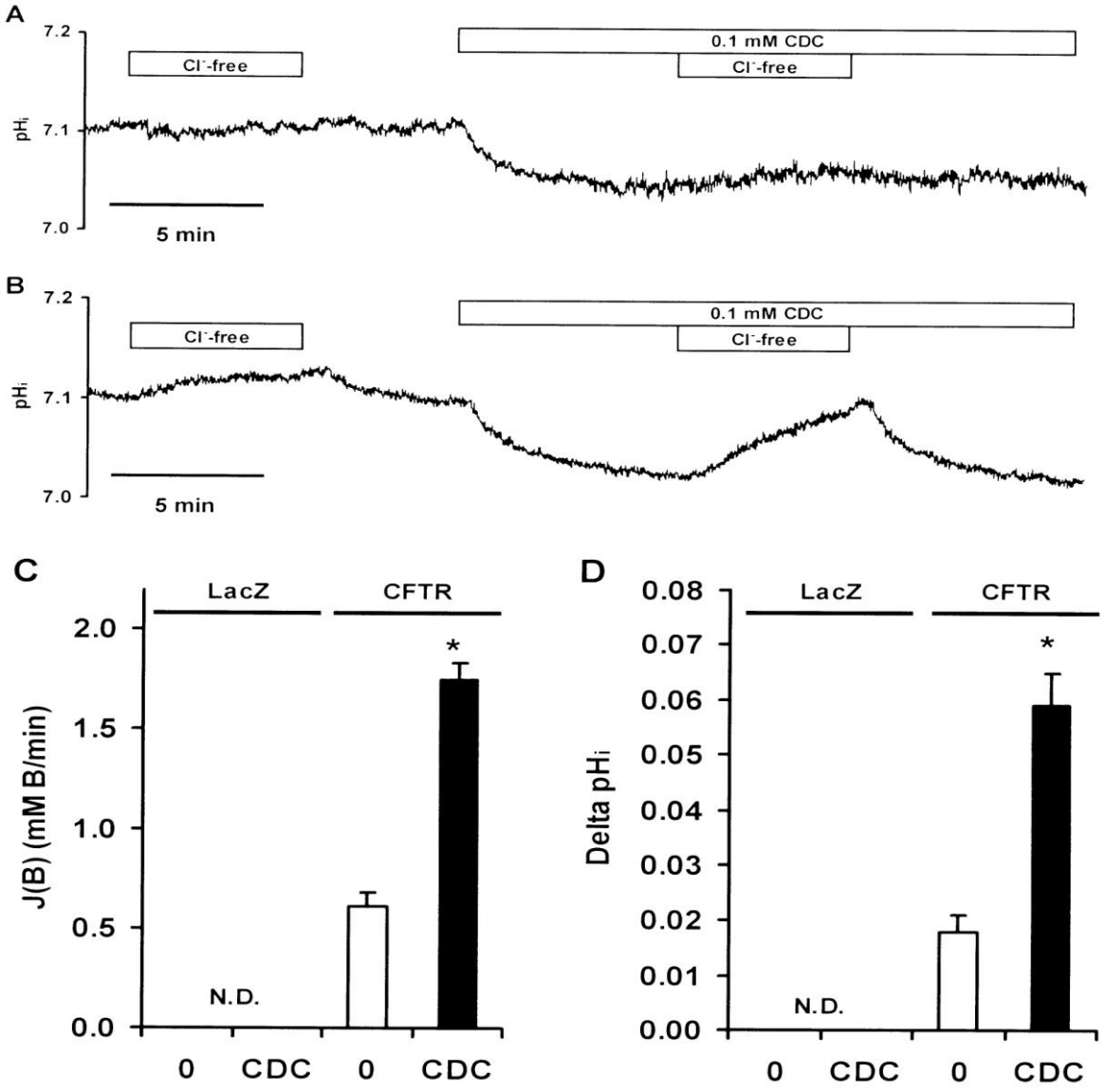

Figure 16. Effect of 0.1 mM CDC on apical Cl^-/HCO_3^- exchange activity in CFPAC-1 cells. The figure shows representative pH_i recordings of **A**: SeV-LacZ and **B**: SeV-CFTR transduced cells (n=6). Cl^-/HCO_3^- exchange activity was assessed by removing Cl^- from the apical standard HCO_3^-/CO_2 solution, first in the absence and then in the presence of 0.1 mM CDC. The bar charts show summary of **C**: base flux and **D**: ΔpH_i in the absence (0) and presence of 0.1 mM CDC. * indicates significant difference ($p<0.05$) *vs* the 0 group. N.D. = not detectable.

3.13. Chenodeoxycholate does not activate CFTR Cl^- currents

The stimulation of apical anion exchange by CDC could be due either to a direct effect on PAT-1 activity (perhaps mediated by an increase in $[Ca^{2+}]_i$) or it could be an indirect effect caused by, for example, an increase in electrodiffusive Cl^- transport through

CFTR. To directly test whether CDC could activate CFTR we performed whole cell patch clamp experiments on single guinea pig pancreatic duct cells (O'Reilly et al., 2000). Administration of 0.1 mM CDC to the bath solution had no effect on whole cell currents (Fig. 17B), whereas characteristic CFTR currents could be activated in the same cell (in 7 out of 10 cells) when it was subsequently exposed to 5 μM forskolin (Fig. 17C). A higher concentration of CDC (0.5 mM) resulted in membrane instability in the majority of cells (5 out of 8) studied.

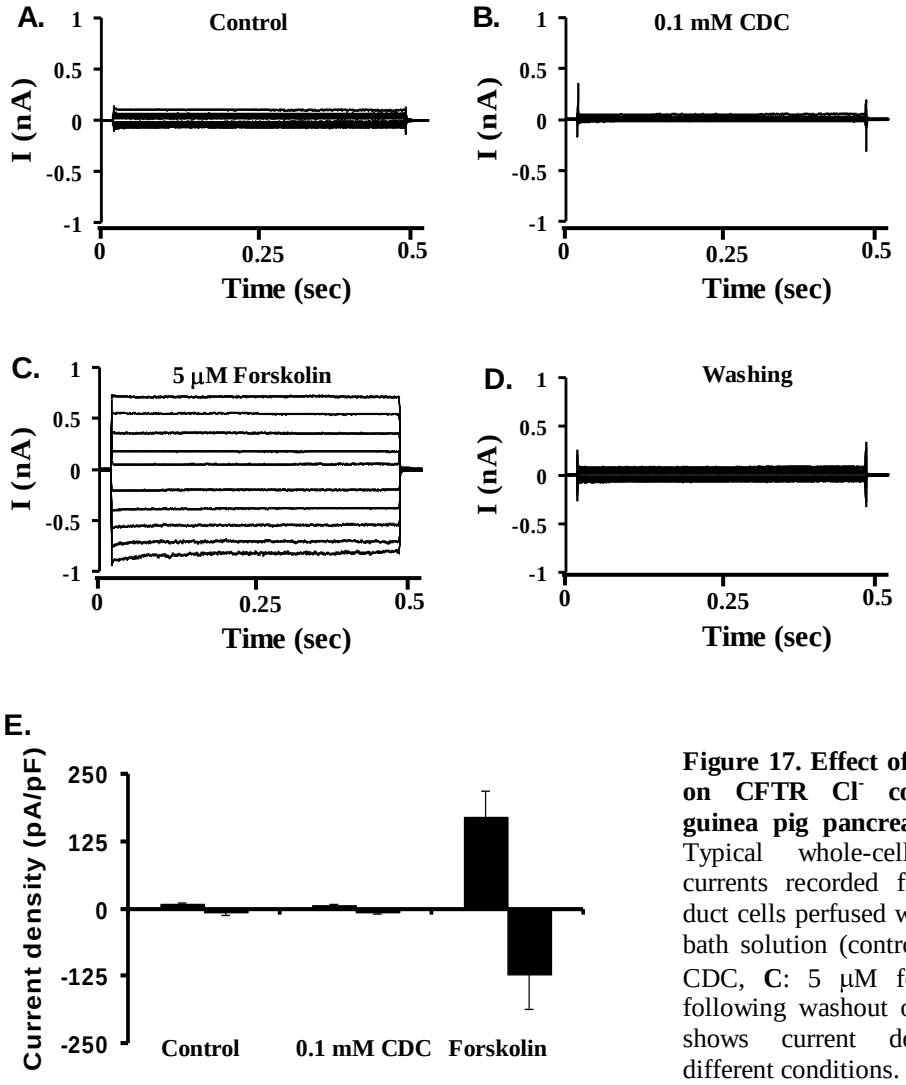

Figure 17. Effect of 0.1 mM CDC on CFTR Cl^- conductance in guinea pig pancreatic duct cells. Typical whole-cell CFTR Cl^- currents recorded from pancreatic duct cells perfused with **A**: standard bath solution (control), **B**: 0.1 mM CDC, **C**: 5 μM forskolin or **D**: following washout of forskolin. **E**: shows current densities under different conditions.

4. Discussion

In the present studies, recombinant SeV vector constructs were utilized as gene transfer agents in polarized monolayer cultures of human CFPAC-1 cells. This cell line is homozygous for the common F508del CFTR mutation, and has no measurable apical Cl^- permeability (Schoumacher et al., 1990). SeV is a single-stranded RNA virus that has been shown to produce efficient cftr gene transfer and expression in airway epithelial cells, both *in vitro* and *in vivo* (Yonemitsu et al., 2000; Tokusumi et al., 2002). CFPAC-1 cells could be efficiently infected by the SeV from the apical side. The virus attaches via both cholesterol and sialic acid receptors bound to gangliosides, present on the luminal surface of the epithelial cells.

The infection of CFPAC-1 cells with the SeV-CFTR construct was associated with an increase in wt CFTR expression and Cl^- transport as well as the induction of the activities of apical Na^+/H^+- and Cl^-/HCO_3^- exchangers, without any effect on the mRNA expression of DRA, PAT-1, NHE2 and NHE3. Basolateral Cl^-/HCO_3^- exchange and Na^+/HCO_3^- co-transport activities were significantly reduced in SeV-CFTR transduced CFPAC-1 cells. Furthermore, apical Cl^-/HCO_3^- exchange activity could be stimulated by cAMP or low doses of CDC. This increase in anion exchange activity was independent of the Cl^- conductance of CFTR.

4.1. The integrity and functional polarity of CFPAC-1 cells after the Sendai virus transduction

CFPAC-1 cells form a polarized monolayer when grown on polyester Transwells. The R_t increased steadily up to 5 days in both the untransduced and transduced cell lines, which suggests the formation of tight junctions. This was confirmed by expression of the tight junction protein, ZO-1, in all the cell lines. Transduction of CFPAC-1 cells by SeV-LacZ or SeV-CFTR vector at both low (MOI=3) and high (MOI=15) did not produce any detrimental effects on cell growth or electrical resistance, at least up to 96 hr post-infection. Our data suggest that the virus was well tolerated by the cells and that even at high virus titers the cells were still able to maintain polarity.

CFPAC-1 cells demonstrate a differential permeability to HCO_3^-/CO_2 at the apical and basolateral membranes (Rakonczay et al., 2006). The apical membrane of the duct cell must resist back-flux of HCO_3^- from the lumen as this would work against HCO_3^- secretion. Wt CFTR expression did not alter the permeability of the apical membrane to CO_2, but in

some monolayers we did observe a small increase in apical HCO_3^- influx following CFTR transduction. This suggests that HCO_3^- influx through transport proteins increases at the apical membrane when CFTR is present, as found by Ishiguro et al. (2000) using isolated guinea pig ducts.

4.2. The hyperexpression of CFTR in CFPAC-1 cells

Mature CFTR protein was only expressed in SeV-CFTR transduced cells. High-levels of CFTR expression has been shown to be associated with biosynthetic and growth abnormalities (Schiavi et al., 1996), so there must be a fine line between the beneficial and toxic effects of CFTR. However, we wanted to make sure that this CFTR was correctly localized to the apical membrane, as CFTR overexpression has previously been shown to result in mislocalisation of the protein (Farmen et al., 2005). Therefore, we also used immunocytochemistry to clearly demonstrate apical localization of CFTR in SeV-CFTR (MOI=3) transduced CFPAC-1 cells. At MOI=3 about 30% of the CFPAC-1 cells express CFTR. However, this relatively low rate of CFTR transduction is sufficient to upregulate apical Cl^-/HCO_3^- exchange activity in the human duct cells.

Hyperexpression of CFTR can alter the molecular physiology of the protein (Mohammad-Panah et al., 1998) and in some cases we observed significant differences in HCO_3^- transport between the MOI = 3 and 15 SeV-CFTR infected cells. For example, basolateral uptake of HCO_3^- was only affected (reduced) in the MOI = 15 SeV-CFTR infected cells and not in the MOI = 3 cells. Furthermore, although resting apical Cl^-/HCO_3^- exchange activity was upregulated in both the MOI = 3 and MOI = 15 SeV-CFTR transduced cells, only the MOI = 3 group responded to cAMP stimulation. Since the key regulatory pathway determining CFTR activity involves elevation of cAMP and activation of PKA, we measured the amount of the 42 kDa PKAcat and PKA activity in CFPAC-1 cells. The amount of PKAcat was similar in uninfected and infected cells, however, PKA activity was reduced in the SeV-CFTR MOI = 15 group providing an explanation as to why the apical exchangers cannot be stimulated with cAMP. The reason for this decrease in PKA activity in the MOI = 15 group remains unclear. However, Mohammad-Panah et al. (1998) showed that hyperexpression of wt CFTR in CFPAC-1 cells caused the appearance of a time-independent, non-rectifying Cl^- current that was insensitive to cAMP stimulation, suggesting that the CFTR channels were permanently activated and not susceptible to cAMP regulation.

4.3. Effect of CFTR expression on Cl^-/HCO_3^- exchange activity in pancreatic cells

Basolateral Cl^-/HCO_3^- exchange activity (most likely mediated by AE2 in CFPAC-1 cells was significantly reduced after the CFTR transduction at high MOIs, and was not influenced by cAMP stimulation. Similarly, Greeley et al. (2001) showed that Cl^-/HCO_3^- exchange (as measured by $^{36}Cl^-$ influx) was decreased by about 33% in corrected CFPAC-1 cells. However, in contrast to these data, basolateral anion exchange activity was not significantly different in main pancreatic ducts isolated from wt versus CF mice (Lee et al., 1999b). These differences between cultured human cells and native murine tissue maybe related to the expression levels of CFTR, which are low in native mouse tissue (Gray et al., 2002). Exactly how CFTR expression inhibits basolateral anion exchange is not clear at the moment, but our real time PCR data indicates that it is not via a reduction in AE2 mRNA levels. One possibility is that an increased Cl^- conductance of the plasma membrane following CFTR expression causes intracellular Cl^- concentration to fall. Thus, when extracellular Cl^- was withdrawn, a reduced outward Cl^- gradient would be available to drive HCO_3^- into the cell.

In contrast to the basolateral membrane, non-infected CFPAC-1 cells as well as LacZ transduced cells displayed no apical Cl^-/HCO_3^- exchange activity under any conditions. Our results clearly show that CFTR expression is associated with the appearance of an apical Cl^-/HCO_3^- exchange activity that can be further enhanced by cAMP stimulation. These results are consistent with Greeley et al. (2001), who reported that total Cl^-/HCO_3^- exchange activity was elevated in non-polarized, stably corrected, CFPAC-1 cells grown on glass coverslips. Similar to our results, this effect was accompanied by enhanced apical Cl^-/HCO_3^- exchanger activity as judged by $^{36}Cl^-$ uptake in polarized monolayers. However, Greeley et al. (2001) found that DRA mRNA was present in the corrected, but not in the non-corrected CFPAC-1 cells, and that PAT-1 expression was enhanced fivefold in the corrected cells, which we did not observe. CFTR has also been shown to activate DRA and PAT-1 in heterologous expression systems (Chernova et al., 2003; Ko et al., 2002, 2004). Lee et al. (1999b) also found that the apical Cl^-/HCO_3^- exchange activity was increased in perfused pancreatic ducts from wt versus CFTR-knockout mice, and that forskolin markedly elevated luminal Cl^-/HCO_3^- exchange activity.

To determine the identity of the apical anion exchanger(s) responsible for the cAMP stimulated Cl^-/HCO_3^- exchange activity, we examined the effect of a high concentration of the disulfonic stilbene H_2-DIDS (500 μM). This compound completely blocked stimulated Cl^-/HCO_3^- exchange. Since the disulfonic stilbene does not inhibit

CFTR from the extracellular side (Akabas, 2000; Chernova et al., 2003; Gray et al., 1993; Melvin et al., 1999) reported that DRA has a low sensitivity to DIDS when Cl^-/HCO_3^- exchange was measured (although Cl^-/SO_4^{2-} exchange by DRA seems to be DIDS-sensitive (Moseley et al., 1999; Silberg et al., 1995), then neither of these transporters are likely to be involved. There is, however, general agreement that PAT-1 is sensitive to block by DIDS (Alvarez et al., 2005; Lohi et al., 2003; Petrovic et al., 2003; Wang et al., 2002). There is no evidence that SLC26 anion exchangers can be activated directly by cAMP. However, activation of SLC26 anion exchangers by phosphorylated CFTR is well described (Shcheynikov et al., 2006), and this is clearly preserved in our CFPAC-1 cells transduced with SeV-CFTR at MOI = 3. Taken together with our semiquantitative and real time RT-PCR data point to PAT-1 as the SLC26 family member expressed on the apical surface of SeV-CFTR infected CFPAC-1 cells. Furthermore, cAMP stimulated apical Cl^-/HCO_3^- exchange activity in SeV-CFTR CFPAC-1 cells was not influenced by alteration of the membrane potential by variation of extracellular K^+ concentration. The electrogenicity of SLC26 transporters is still a matter of debate (Alper et al., 2006; Ko et al., 2002; Mount & Romero, 2004). Our results seem to be in accord with Alper et al. (2006) who have shown that human PAT-1 mediates electroneutral Cl^-/HCO_3^- exchange.

In order to test whether the Cl^- conductance of CFTR was necessary for cAMP-dependent activation of apical Cl^-/HCO_3^- exchange in SeV-CFTR (MOI = 3) CFPAC-1 cells, we tested the effect of $CFTR_{inh}$-172. This compound completely inhibited CFTR as assessed by the iodide efflux assay, but it had no effect on Cl^-/HCO_3^- exchange in SeV-CFTR transduced cells. Thus, it would appear that there is no strong coupling between CFTR ion transport and anion exchange activity, a conclusion consistent with results in native mouse pancreatic duct (Lee et al., 1999a). However, Simpson et al. (2005), using a different (non-specific) CFTR inhibitor, glybenclamide, showed that this compound did to reduce resting Cl^-/HCO_3^- exchange in mouse intestine. How CFTR expression leads to an upregulation of apical anion exchange activity is still not fully understood, but recent work has shown that SLC26A3, A4, and A6 physically and functionally interact with CFTR (Shcheynikov et al., 2006). Furthermore, phosphorylation of CFTR on its R domain stimulates anion exchange activity which appears to be preserved in our CFTR-transduced cells. Interestingly, CFTR activity appears to be enhanced in pancreatic ducts from SLC26A6 knockout mice (Wang et al., 2006), suggesting that the exchanger tonically inhibits CFTR. Lack of SLC26A6 led to enhanced spontaneous, but reduced cAMP-stimulated fluid secretion, illustrating the important role the exchanger plays in both basal

and stimulated pancreatic HCO_3^- secretion. However, in another SLC26A6 knockout mouse model no differences were observed in fluid or HCO_3^- secretion between wt and knockout animals, a finding explained by a compensatory upregulation in SLC26A3 activity in the knockout animals (Ishiguro et al., 2007).

4.4. Apical Na^+/H^+ exchange

CFTR expression resulted in a marked upregulation of apical NHE activity in CFPAC-1 cells. Although it is possible that this effect could be due to apical bath Na^+ accessing basolateral NHE1 (given the low paracellular resistance of the CFPAC-1 monolayers), Ahn et al. (2001) observed similar results and found an increased luminal Na^+-dependent pH_i recovery from an acid load in microperfused pancreatic ducts from isolated wt versus F508del mice. This effect probably resulted from reduced levels of NHE3 expression in the knockout animals (Ahn et al., 2001). However, we must note that we could not detect NHE2 or NHE3 expression by RT-PCR in our CFPAC-1 cells. In contrast to our data, stimulation of the wt mouse ducts with forskolin dose-dependently inhibited luminal Na^+-dependent pH_i recovery. Our failure to detect an inhibitory effect of forskolin on apical NHE in the MOI = 15 SeV-CFTR group was not surprising since these cells had no detectable PKA activity. However, the MOI = 3 group, which did exhibit PKA activity, behaved similarly. It is possible that human pancreatic duct cells either express a different, cAMP-insensitive, NHE isoform in their apical membrane or that apical NHE is regulated by another mechanism in human cells, for example, by an interaction with Cl^-/HCO_3^- exchangers (Lamprecht et al., 2002).

4.5. Effect of chenodeoxycholate on CFPAC-1 cells

In this study we investigated the effect of CDC on the pH_i and $[Ca^{2+}]_i$ of CFPAC-1 pancreatic duct cells. We also wanted to address the specific issue as to whether CFTR was involved in the bile-acid induced increase in HCO_3^- secretion that we have previously reported in guinea pig ducts (Venglovecz et al., 2008). To do this we have studied apical Cl^-/HCO_3^- exchange activity in CFPAC-1 cells either lacking or expressing CFTR.

It has been demonstrated that bile acids induce Ca^{2+} signals in both pancreatic acinar cells and in guinea pig ductal cells (Fischer et al., 2007; Gerasimenko et al., 2006; Venglovecz et al., 2008 Voronina et al., 2002). We have shown that CDC also causes a dose-dependent increase in $[Ca^{2+}]_i$ in human pancreatic duct cells. In accordance with our earlier findings on guinea pig ducts, apical application of CDC to CFPAC-1 cells resulted

in a greater elevation of $[Ca^{2+}]_i$ compared to basolateral application. These bile acid-induced Ca^{2+} signals were not dependent on the expression of CFTR. In contrast to our findings, in cholangiocytes, ursodeoxycholic acid only initiated Ca^{2+} signaling in cells expressing CFTR (Fiorotto et al., 2007).

Unconjugated bile salts, such as CDC, are weak acids and can therefore pass through cell membranes either by passive diffusion or via bile acid transporters (Trauner & Boyer, 2003.). Basolateral or luminal administration of CDC dose-dependently decreased the pH_i of the CFPAC-1 cells. Similarly, it has been reported that 0.5 – 1.5 mM ursodeoxycholate also caused a dose-dependent, rapid, intracellular acidification in bile duct epithelial cells (Alvaro et al., 1993). As for $[Ca^{2+}]_i$, the effect of CDC on the pH_i of CFPAC-1 cells was greater when the bile acid was given from the apical side. Differential effects of bile acids have also been reported in dog pancreatic duct cells (Okolo et al., 2002). However, in the dog cells, the basolateral membrane was much more sensitive to bile acid-induced damage compared to the luminal membrane (Okolo et al., 2002). Interestingly, in our experiments the CDC-induced acidosis was somewhat higher in CFTR-deficient pancreatic duct cells. This may be due to increased active uptake (via bile-acid transporters) of CDC in CF cells, but further experiments are required to resolve this issue. Note that the absorption of taurocholate has been reported to be either reduced (Hardcastle et al., 2004) or increased (Stelzner et al., 2001) in the ileum of transgenic CF mice with the F508del mutation. CDC stimulation (0.1 mM) of Cl^-/HCO_3^- exchange activity was only observed in cells expressing CFTR, strongly suggesting that the presence of CFTR is necessary for this effect. In similarity to our findings, Fiorotto et al. (2007) reported that 0.1 mM ursodeoxycholate significantly elevated fluid secretion from intrahepatic mouse bile duct units in normal, but not in CFTR-defective mice.

We also wanted to investigate whether the CDC-induced increase in apical Cl^-/HCO_3^- exchange activity was linked to enhanced Cl^- transport by CFTR. Using whole cell current recording we found that 0.1 mM CDC did not activate CFTR and, therefore, conclude that stimulation of CFTR does not underlie the effect of CDC of the anion exchanger. Our data contrast with the results of Bijvelds et al. (2005) who found that luminal administration of 0.5 mM taurocholate did stimulate CFTR-dependent electrogenic Cl^- transport in the murine ileum. These contrasting results may be due to differences in species, tissue, and the type and concentration of bile acids used. However, our results suggest that the increase in anion exchange activity evoked by CDC either reflects a direct effect of the bile acid on the apical exchanger (most likely PAT-1) or involves some other,

indirect mechanism. The fact that the CDC-induced increase in anion exchange activity observed in guinea pig pancreatic ducts was entirely dependent on a rise in $[Ca^{2+}]_i$ (Venglovecz et al., 2008) implies that bile acids do not directly modulate SLC26 transporter activity. If (in contrast to our results) PAT-1 is indeed electrogenic and transports $2HCO_3^-$:$1Cl^-$ (Ko et al., 2002), an alternate scenario would involve a CDC-dependent opening of Ca^{2+}-dependent K^+ channels via Ca^{2+} release from internal stores. The increase in K^+ conductance would hyperpolarize the membrane potential and thereby stimulate electrogenic HCO_3^- secretion via PAT-1.

4.6. Conclusions

We conclude that SeV is an effective CFTR gene transfer vector for human pancreatic duct cells. As SeV-mediated CFTR gene transfer is much more effective via the apical as compared to the basolateral membrane, efficient gene transfer into the pancreas *in vivo* would probably require retrograde injection of the vector into the pancreatic duct. Moreover, as 62% of CF patients are born with a non-functional pancreas (Waters et al., 1990), gene therapy would need to be initiated *in utero* in the majority of cases. Thus, the smaller group of patients who are pancreatic sufficient at birth, but who become pancreatic insufficient in later life, might be best helped by gene therapy.

Importantly, CFTR transduced CF duct cells maintain their normal epithelial polarity and evidence restoration of Cl^- and HCO_3^- transport processes at the apical membrane. The CFTR Cl^- channel regulates the activities of SLC26 and SLC4 (previously AE) families of anion transporters and NHEs without affecting their mRNA expression. We have demonstrated that apical anion exchange in the duct cell is mediated by SCL26A6. The activity of SLC26A6 is upregulated by cAMP stimulation, whereas the activities of SLC4A2 and apical NHE transporters are not influenced by stimulated secretion.

The administration of CDC to pancreatic duct cells caused dose-dependent decrease in pH_i and increase in $[Ca^{2+}]_i$. Small doses of CDC stimulated apical Cl^-/HCO_3^- exchange activity independently of CFTR transport of Cl^-. We speculate that CDC-induced HCO_3^- secretion would flush toxic bile salts out of the ductal tree and may serve as a defense mechanism against acute biliary pancreatitis.

Taken together, this work lead to an improved understanding of the regulation of acid/base transporters in the diseased (CF) and corrected (with wt CFTR) pancreatic ductal epithelium.

5. ACKNOWLEDGEMENTS

I would like to thank the people who have helped and inspired me during my doctoral studies.

I am grateful to **Prof. János Lonovics** and **Prof. Tibor Wittmann**, past and present head of the First Department of Medicine, who gave me the opportunity to work in the department.

My warm thanks are due to **Prof. Tamás Takács** who provided the opportunity to work in his laboratory. I am indeed grateful for his valuable advice and help.

I wolud like express my deep and sincere gratitude to my supervisors **Dr. Zoltán Rakonczay Jr.** and **Dr. Péter Hegyi.** Their wide knowledge and their logical way of thinking have been of great value for me. Their understanding and encouragement provided a good basis for the present thesis.

I wish to thank **Prof. Barry E. Argent** and **Dr. Mike A. Gray,** our collaborators from the University of Newcastle, UK for their extensive discussions of my work and interesting explorations.

I would also like to thank my colleagues and friends, **Petra Pallagi, Viktória Venglovecz, Klaudia Farkas, Andrea Schnúr, Béla Ózsvári, József Maléth, Mátyás Czepán,** and **György Biczó** for all the emontional support, enterainment and care they provided.

This work would not have been possible to accomplish without the assistance of **Zoltánné Fuksz, Edit Magyarné Pálfi, Ágnes Sitkei, Miklósné Árva.**

I'm grateful to **Prof. András Varró,** the head of Department of Pharmacology and Pharmacotherapy, who provided us the opportunity to work in his department.

I would also like to thank my **co-authors** for their help. **DNAVEC Corporation** supplied the SeV constructsOur research was supported by grants from **OTKA, MTA and NKTH**.

My deepest gratitude goes to **my family** for their unflagging love and support throughout my life; this dissertation wolud have been impossible to accomplish without their help. I dedicate this thesis to them.

6. REFERENCES

Ahn W, Kim KH, Lee JA, et al. 2001. Regulatory interaction between the cystic fibrosis transmembrane conductance regulator and HCO_3^- salvage mechanisms in model systems and the mouse pancreatic duct. J Biol Chem 276: 17236-17243.

Akabas MH. 2000. Cystic fibrosis transmembrane conductance regulator. Structure and function of an epithelial chloride channel. J Biol Chem 275: 3729-3732.

Alper SL, Stewart AK, Chernova MN, et al. 2006. Anion exchangers in flux: Functional differences between human and mouse SLC26A6 polypeptides. Novartis Found Symp 273: 107-119.

Alvarez BV, Vilas GL, Casey JR. 2005. Metabolon disruption: A mechanism that regulates bicarbonate transport. EMBO J 24: 2499-2511.

Alvaro D, Mennone A, Boyer JL. 1993. Effect of ursodeoxcholic acid on intracellular pH regulation in isolated rat bile duct epithelial cells. Am J Physiol Gastrointest Liver Physiol. 28: G783-791.

Argent BE, Gray MA, Steward MC, et al. 2006. Cell physiology of pancreatic ducts. In: Johnson LR, editor. Physiology of the Gastrointestinal Tract 4th edition San Diego: Elsevier. pp. 1371-1396.

Bijvelds MJ, Jorna H, Verkade HJ, et al. 2005. Activation of CFTR by ASBT-mediated bile salt absorption. Am J Physiol Gastrointest Liver Physiol. 289: G870-879.

Chang XB, Tabcharani JA, Hou YX, et al. 1993. Protein kinase A (PKA) still activates CFTR chloride channel after mutagenesis of all 10 PKA consensus phosphorylation sites. J Biol Chem 268: 11304-11311.

Cheng SH, Gregory RJ, Marshall J et al. 1990. Defective intracellular transport and processing of CFTR is the molecular basis of most cystic fibrosis. Cell 65: 827-834.

Chernova MN, Jiang L, Shmukler BE, et al. 2003. Acute regulation of the SLC26A3 congenital chloride diarrhoea anion exchanger (DRA) expressed in Xenopus oocytes. J Physiol 549: 3-19.

Cheung CY, Wang XF, Chan HC. 1998. Stimulation of HCO_3^- secretion across cystic fibrosis pancreatic duct cells by extracellular ATP. Biol Signals Recept 17: 321-327.

Choi JY, Muallem D, Kiselyov K, et al. 2001. Aberrant CFTR-dependent HCO_3^- transport in mutations associated with cystic fibrosis. Nature 410: 94-97.

Criddle DN, Gerasimenko JV, Baumgartner HK, et al. 2007. Calcium signalling and pancreatic cell death: apoptosis or necrosis? Cell Death Differ 14: 1285-1294.

Dehaye JP, Nagy Á, Premkumar A, et al. 2003. Identification of a functionally important conformation-sensitive region of the secretory Na+-K+-2Cl- cotransporter (NKCC1). J Biol Chem 278: 11811-7.

Demeter I, Hegyesi O, Nagy ÁK, et al. 2009. Bicarbonate transport by the human pancreatic ductal cell line HPAF. Pancreas. 38: 913-20.

Farinha CM, Mendes F, Roxo-Rosa M, et al. 2004. A comparison of 14 antibodies for the biochemical detection of the cystic fibrosis transmembrane conductance regulator protein. Mol Cell Probes 18: 235-242.

Farinha CM, Penque D, Roxo-Rosa M, et al. 2004. Biochemical methods to assess CFTR expression and membrane localization. J Cyst Fibros 3: 73-77.

Farmen SL, Karp PH, Ng P, et al. 2005. Gene transfer of CFTR to airway epithelia: low levels of expression are sufficient to correct Cl^- transport and overexpression can generate basolateral CFTR. Am J Physiol Lung Cell Mol Physiol. 289: L1123-1130.

Ferrari S, Griesenbach U, Iida A, et al. 2007. Sendai virus-mediated CFTR gene transfer to the airway epithelium. Gene Ther 14: 1371-9.

Fiorotto R, Spirlì C, Fabris L, et al. 2007. Ursodeoxycholic acid stimulates cholangiocyte fluid secretion in mice via CFTR-dependent ATP secretion. Gastroenterology. 133: 1603-1613.

Fischer L, Gukovskaya AS, Penninger JM, et al. 2007. Phosphatidylinositol 3-kinase facilitates bile acid-induced Ca2+ responses in pancreatic acinar cells. Am J Physiol Gastrointest Liver Physiol. 292: G875-G886.

Fuerst TR, Niles EG, Studier FW, Moss B. 1986. Eukaryotic transient-expression system based on recombinant vaccinia virus that synthesizes bacteriophage T7 RNA polymerase. Proc Natl Acad Sci USA 83: 8122-8126.

Gerasimenko JV, Flowerdew SE, Voronina SG, et al. 2006. Bile acids induce Ca2+ release from both the endoplasmic reticulum and acidic intracellular calcium stores through activation of inositol trisphosphate receptors and ryanodine receptors. J Biol Chem. 281:40154-40163.

Gray MA, Pollard CE, Harris A, et al. 1990. Anion selectivity and block of the small-conductance chloride channel on pancreatic duct cells. Am J Physiol 259: C752-C761.

Gray MA, Plant S, Argent BE. 1993. cAMP-regulated whole cell chloride currents in pancreatic duct cells. Am J Physiol 264: C591-C602.

Gray MA, Winpenny JP, Porteous DJ, et al. 1994. CFTR and calcium-activated chloride currents in pancreatic ducts of a transgenic CF mouse. Am J Physiol. 266: C213–C221.

Gray MA, Winpenny JP, Verdon B, et al. 2002. Properties and role of calcium-activated chloride channels in pancreatic duct cells. In: Fuller CM , editor. Current topics in Membranes,Vol. 53. Calcium-activated chloride channels. San Diego: Academic Press. pp. 231-256.

Greeley T, Shumaker H, Wang Z, et al. 2001. Downregulated in adenoma and putative anion transporter are regulated by CFTR in cultured pancreatic duct cells. Am J Physiol 281: G1301-G1308.

Hardcastle J, Harwood MD, Taylor CJ. 2004. Absorption of taurocholic acid by the ileum of normal and transgenic DeltaF508 cystic fibrosis mice. J Pharm Pharmacol. 56: 445-552.

Harlow E, Lane D. 1988. Antibodies: A Laboratory Manual. Cold Spring Harbor: Cold Spring Harbor Laboratory Press.

Hegyi P, Gray MA, Argent BE. 2003. Substance P inhibits bicarbonate secretion from guinea pig pancreatic ducts by modulating an anion exchanger. Am J Physiol Cell Physiol 285: C268-76.

Hegyi P, Ördög B, Rakonczay Z Jr, et al. 2005. The effect of herpesvirus infection on pancreatic duct cell secretion. World J Gastroenterol 38: 5997-6002.

Hegyi P, Rakonczay Z, Jr, Gray MA, et al. 2004. Measurement of intracellular pH in pancreatic duct cells: A new method for calibrating the fluorescence data. Pancreas 28: 427-434.

Hegyi P, Rakonczay Z Jr. 2007. The inhibitory pathways of pancreatic ductal bicarbonate secretion. Int J Biochem Cell Biol 39: 25-30.

Hegyi P, Rakonczay Z Jr, Farkas K, et al. 2008. Controversies in the role of SLC26 anion exchangers in pancreatic ductal bicarbonate secretion. Pancreas 37:232-4.

Hegyi P, Rakonczay Z Jr, Tiszlavicz L, et al. 2005. Protein kinase C mediates the inhibitory effect of substance P on HCO_3^- secretion from guinea pig pancreatic ducts. Am J Physiol Cell Physiol 288:C1030-41.

Hughes L, Li KH, Sheppard DN, et al. 2004. Use of an iodide-selective electrode to measure CFTR Cl^- channel activity.
http://central.igc.gulbenkian.pt/cftr/hughes_iodid_selective_electrode_measure_cftr_cl_activity.pdf

Ishiguro H, Naruse S, Kitagawa M, et al. 2000. CO_2 permeability and bicarbonate transport in microperfused interlobular ducts isolated from the guinea-pig pancreas. J Physiol 528: 305-315.

Ishiguro H, Namkung W, Yamamoto A, et al. 2007. Effect of Slc26a6 deletion on apical Cl^-/HCO_3^- exchanger activity and cAMP-stimulated bicarbonate secretion in pancreatic duct. Am J Physiol 292: G447-G455.

Kato A, Sakai Y, Shioda T, et al. 1996. Initiation of Sendai virus multiplication from transfected cDNA or RNA with negative or positive sense. Genes Cells 1: 569-579.

Ko SB, Shcheynikov N, Choi JY, et al. 2002. A molecular mechanism for aberrant CFTR-dependent HCO_3^- transport in cystic fibrosis. EMBO J 21: 5662-5672.

Ko SB, Zeng W, Dorwart MR, et al. 2004. Gating of CFTR by the STAS domain of SLC26 transporters. Nat Cell Biol 6: 343-350.

Lamprecht G, Heil A, Baisch S, et al. 2002. The down regulated in adenoma (dra) gene product binds to the second PDZ domain of the NHE3 kinase A regulatory protein (E3KARP), potentially linking intestinal Cl^-/HCO_3^- exchange to Na^+/H^+ exchange. Biochemistry 41: 12336-12342.

Lee MG, Choi JY, Luo X, et al. 1999a. Cystic fibrosis transmembrane conductance regulator regulates luminal Cl^-/HCO_3^- exchange in mouse submandibular and pancreatic ducts. J Biol Chem 274: 14670-14677.

Lee MG, Wigley WC, Zeng W, et al. 1999b. Regulation of Cl^-/HCO_3^- exchange by cystic fibrosis transmembrane conductance regulator expressed in NIH 3T3 and HEK 293 cells. J Biol Chem 274: 3414-3421.

Lee MG, Ahn W, Choi JY, et al. 2000. Na^+-dependent transporters mediate HCO_3^- salvage across the luminal membrane of the main pancreatic duct. J Clin Invest 105: 1651-1658.

Lee MG, Muallem S. 2008. Pancreatitis: the neglected duct. Gut 57: 1037-1039.

Linsdell P, Tabcharani JA, Rommens JM, et al. 1997. Permeability of wild-type and mutant cystic fibrosis transmembrane conductance regulator chloride channels to polyatomic anions. J Gen Physiol 110: 355-364.

Livak KJ, Schmittgen TD. 2001. Analysis of relative gene expression data using real-time quantitative PCR and the 2(-Delta Delta C(T)). Methods 25: 402-408.

Lohi H, Lamprecht G, Markovich D, et al. 2003. Isoforms of SLC26A6 mediate anion transport and have functional PDZ interaction domains. Am J Physiol 284: C769-C779.

Ma T, Thiagarajah JR, Yang H, et al. 2002. Thiazolidinone CFTR inhibitor identified by high-throughput screening blocks cholera toxin-induced intestinal fluid secretion. J Clin Invest 110: 1651-1658.

Maléth J, Venglovecz V, Rázga Z, et al. 2009. The non-conjugated chenodeoxycholate induces severe mitochondrial damage and inhibits bicarbonate transport mechanisms in pancreatic duct cells. Gut (accepted)

Marteau C, Silviani V, Ducroc R, et al. 1995. Evidence for apical Na^+/H^+ exchanger in bovine main pancreatic duct. Dig Dis Sci 40: 2336-2340.

Melvin JE, Park K, Richardson L, et al. 1999. Mouse down-regulated in adenoma (DRA) is an intestinal Cl^-/HCO_3^- exchanger and is up-regulated in colon of mice lacking the NHE3 Na^+/H^+ exchanger. J Biol Chem 274: 22855-22861.

Mohammad-Panah R, Demolombe S, Riochet D, et al. 1998. Hyperexpression of recombinant CFTR in heterologous cells alters its physiological properties. Am J Physiol 274: C310-C318.

Moseley RH, Hoglund P, Wu GD, et al. 1999. Downregulated in adenoma gene encodes a chloride transporter defective in congenital chloride diarrhea. Am J Physiol 276: G185-G192.

Mount DB, Romero MF. 2004. The SLC26 gene family of multifunctional anion exchangers. Pflugers Arch 447: 710-721.

Muimo R, Hornickova Z, Riemen CE, et al. 2000. Histidine phosphorylation of annexin I in airway epithelia. J Biol Chem 275: 36632-36636.

Nagy Á, Turner RJ. 2007. The membrane integration of a naturally occurring alpha-helical hairpin. Biochem Biophys Res Commun 356: 392-7.

Namkung W, Lee JA, Ahn W, et al. 2003. Ca^{2+} activates cystic fibrosis transmembrane conductance regulator- and Cl^--dependent HCO_3^- transport in pancreatic duct cells. J Biol Chem 278:200-207.

Okolo C, Wong T, Moody MW, et al. 2002. Effect of bile acids on dog pancreatic duct epithelial cell secretion and monolayer resistance. Am J Physiol Gastrointest Liver Physiol.283: G1042-1050.

O'Reilly CM, Winpenny JP, Argent BE, et al. 2000. Cystic fibrosis transmembrane conductance regulator currents in guinea pig pancreatic duct cells: inhibition by bicarbonate ions. Gastroenterology 118 :1187-1196.

Pandol SJ, Saluja AK, Imrie CW, et al. 2007. Acute pancreatitis: bench to the bedside. Gastroenterology 132: 1127-1151.

Park M, Ko SB, Choi JY, Muallem G, et al. 2002. The cystic fibrosis transmembrane conductance regulator interacts with and regulates the activity of HCO_3^- salvage transporter human Na^+-HCO_3^- cotransport isoform 3. J Biol Chem 277: 50503-50509.

Petrovic S, Ma L, Wang Z, Soleimani M. 2003. Identification of an apical Cl^-/HCO_3^-exchanger in rat kidney proximal tubule. Am J Physiol 285: C608-C617.

Rakonczay Z Jr, Fearn A, Hegyi P, et al. 2006. Characterisation of H^+ and HCO_3^- transporters in CFPAC-1 human pancreatic duct cells. World J Gastroenterol 12: 885-895.

Schiavi SC, Abdelkader N, Reber S, et al. 1996. Biosynthetic and growth abnormalities are associated with high-level expression of CFTR in heterologous cells. Am J Physiol 270: C341-351.

Schoumacher RA, Ram J, Iannuzzi MC, et al. 1990. A cystic fibrosis pancreatic adenocarcinoma cell line. Proc Natl Acad Sci USA 87: 4012-4016.

Shcheynikov N, Ko SB, Zeng W, et al. 2006. Regulatory interaction between CFTR and the SLC26 transporters. Novartis Found Symp 273: 177-186.

Shiotani A, Fukumura M, Maeda M, et al. 2001. Skeletal muscle regeneration after insulin-like growth factor I gene transfer by recombinant Sendai virus vector. Gene Ther 8: 1043-1050.

Silberg DG, Wang W, Moseley RH, et al. 1995. The down regulated in adenoma (dra) gene encodes an intestine-specific membrane sulfate transport protein. J Biol Chem 270: 11897-11902.

Simpson JE, Gawenis LR, Walker NM, et al. 2005. Chloride conductance of CFTR facilitates basal Cl^-/HCO_3^- exchange in the villous epithelium of intact murine duodenum. Am J Physiol 288: G1241-G1251.

Stelzner M, Somasundaram S, Lee SP, et al. 2001. Ileal mucosal bile acid absorption is increased in Cftr knockout mice. BMC Gastroenterol 1: 10.

Steward MC, Ishiguro H, Case RM. 2005. Mechanisms of bicarbonate secretion in the pancreatic duct. Annu Rev Physiol 67: 377-409.

Szűcs Á, Demeter I, Burghardt B, et al. 2006. Vectorial bicarbonate transport by Capan-1 cells: a model for human pancreatic ductal secretion. Cell Physiol Biochem 18: 253-64.

Thomas JA, Buchsbaum RN, Zimniak A, et al. 1979. Intracellular pH measurements in Ehrlich ascites tumor cells utilizing spectroscopic probes generated in situ. Biochemistry 18: 2210-2218

Tokusumi T, Iida A, Hirata T, et al. 2002. Recombinant Sendai viruses expressing different levels of a foreign reporter gene. Virus Res 86: 33-38.

Trauner M, Boyer JL. 2003. Bile salt transporters: Molecular characterization, function, and regulation. Physiol Rev 83: 633-671.

Yonemitsu Y, Kitson C, Ferrari S, et al. 2000. Efficient gene transfer to airway epithelium using recombinant Sendai virus. Nat Biotechnol 18: 970-973.

Venglovecz V, Rakonczay Z Jr, Ózsvári B, et al. 2008. Differential effects of bile acids on pancreatic ductal bicarbonate secretion in guinea pig. Gut 57: 1102-1112

Voronina S, Longbotton R, Sutton R, et al. 2002. Bile acids induce calcium signals in mouse pancreatic acinar cells: implications for bile-induced pancreatic pathology. J Physiol. 540:49Y55.

Wallrapp C, Muller-Pillasch F, Solinas-Toldo S, et al. 1997. Characterization of a high copy number amplification at 6q24 in pancreatic cancer identifies c-myb as a candidate oncogene. Cancer Res 57: 3135-3139.

Wang Y, Soyombo AA, Shcheynikov N, et al. 2006. Slc26a6 regulates CFTR activity in vivo to determine pancreatic duct HCO_3^- secretion: Relevance to cystic fibrosis. EMBO J 25: 5049-5057.

Wang Z, Petrovic S, Mann E, et al. 2002. Identification of an apical Cl^-/HCO_3^- exchanger in the small intestine. Am J Physiol 282: G573-G579.

Waters DL, Dorney SFA, Gaskin KJ, et al. 1990. Pancreatic function in infants identified as having cystic-fibrosis in a neonatal screening program. N Engl J Med 322: 303-308.

Weintraub WH, Machen TE. 1989. pH regulation in hepatoma cells: Roles for Na-H exchange, Cl--HCO_3 exchange, and Na-HCO_3^- cotransport. Am J Physiol 257: G317-G327.

Zsembery A, Strazzabosco M, Graf J, 2000. Ca^{2+}-activated Cl^- channels can substitute for CFTR in stimulation of pancreatic duct bicarbonate secretion. FASEB J 14:2345-2356.

7. ANNEX

CFTR Expression But Not Cl^- Transport Is Involved in the Stimulatory Effect of Bile Acids on Apical Cl^-/HCO_3^- Exchange Activity in Human Pancreatic Duct Cells

Imre Ignáth, MSc, Péter Hegyi, MD, PhD,* Viktória Venglovecz, PhD,† Csilla A. Székely, MSc,* Georgina Carr, PhD,‡ Mamoru Hasegawa, PhD,§ Makoto Inoue, PhD,§ Tamás Takács, MD, PhD, DSc,* Barry E. Argent, PhD,‡ Michael A. Gray, PhD,‡ and Zoltán Rakonczay Jr, MD, PhD**

Objectives: Low doses of chenodeoxycholate (CDC) stimulate apical anion exchange and HCO_3^- secretion in guinea pig pancreatic duct cells (*Gut.* 2008;57:1102–1112). We examined the effects of CDC on intracellular pH (pH_i), intracellular Ca^{2+} concentration ($[Ca^{2+}]_i$), and apical Cl^-/HCO_3^- exchange activity in human pancreatic duct cells and determined whether any effects were dependent on cystic fibrosis transmembrane conductance regulator (CFTR) expression and Cl^- channel activity.

Methods: Polarized CFPAC-1 cells (expressing F508del CFTR) were transduced with Sendai virus constructs containing complementary DNAs for either wild-type CFTR or β-galactosidase. Microfluorimetry was used to record pH_i and $[Ca^{2+}]_i$ and apical Cl^-/HCO_3^- exchange activity. Patch clamp experiments were performed on isolated guinea pig duct cells.

Results: Chenodeoxycholate induced a dose-dependent intracellular acidification and a marked increase in $[Ca^{2+}]_i$ in CFPAC-1 cells. CFTR expression slightly reduced the rate of acidification but did not affect the $[Ca^{2+}]_i$ changes. Luminal administration of 0.1 mmol/L of CDC significantly elevated apical Cl^-/HCO_3^- exchange activity but only in cells that expressed CFTR. However, CDC did not activate CFTR Cl^- conductance.

Conclusions: Bile salts modulate pH_i, $[Ca^{2+}]_i$, and apical anion exchange activity in human pancreatic duct cells. The stimulatory effect of CDC on anion exchangers requires CFTR expression but not CFTR channel activity.

Key Words: pancreatic duct cells, CFTR, Cl^-/HCO_3^- exchange, chenodeoxycholate, Sendai virus

(*Pancreas* 2009;00: 00–00)

The pancreatic ductal epithelium secretes a HCO_3^--rich alkaline fluid that flushes digestive enzymes (secreted by acinar cells) down the ductal tree and into the duodenum and also helps to neutralize acid chyme entering the duodenum from the stomach.[1] We have recently shown that luminal administration of a low dose (0.1 mmol/L) of the unconjugated bile salt, chenodeoxycholate (CDC), significantly elevated apical Cl^-/HCO_3^- exchange activity and HCO_3^- secretion in guinea pig pancreatic ducts and that these effects were Ca^{2+} dependent.[2] In contrast, a higher dose of CDC (1 mmol/L) strongly inhibited ductal HCO_3^- transport.[2]

The stimulatory effect of 0.1 mmol/L of CDC on apical Cl^-/HCO_3^- exchange activity in intact ducts is most likely mediated by up-regulation of SLC26A6 (putative anion transporter 1 [PAT-1]) because it was blocked by 4,4′-diisothiocyanodihydrostilbene-2,2′-disulphonate.[2] Under physiological conditions, ductal HCO_3^- secretion is regulated by a direct interaction between the SLC26 family Cl^-/HCO_3^- exchangers and cystic fibrosis transmembrane conductance regulator (CFTR).[3,4] Therefore, assessing whether the stimulatory effects of CDC on anion exchange activity and HCO_3^- secretion are dependent on CFTR expression and functional Cl^- channel activity should help to clarify the underlying mechanism.[5]

Therefore, the main aim of this study was to investigate the effects of 0.1 mmol/L of CDC on intracellular pH (pH_i), intracellular calcium concentration ($[Ca^{2+}]_i$), and apical Cl^-/HCO_3^- exchange activity in normal and cystic fibrosis human pancreatic duct cells. All these experiments were performed on polarized human CFPAC-1 cells, which are homozygous for the *F508del CFTR* mutation. CFPAC-1 cells were ideal for these investigations because they can be efficiently transduced with wild-type CFTR using a Sendai virus (SeV) construct, and they also express SLC26A6, which is functional only when wild-type CFTR is present in the cells.[6] Finally, we wanted to test whether CDC increased CFTR Cl^- channel activity, and for these experiments, we used guinea pig pancreatic duct cells in which CFTR activity and its regulation have been well characterized.[7]

MATERIALS AND METHODS

Materials and Solutions

All the laboratory chemicals, the cell culture reagents, and the CDC were purchased from Sigma-Aldrich (Budapest, Hungary). 2′,7′-*bis*-(2-carboxyethyl)-5(6)-carboxyfluorescein-acetoxymethyl ester (BCECF-AM) and 2-(6-(*bis*(carboxymethyl) amino)-5-(2-(2-(bis(carboxymethyl)amino)-5-methylphenoxy) ethoxy)-2-benzofuranyl)-5-oxazolecarboxylic acetoxymethyl ester (Fura-2 AM) were from Molecular Probes Inc (Eugene, Ore). The stock solution of BCECF-AM (2 mmol/L) was prepared in dimethyl sulfoxide. Five millimoles per liter of Fura-2 AM was dissolved in 20% pluronic F-127 in dimethyl sulfoxide. Nigericin (10 mmol/L) and forskolin (50 mmol/L) were dissolved in ethanol and stored at −20°C. Polyester Transwells were supplied

From the *First Department of Medicine, and †Department of Pharmacology and Pharmacotherapy, University of Szeged, Szeged, Hungary; ‡Epithelial Research Group, Institute for Cell and Molecular Biosciences, University of Newcastle, Newcastle upon Tyne, United Kingdom; and §DNAVEC Corporation, Tsukuba, Ibaraki, Japan.

Received for publication March 18, 2009; accepted June 25, 2009.

Reprints: Zoltán Rakonczay Jr, MD, PhD, First Department of Medicine, University of Szeged PO Box 427, 6701 Szeged, Hungary (e-mail: raz@in1st.szote.u-szeged.hu).

This study was supported by the Hungarian Scientific Research Fund (PF63951 and K78311 to Z.R. Jr and PD78087 to V.V.), the Hungarian Academy of Sciences (BO 00334/08/5 to P.H. and BO 00218/06 to Z.R. Jr), The Physiological Society (United Kingdom), and a joint international grant (Hungarian Academy of Sciences and The Royal Society) to P.H. and M.A.G.

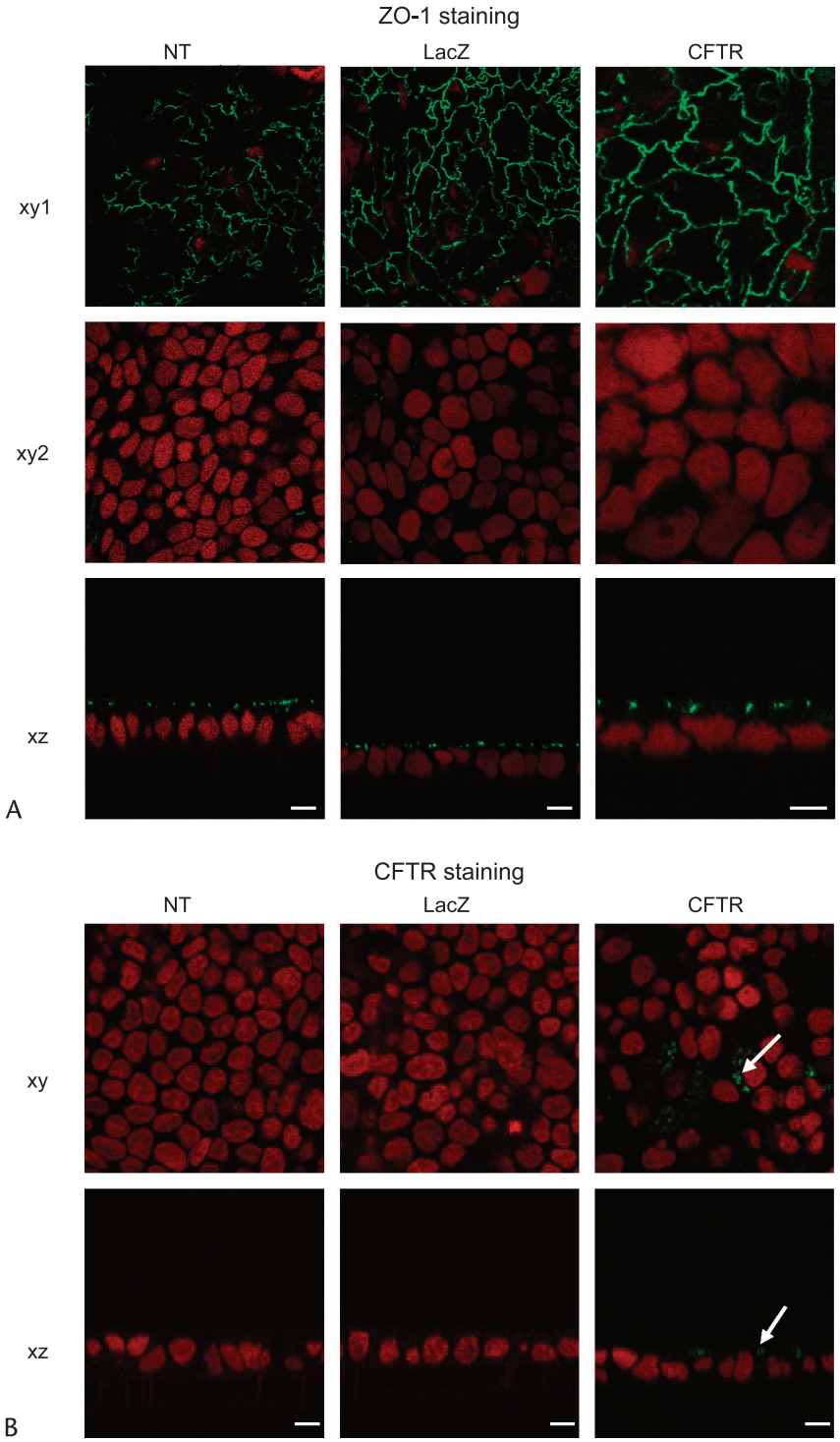

FIGURE 1. ZO-1 and CFTR expression in untransduced and SeV-LacZ or SeV-CFTR CFPAC-1 pancreatic duct cells. CFPAC-1 monolayers were fixed and stained for ZO-1 (A) or CFTR expression (B) 2 days after being transduced with SeV-LacZ or SeV-CFTR. A, ZO-1 was localized to the apical part of the cells (see xy1 and xz sections) and showed a characteristic chicken-wire pattern (green staining in the xy1 section) in both the untransduced and transduced CFPAC-1 cells, consistent with its expression at the tight junctions. The xy2 section shows the nuclei of cells stained (red) with propidium iodide. No difference was observed in ZO-1 expression between the different cell lines. B, CFTR expression could only be detected in the apical membrane of SeV-CFTR–transduced CFPAC-1 cells (green staining in xy and xz sections). Scale bars are equal to 10 μm. Note that in the ZO-1 images, the scale bar for SeV-CFTR–transduced cells is larger compared with the SeV-LacZ and untransduced cells.

by Corning-Costar (Buckinghamshire, United Kingdom). The standard 4-(2-hydroxyethyl)-1-piperazineethanesulfonic acid (HEPES)–buffered solution contained the following (in millimoles per liter): NaCl, 130; KCl, 5; $MgCl_2$, 1; $CaCl_2$, 1; Na-HEPES (pH 7.4 with HCl), 10; and D-glucose, 10. The standard HCO_3^--buffered solution contained the following (in millimoles per liter): NaCl, 115; KCl, 5; $MgCl_2$, 1; $CaCl_2$, 1; Na-HCO_3, 25; and D-glucose, 10. The Cl^--free HCO_3^- solution contained the following (in millimoles per liter): Na-gluconate, 115; K_2SO_4, 2.5; Ca-gluconate, 6; Mg-gluconate, 1; Na-HCO_3, 25; and D-glucose, 10. The HCO_3^--containing solutions were continuously equilibrated with 5% CO_2–95% O_2 to maintain the pH at 7.4. For patch clamp experiments, the pipette solution contained the following (in millimoles per liter): CsCl, 110; $MgCl_2$, 2; ethylene glycol-*bis*(β-aminoethyl ether)-*N*,*N*,*N*′,*N*′-tetraacetic acid, 5; HEPES, 10; and Na_2ATP (pH 7.2 with CsOH), 1. The osmolarity of the pipette solution was 240 mOsm/L. The standard bath solution contained the following (in millimoles per liter): NaCl, 145; KCl, 4.5; $CaCl_2$, 2; $MgCl_2$, 1; HEPES (pH 7.4 with NaOH, 300 mOsm/L), 10; and glucose, 5.

Culturing of CFPAC-1 Cells

CFPAC-1 cells (passage numbers 50–70) were obtained from Prof R.A. Frizzell (University of Pittsburgh, Pittsburgh, Pa); grown in Iscove's modified Dulbecco's medium supplemented with 10% fetal calf serum, 2 mmol/L of glutamine, 100 units per milliliter of penicillin, and 0.1 mg/mL of streptomycin; and cultured as described previously.[6] The medium was changed every 1 to 2 days. Cells were maintained at 37°C in a humidified atmosphere containing 5% CO_2. Cell monolayers were prepared by seeding at high density (300,000–350,000 cells per square centimeter) onto polyester permeable supports (Transwells:

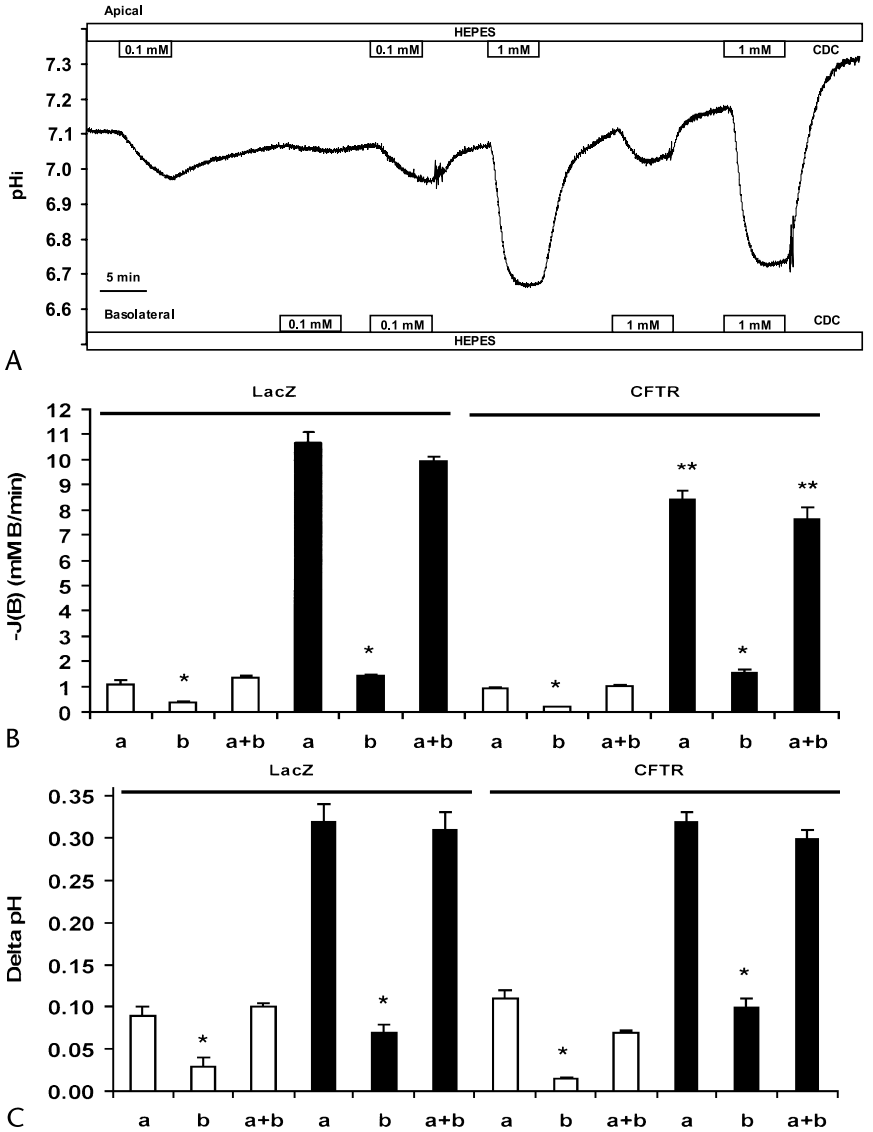

FIGURE 2. Differential effect of CDC on pH_i of CFPAC-1 cells. A, The figure shows a representative pH_i recording from SeV-CFTR–transduced CFPAC-1 cells. Either 0.1 or 1 mmol/L CDC was administered in standard HEPES solution from the apical (a) and/or the basolateral (b) membrane. Rate of intracellular acidification (B) and net change in pH_i (C) in response to 0.1 mmol/L (open bars) or 1 mmol/L (filled bars) chenodeoxycholate administration in SeV-LacZ– and SeV-CFTR–transduced CFPAC-1 cells. Significant difference ($P < 0.05$) versus *the apical administration or the **SeV-LacZ group.

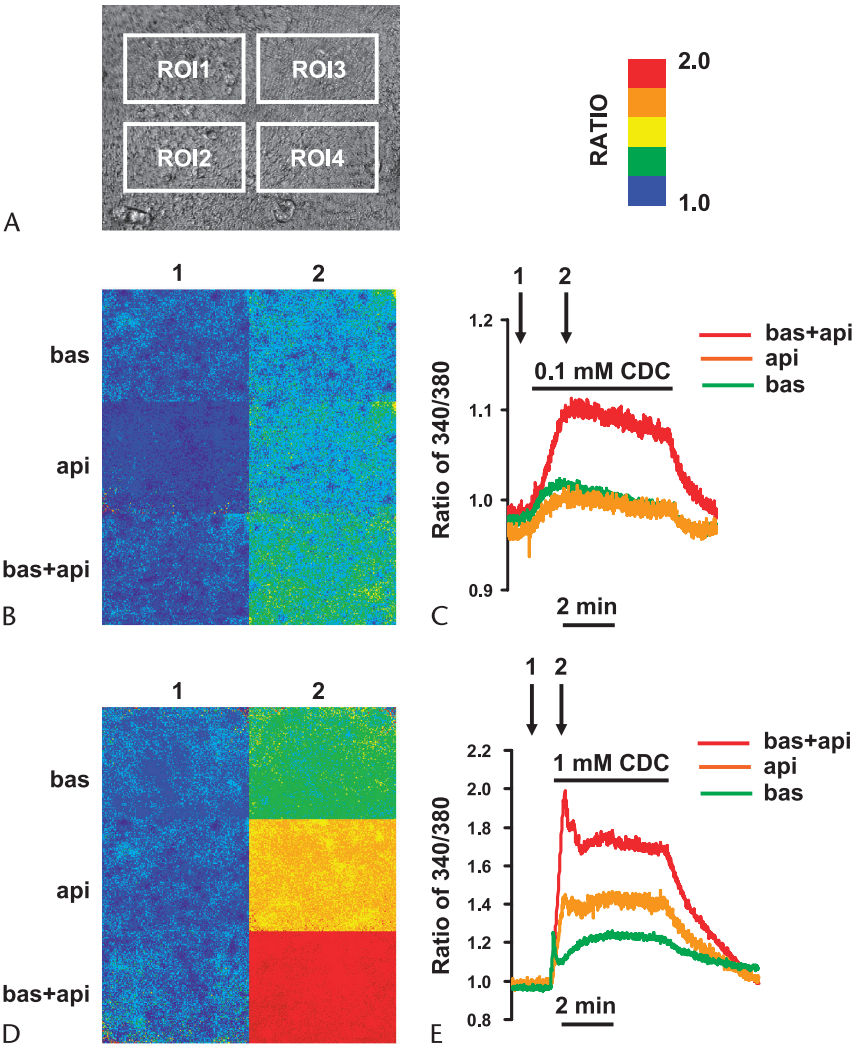

FIGURE 3. Effect of CDC on $[Ca^{2+}]_i$ in CFPAC-1 duct cells. CFPAC-1 cells were loaded with 5 μmol/L Fura-2. A, Four to 5 small areas (ROIs, regions of interests) of 180 to 240 cells were excited with light at wavelengths of 340 and 380 nm, and the 340:380 fluorescence emission ratio was measured at 535 nm. The figure shows fluorescence ratio images (B and D) and representative 340:380 ratio traces (C and E) of CFPAC-1 cells perfused with 0.1 mmol/L (B and C) or 1 mmol/L CDC (D and E) from the basolateral (bas) and/or apical (api) side. In the fluorescent ratio images, an increase in $[Ca^{2+}]_i$ is denoted by a change from a cold color (blue) to a warmer color (yellow to red); see scale on top. Pictures were taken before (1) and soon after exposure of CDC (2).

diameter, 12 mm; pore size, 0.4 μm). Cell confluence was checked by microscopy and determination of transepithelial electrical resistance (R_T) using an EVOM-G voltohmmeter (World Precision Instruments, Sarasota, Fla).

Isolation of Guinea Pig Pancreatic Duct Cells

For patch clamp experiments, small intralobular and interlobular ducts were isolated from guinea pig (weighing 150–250 g) pancreas, cultured overnight, and dissociated into single cells as described previously.[8]

Recombinant SeV Constructs and Infection of CFPAC-1 Cells

Sendai virus constructs containing the wild-type CFTR (SeV-CFTR) or the β-galactosidase (SeV-LacZ) gene were prepared as described previously.[9,10] CFPAC-1 monolayers were infected with SeV-CFTR or SeV-LacZ (nuclear localized) from the apical side 3 days after seeding (multiplicity of infection [MOI], 3; see details in Rakonczay et al[6]). Control (ie, uninfected) CFPAC-1 cells were subjected to a similar protocol, but the virus aliquots were substituted with serum-free Iscove's modified Dulbecco's medium. Experiments were performed 48 to 96 hours after infection.

To estimate the efficiency of the gene transfer, β-galactosidase activity was detected by in situ staining in CFPAC-1 cells transduced with SeV-LacZ or SeV-CFTR.[6] LacZ activity was measured between 48 and 96 hours after infection. The application of SeV-LacZ to the apical membrane at an MOI of 3 resulted in a strong, homogenous LacZ activity in 30 +/− 3% (mean +/− SEM) of CFPAC-1 cells in the cultures (n = 6). Untransduced cells or cells transduced with SeV-CFTR did not show any LacZ activity.

Immunocytochemistry

Two days after infection with SeV-LacZ or SeV-CFTR, CFPAC-1 monolayers were washed with phosphate-buffered saline (PBS) and then fixed and permeabilized with methanol on ice for 15 minutes. The monolayers were blocked in 3% horse

serum for 1 hour. The cells were then incubated overnight at 4°C with mouse anti–ZO-1 (33-9100; Zymed Laboratories, San Francisco, Calif) or anti-CFTR (MAB3480; Chemicon, Temecula, Calif) antibody (1:100). After 3 washes with PBS, the cells were incubated in 3% goat serum for 1 hour and goat anti–mouse FITC secondary antibody (Alexa Fluor 488, 1:100; Invitrogen, Paisley, United Kingdom) for 1 hour. The filters were washed in PBS and incubated in 1 μg/mL of propidium iodide (Invitrogen) for 5 to 10 minutes (to stain the nuclei of cells) and were mounted in Vectashield mounting medium (Vector Laboratories Ltd, Peterborough, United Kingdom). Control experiments omitted the primary antibody (and were negative). Staining was visualized using confocal laser microscopy (TCS-NT with Kr-Ar laser; Leica, Milton Keynes, United Kingdom) with appropriate excitation and emission filter sets. A gallery of 10 to 20 optical sections (0.5-μm-thick) through the *x-y* and the *z* planes were obtained.

Measurement of Intracellular pH and $[Ca^{2+}]$

Intracellular pH (pH_i) was estimated as described previously.[6,11,12] Briefly, after loading the cells with 2 μmol/L of BCECF-AM, the Transwells were transferred to a perfusion chamber mounted on an IX71 inverted Olympus microscope (Olympus, Tokyo, Japan). Apical and basal bath volumes were 0.5 and 1 mL, and the perfusion rates were 3 and 6 mL/min, respectively. pH_i was measured using a Cell^R imaging system (Olympus). Four to 5 small areas (regions of interest) of 180 to 240 cells were excited with light at wavelengths of 490 and 440 nm, and the 490:440 fluorescence emission ratio was measured at 535 nm. In situ calibration of the fluorescence signal was performed using the high K^+-nigericin technique.[11]

Measurement of intracellular Ca^{2+} concentration ($[Ca^{2+}]_i$) was performed using the same method, except that the cells were loaded with the Ca^{2+}-sensitive fluorescent dye Fura-2 AM (5 μmol/L) for 60 minutes. For excitation, 340- and 380-nm filters were used, and the changes in $[Ca^{2+}]_i$ were calculated from the fluorescence ratio (F_{340}/F_{380}) measured at 510 nm.

Net Change in pH_i (ΔpH_i) and Calculation of Base Flux

The net change in pH_i (ΔpH_i) was measured by determining the pH_i immediately before and at the peak level after the changes of solutions by averaging the values of 80 data points. The intrinsic buffering capacity (β_i) and the total buffering capacity (β_{total}) of CFPAC-1 cells was estimated according to the NH_4^+ prepulse technique.[6] The initial rates of change of pH_i (over 30–60 seconds) resulting from solution changes were used to calculate transmembrane base flux (J_B). J_B is equal to the change of pH_i / $\Delta t \times \beta_i$. The β_i value used in the calculation of J_B was obtained by using the mean pH_i value during a 30-second period immediately before changing solutions. We denote base influx as J_B and base efflux as $-J_B$. The units of J_B are mmol/L of base equivalent (B) per minute.

Electrophysiology

Patch pipettes were pulled from borosilicate glass and had resistances of between 3 and 5 MΩ after fire polishing. Seal

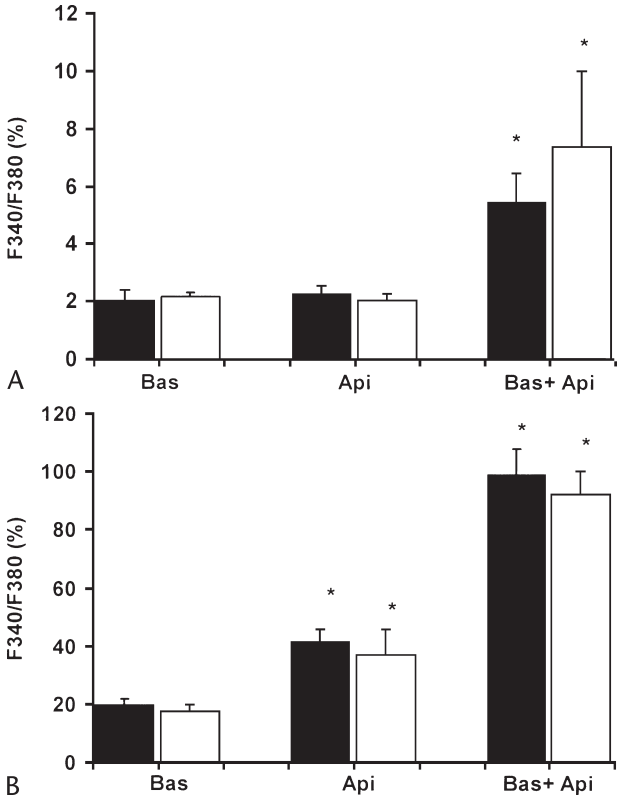

FIGURE 4. Summary of changes in $[Ca^{2+}]_i$ caused by CDC in SeV-LacZ– and SeV-CFTR–transduced CFPAC-1 cells. Addition of 0.1 mmol/L (A) or 1 mmol/L of CDC (B) to SeV-LacZ– (filled bars) or SeV-CFTR–transduced CFPAC-1 cells (open bars) caused a significant increase in $[Ca^{2+}]_i$. The 1-mmol/L CDC caused a significantly higher Ca^{2+} signal from the apical (api) membrane versus from the basolateral (bas) membrane. Bilateral administration of CDC elevated $[Ca^{2+}]_i$ to an even greater extent. There was no significant difference in $[Ca^{2+}]_i$ in response to the CDC between SeV-LacZ– and SeV-CFTR–transduced cells. The percent changes in F_{340}/F_{380} ratio were calculated using the peak $[Ca^{2+}]_i$ responses (Fig. 3). *Significant difference ($P < 0.05$) versus the basolateral administration.

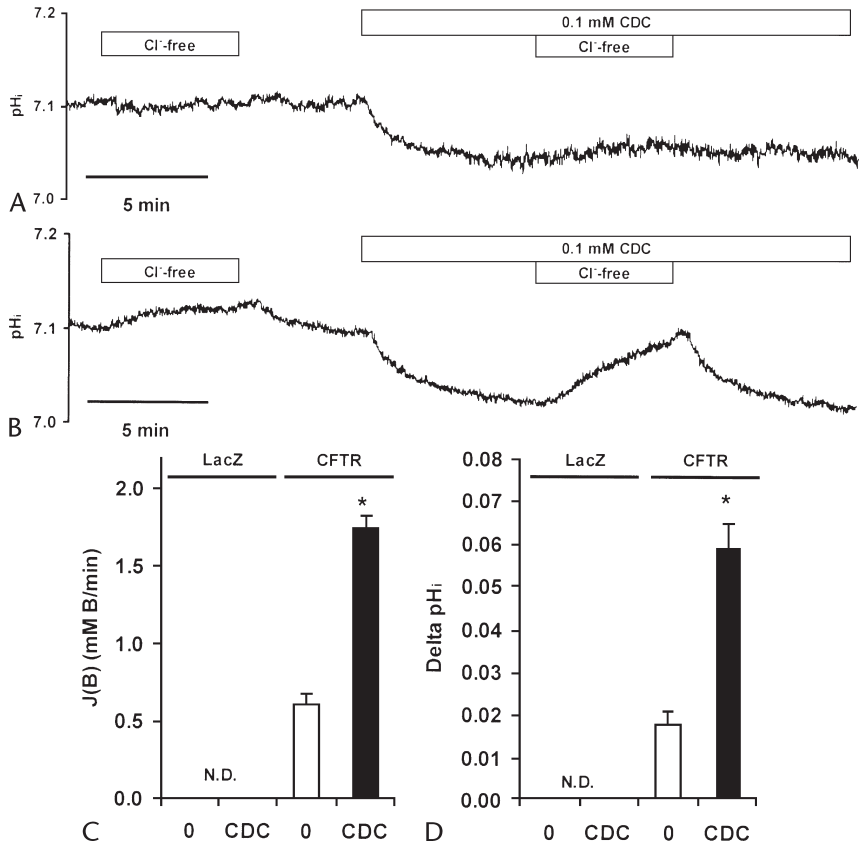

FIGURE 5. Effect of 0.1 mmol/L of CDC on apical Cl^-/HCO_3^- exchange activity in CFPAC-1 cells. Representative pH_i recordings of SeV-LacZ– (A) and SeV-CFTR–transduced cells (n = 6) (B). Cl^-/HCO_3^- exchange activity was assessed by removing Cl^- from the apical standard HCO_3^-/CO_2 solution, first in the absence and then in the presence of 0.1 mmol/L of CDC. The bar charts showing the summary of base flux (C) and ΔpH_i (D) in the absence (0) and presence of 0.1 mmol/L of CDC. *Significant difference ($P < 0.05$) versus the 0 group. N.D. indicates not detectable.

resistances were typically between 5 and 10 GΩ. An EPC-7 amplifier (List Electronic, Darmstadt, Germany) was used to record whole-cell currents from single duct cells at room temperature.[7] Current-voltage (*I*/*V*) relationships were obtained by holding V_m at 0 mV and clamping to ±100 mV in 20-mV increments for 500 milliseconds with an 800-millisecond interval between each pulse. Data were filtered at 1 kHz, sampled at 2 kHz with a CED 1401 interface (Cambridge Electronic Design, Cambridge, England), and stored on computer hard disc. *I*/*V* plots were constructed using the mean current measured during a 4-millisecond period starting 495 milliseconds into the voltage pulse. Reversal potentials (E_{rev}) and current densities were determined from *I*/*V* plots after fitting a third-order polynomial using regression analysis. The mean current amplitudes were calculated at E_{rev} +/− 60 mV and normalized to cell capacitance (pF) measured using the EPC-7 amplifier. Series resistance (R_s) compensation was routinely used (50%–70%). V_m was corrected for current flow (I) across the uncompensated fraction of R_s using the relationship $V_m = V_p - I \times R_s$, where V_p is the pipette potential. V_m was also corrected for liquid junction potentials using the program JPCalc (Professor Peter H. Barry, University of New South Wales, Australian) and have been applied to V_m.

Statistical Analyses

To avoid errors arising from the variation in the rate and magnitude of HCO_3^- flux between different sets of monolayers, we performed the respective measurements in random order on the same day from one set of cell cultures. Whenever possible, internal control experiments were carried out. Data are presented as mean (SEM). Statistical analyses were determined using either the Student's paired or unpaired *t* test or the analysis of variance as appropriate. $P < 0.05$ was accepted as statistically significant.

RESULTS

Unless stated otherwise, there was no significant difference between data obtained from uninfected and SeV-LacZ–infected CFPAC-1 cells.

Expression of ZO-1 and CFTR in Polarized Cultures of Untransduced and SeV-Transduced CFPAC-1 Cells

CFPAC-1 cells grown on polyester Transwells became confluent 2 to 3 days after seeding, as judged by visual observation. Epithelial integrity, as judged by the measurement of R_T, increased steadily for 4 to 5 days up to a maximum of 256 (10) $\Omega \times cm^2$ in the untransduced cells. R_T was not significantly different in the SeV-LacZ (266 [10] $\Omega \times cm^2$) versus the SeV-CFTR–infected cells (253 [9] $\Omega \times cm^2$; n = 35–38).

As shown in Figure 1A, the tight junction protein ZO-1 was localized to the apical part of the cells and showed a characteristic "chicken-wire" pattern in both the control and the SeV-transduced CFPAC-1 cells, consistent with its expression at the tight junctions. No difference was observed in ZO-1

expression between the different cell lines. CFTR expression was only detected in the SeV-CFTR–transduced CFPAC-1 cells (Fig. 1B) and was localized solely to the apical plasma membrane.

Effect of CDC on pH_i

Administration of CDC (0.1 and 1.0 mmol/L) in standard HEPES solution caused a dose-dependent decrease in the pH_i of CFPAC-1 cells (Figs. 2A–C). However, at both doses tested, apical administration of CDC resulted in a markedly higher rate of intracellular acidification as compared with basolateral administration (Figs. 2B, C). Moreover, the $-J$(B) response to 1 mmol/L of CDC was significantly lower in cells transduced with CFTR versus LacZ (Fig. 2B), probably indicating that CFTR expression had reduced the rate at which the bile acid entered the duct cells. However, the ΔpH_i values induced by CDC were unaffected by CFTR expression (Fig. 2C).

Effect of CDC on $[Ca^{2+}]_i$

Exposure of duct cells to CDC caused a dose-dependent increase in $[Ca^{2+}]_i$ (Figs. 3 and 4). Figure 3 shows that 0.1 mmol/L of CDC typically evoked a relatively slow rise in $[Ca^{2+}]_i$ to a peak value, which then declined slowly (Figs. 3B, C). In contrast, 1 mmol/L of CDC typically caused a fast rise in $[Ca^{2+}]_i$ to a peak that was followed by a maintained plateau phase (Figs. 3D, E). In accordance with our earlier findings in guinea pig ducts, apical 1 mmol/L of CDC caused a significantly larger Ca^{2+} signal when compared with the same dose applied from the basolateral membrane (compare Figs. 3D, E). Bilateral administration of CDC (at both 0.1 and 1.0 mmol/L of doses) elevated $[Ca^{2+}]_i$ to an even greater extent (Figs. 3C, E).

Figure 4 is a summary of the $[Ca^{2+}]_i$ data and shows that expression of CFTR had no effect on the $[Ca^{2+}]_i$ response to CDC administration, indicating that CFTR expression was not obligatory for CDC-induced Ca^{2+} signaling.

CFTR Expression Is Required for CDC-Induced Increase in Apical Cl^-/HCO_3^- Exchange Activity

In SeV-LacZ–transduced CFPAC-1 cells, removal of Cl^- from the standard HCO_3^-/CO_2 solution perfusing the apical membrane of the monolayers had no effect on pH_i, either in the absence or presence of 0.1 mmol/L of CDC (Fig. 5A). However, Cl^- removal from the apical membrane of SeV-CFTR–transduced cells (Fig. 5B) caused a clear alkalinization of pH_i (J_B, 0.61 [0.07] mmol/L of B per minute; ΔpH_i, 0.018 [0.003]), which was significantly increased by approximately 3-fold

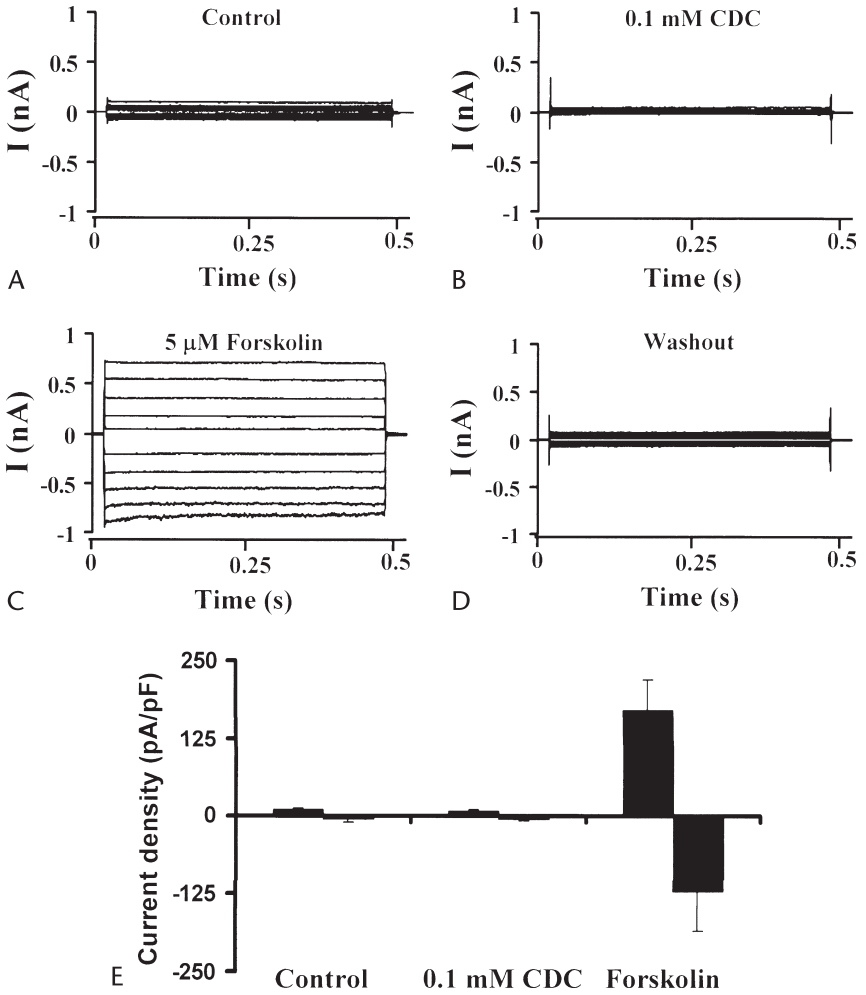

FIGURE 6. Effect of 0.1 mmol/L of CDC on CFTR Cl^- conductance in guinea pig pancreatic duct cells. Typical whole-cell CFTR Cl^- currents recorded from pancreatic duct cells perfused with standard bath solution (control) (A), 0.1 mmol/L of CDC (B), or 5 μmol/L of forskolin (C) or following washout of forskolin (D). E, Current densities under different conditions.

(J_B, 1.75 [0.08] mmol/L of B per minute; ΔpH_i, 0.059 [0.006]) in the presence of 0.1 mmol/L of CDC (Figs. 5C, D).

Chenodeoxycholate Does Not Activate CFTR Cl^- Currents

The stimulation of apical anion exchange by CDC (Fig. 5) could be due either to a direct effect on SLC26A6 activity (perhaps mediated by an increase in $[Ca^{2+}]_i$), or it could be an indirect effect caused by, for example, an increase in electrodiffusive Cl^- transport through CFTR. To directly test whether CDC could activate CFTR, we performed whole-cell patch clamp experiments on single guinea pig pancreatic duct cells.[13] Administration of 0.1 mmol/L of CDC to the bath solution had no effect on whole-cell currents (Fig. 6B), whereas characteristic italic> /italic> currents could be activated in the same cell (in 7 of 10 cells) when it was subsequently exposed to 5 μmol/L of forskolin (Fig. 6C). A higher concentration of CDC (0.5 mmol/L) resulted in membrane instability in most (5 of 8) cells studied.

DISCUSSION

The key transporters that control HCO_3^- secretion across the apical membrane of the pancreatic duct cell are CFTR and SLC26 anion exchangers (most likely SLC26A6 and/or SLC26A3).[1,4] In this study, our main aim was to test the effect of the unconjugated bile acid, CDC, on the activity of these transporters in human pancreatic duct cells. Moreover, we wanted to address the specific issue as to whether CFTR was involved in the bile acid–induced increase in HCO_3^- secretion that we have previously reported in guinea pig ducts.[2] To do this, we have studied apical Cl^-/HCO_3^- exchange activity in human pancreatic duct cells either lacking or expressing CFTR.

CFPAC-1 cells form a polarized monolayer when grown on polyester Transwells. The Rt increased steadily up to 5 days in both the untransduced and transduced cell lines, which suggests the formation of tight junctions. This is confirmed by expression of the tight junction protein, ZO-1, in all the cell lines. We have previously used Western blotting to demonstrate the expression of CFTR in SeV-CFTR–transduced CFPAC-1 cells. However, we wanted to make sure that this CFTR was correctly localized to the apical membrane, as CFTR overexpression has previously been shown to result in mislocalization of the protein.[14] Therefore, in this study, we have used immunocytochemistry to clearly demonstrate apical localization of CFTR in SeV-CFTR–transduced CFPAC-1 cells (MOI, 3). At a MOI of 3, approximately 30% of the CFPAC-1 cells express CFTR.[6] However, this relatively low rate of CFTR transduction is sufficient to up-regulate apical Cl^-/HCO_3^- exchange activity in the human duct cells.[6] We have previously shown that cells transduced with SeV-CFTR at a higher virus titer (MOI, 15) have a higher rate of transduction (approximately 70%). However, we chose not to use an MOI of 15 cells for this study because they exhibit a constitutively active apical Cl^-/HCO_3^- exchanger. This constitutive activity cannot be further increased by cyclic adenosine monophosphate, suggesting that in these cells transduced with a MOI of 15, anion exchange was already maximally activated.[6]

It has been demonstrated that bile acids induce Ca^{2+} signals in both pancreatic acinar cells[15–17] and in guinea pig ductal cells.[2] In the present study, we have shown that CDC also causes a dose-dependent increase in $[Ca^{2+}]_i$ in human pancreatic duct cells. In accordance with our earlier findings on guinea pig ducts, apical application of CDC to CFPAC-1 cells resulted in a greater elevation of $[Ca^{2+}]_i$ compared with basolateral application. These bile acid–induced Ca^{2+} signals were not dependent on the expression of CFTR. In contrast to our findings, in cholangiocytes, ursodeoxycholic acid only initiated Ca^{2+} signaling in cells expressing CFTR.[18]

Unconjugated bile salts, such as CDC, are weak acids and can therefore pass through cell membranes either by passive diffusion or via bile acid transporters.[19] Basolateral or luminal administration of CDC dose-dependently decreased the pH_i of the CFPAC-1 cells. Similarly, it has been reported that 0.5 to 1.5 mmol/L of ursodeoxycholate also caused a dose-dependent, rapid, intracellular acidification in bile duct epithelial cells.[20] As for $[Ca^{2+}]_i$, the effect of CDC on the pH_i of CFPAC-1 cells was greater when the bile acid was given from the apical side. Differential effects of bile acids have also been reported in dog pancreatic duct cells.[21] In these cells, the basolateral membrane was much more sensitive to bile acid–induced damage compared with the luminal membrane.[21] Interestingly, in our experiments, the CDC-induced acidosis was somewhat higher in CFTR-deficient pancreatic duct cells. This may be because of increased active uptake (via bile acid transporters) of CDC in CF cells, but further experiments are required to resolve this issue. Note that the absorption of taurocholate has been reported to be either reduced[22] or increased[23] in the ileum of transgenic CF mice with the *F508del CFTR* mutation.

We next tested the effect of 0.1 mmol/L of CDC on the Cl^-/HCO_3^- exchange activity of CFPAC-1 cells either lacking or expressing wild-type CFTR. Chenodeoxycholate stimulation of Cl^-/HCO_3^- exchange activity was only observed in cells expressing CFTR, strongly suggesting that the presence of CFTR is necessary for this effect. Similar to our findings, Fiorotto et al[18] reported that 0.1 mmol/L of ursodeoxycholate significantly elevated fluid secretion from intrahepatic mouse bile duct units in normal but not in CFTR-defective mice.

We also wanted to investigate whether the CDC-induced increase in Cl^-/HCO_3^- exchange activity was linked to enhanced Cl^- transport by CFTR. Using whole-cell current recording, we found that 0.1 mmol/L of CDC did not activate CFTR and therefore conclude that stimulation of CFTR does not underlie the effect of CDC of the anion exchanger. Our data contrast with the results of Bijvelds et al,[24] who found that luminal administration of 0.5 mmol/L of taurocholate did stimulate CFTR-dependent electrogenic Cl^- transport in the murine ileum. These contrasting results may be due to differences in species and tissues and the type and concentration of bile acids used. However, our results suggest that the increase in anion exchange activity evoked by CDC either reflects a direct effect of the bile acid on the apical exchanger or involves some other, indirect, mechanism. The CDC-induced increase in anion exchange activity observed in guinea pig pancreatic ducts that was entirely dependent on a rise in $[Ca^{2+}]_i$[2] implies that bile acids do not directly modulate SLC26 transporter activity. Because SLC26A6 is thought to be electrogenic and transports $2HCO_3^-:1Cl^-$,[25] an alternate scenario would involve a CDC-dependent opening of Ca^{2+}-dependent K^+ channels via Ca^{2+} release from internal stores. The increase in K^+ conductance would hyperpolarize the membrane potential and thereby stimulate electrogenic HCO_3^- secretion via SLC26A6.

Finally, obstruction of the ampulla of Vater by gallstones that have migrated down the common bile duct is a major risk factor for acute pancreatitis.[26] The consequent obstruction of bile and pancreatic juice outflow into the duodenum might cause bile reflux into the pancreas. In pancreatic acinar cells, bile acids cause a global elevation of $[Ca^{2+}]_i$, which leads to trypsinogen activation and, subsequently, to cell death.[27] However, the role of pancreatic duct cells in the pathogenesis of acute pancreatitis is unclear. Our earlier studies on guinea pig pancreatic ducts[2,28] and this current study on human duct cells suggest that toxic

factors known to induce acute pancreatitis (such as viruses and bile acids) stimulate HCO_3^- secretion. Therefore, we speculate that CDC-induced HCO_3^- secretion would flush toxic bile salts out of the ductal tree and may serve as a defense mechanism against acute biliary pancreatitis.

REFERENCES

1. Steward MC, Ishiguro H, Case RM. Mechanisms of bicarbonate secretion in the pancreatic duct. *Annu Rev Physiol*. 2005;67:377–409.
2. Venglovecz V, Rakonczay Z Jr, Ózsvári B, et al. Differential effects of bile acids on pancreatic ductal bicarbonate secretion in guinea pig. *Gut*. 2008;57:1102–1112.
3. Choi JY, Muallem D, Kiselyov K, et al. Aberrant CFTR-dependent HCO_3^- transport in mutations associated with cystic fibrosis. *Nature*. 2001;10:94–97.
4. Shcheynikov N, Ko SB, Zeng W, et al. Regulatory interaction between CFTR and the SLC26 transporters. *Novartis Found Symp*. 2006;273: 177–186.
5. Lee MG, Muallem S. Pancreatitis: the neglected duct. *Gut*. 2008;57: 1037–1039.
6. Rakonczay Z Jr, Hegyi P, Hasegawa M, et al. CFTR gene transfer to human cystic fibrosis pancreatic duct cells using a Sendai virus vector. *J Cell Physiol*. 2008;214:442–455.
7. Gray MA, Plant S, Argent BE. cAMP-regulated whole cell chloride currents in pancreatic duct cells. *Am J Physiol*. 1993;264:C591–C602.
8. Gray MA, Winpenny JP, Porteous DJ, et al. CFTR and calcium-activated chloride currents in pancreatic ducts of a transgenic CF mouse. *Am J Physiol*. 1994;266:C213–C221.
9. Ferrari S, Griesenbach U, Iida A, et al. Sendai virus-mediated CFTR gene transfer to the airway epithelium. *Gene Ther*. 2007;14:1371–1379.
10. Yonemitsu Y, Kitson C, Ferrari S, et al. Efficient gene transfer to airway epithelium using recombinant Sendai virus. *Nat Biotechnol*. 2000;18: 970–973.
11. Hegyi P, Rakonczay Z Jr, Gray MA, et al. Measurement of intracellular pH in pancreatic duct cells: a new method for calibrating the fluorescence data. *Pancreas*. 2004;28:427–434.
12. Thomas JA, Buchsbaum RN, Zimniak A, et al. Intracellular pH measurements in Ehrlich ascites tumor cells utilizing spectroscopic probes generated in situ. *Biochemistry*. 1979;18:2210–2218.
13. O'Reilly CM, Winpenny JP, Argent BE, et al. Cystic fibrosis transmembrane conductance regulator currents in guinea pig pancreatic duct cells: inhibition by bicarbonate ions. *Gastroenterology*. 2000; 118:1187–1196.
14. Farmen SL, Karp PH, Ng P, et al. Gene transfer of CFTR to airway epithelia: low levels of expression are sufficient to correct Cl^- transport and overexpression can generate basolateral CFTR. *Am J Physiol Lung Cell Mol Physiol*. 2005;289:L1123–L1130.
15. Fischer L, Gukovskaya AS, Penninger JM, et al. Phosphatidylinositol 3-kinase facilitates bile acid-induced Ca^{2+} responses in pancreatic acinar cells. *Am J Physiol Gastrointest Liver Physiol*. 2007;292:G875–G886.
16. Gerasimenko JV, Flowerdew SE, Voronina SG, et al. Bile acids induce Ca^{2+} release from both the endoplasmic reticulum and acidic intracellular calcium stores through activation of inositol trisphosphate receptors and ryanodine receptors. *J Biol Chem*. 2006;281:40154–40163.
17. Voronina S, Longbotton R, Sutton R, et al. Bile acids induce calcium signals in mouse pancreatic acinar cells: implications for bile-induced pancreatic pathology. *J Physiol*. 2002;540:49–55.
18. Fiorotto R, Spirlì C, Fabris L, et al. Ursodeoxycholic acid stimulates cholangiocyte fluid secretion in mice via CFTR-dependent ATP secretion. *Gastroenterology*. 2007;133:1603–1613.
19. Trauner M, Boyer JL. Bile salt transporters: molecular characterization, function, and regulation. *Physiol Rev*. 2003;83:633–671.
20. Alvaro D, Mennone A, Boyer JL. Effect of ursodeoxcholic acid on intracellular pH regulation in isolated rat bile duct epithelial cells. *Am J Physiol Gastrointest Liver Physiol*. 1993;28:G783–G791.
21. Okolo C, Wong T, Moody MW, et al. Effect of bile acids on dog pancreatic duct epithelial cell secretion and monolayer resistance. *Am J Physiol Gastrointest Liver Physiol*. 2002;283:G1042–G1050.
22. Hardcastle J, Harwood MD, Taylor CJ. Absorption of taurocholic acid by the ileum of normal and transgenic DeltaF508 cystic fibrosis mice. *J Pharm Pharmacol*. 2004;56:445–552.
23. Stelzner M, Somasundaram S, Lee SP, et al. Ileal mucosal bile acid absorption is increased in Cftr knockout mice. *BMC Gastroenterol*. 2001;1:10.
24. Bijvelds MJ, Jorna H, Verkade HJ, et al. Activation of CFTR by ASBT-mediated bile salt absorption. *Am J Physiol Gastrointest Liver Physiol*. 2005;289:G870–G879.
25. Ko SB, Shcheynikov N, Choi JY, et al. A molecular mechanism for aberrant CFTR-dependent HCO_3^- transport in cystic fibrosis. *EMBO J*. 2002;21:5662–5672.
26. Pandol SJ, Saluja AK, Imrie CW, et al. Acute pancreatitis: bench to the bedside. *Gastroenterology*. 2007;132:1127–1151.
27. Criddle DN, Gerasimenko JV, Baumgartner HK, et al. Calcium signalling and pancreatic cell death: apoptosis or necrosis? *Cell Death Differ*. 2007;14:1285–1294.
28. Hegyi P, Ördög B, Rakonczay Z Jr, et al. The effect of herpesvirus infection on pancreatic duct cell secretion. *World J Gastroenterol*. 2005;38:5997–6002.

Journal of Cellular Physiology

CFTR Gene Transfer to Human Cystic Fibrosis Pancreatic Duct Cells Using a Sendai Virus Vector

ZOLTÁN RAKONCZAY JR,[1,2] PÉTER HEGYI,[1,2] MAMORU HASEGAWA,[3] MAKOTO INOUE,[3] JUN YOU,[3] AKIHIRO IIDA,[3] IMRE IGNÁTH,[2] ERIC W.F.W. ALTON,[4] UTA GRIESENBACH,[4] GABRIELLA ÓVÁRI,[5] JÁNOS VÁG,[5] ANA C. DA PAULA,[6] RUSSELL M. CRAWFORD,[8] GÁBOR VARGA,[5] MARGARIDA D. AMARAL,[6,7] ANIL MEHTA,[8] JÁNOS LONOVICS,[2] BARRY E. ARGENT,[1] AND MICHAEL A. GRAY[1]*

[1]*Institute for Cell and Molecular Biosciences, University of Newcastle, Newcastle upon Tyne, United Kingdom*

[2]*First Department of Medicine, University of Szeged, Szeged, Hungary*

[3]*DNAVEC Corporation, Tsukuba, Ibaraki, Japan*

[4]*Department of Gene Therapy, National Heart and Lung Institute, Imperial College, London, United Kingdom*

[5]*Molecular Oral Biology Research Group, Department of Oral Biology, Semmelweis University and Hungarian Academy of Sciences, Budapest, Hungary*

[6]*Centre of Human Genetics, National Institute of Health, Lisboa, Portugal*

[7]*Department of Chemistry & Biochemistry, University of Lisboa, Lisboa, Portugal*

[8]*Division of Maternal and Child Health Sciences, Ninewells Hospital Medical School, Dundee, Scotland, United Kingdom*

Cystic fibrosis (CF) is a fatal inherited disease caused by the absence or dysfunction of the CF transmembrane conductance regulator (CFTR) Cl^- channel. About 70% of CF patients are exocrine pancreatic insufficient due to failure of the pancreatic ducts to secrete a HCO_3^--rich fluid. Our aim in this study was to investigate the potential of a recombinant Sendai virus (SeV) vector to introduce normal CFTR into human CF pancreatic duct (CFPAC-1) cells, and to assess the effect of CFTR gene transfer on the key transporters involved in HCO_3^- transport. Using polarized cultures of homozygous F508del CFPAC-1 cells as a model for the human CF pancreatic ductal epithelium we showed that SeV was an efficient gene transfer agent when applied to the apical membrane. The presence of functional CFTR was confirmed using iodide efflux assay. CFTR expression had no effect on cell growth, monolayer integrity, and mRNA levels for key transporters in the duct cell (pNBC, AE2, NHE2, NHE3, DRA, and PAT-1), but did upregulate the activity of apical Cl^-/HCO_3^- and Na^+/H^+ exchangers (NHEs). In CFTR-corrected cells, apical Cl^-/HCO_3^- exchange activity was further enhanced by cAMP, a key feature exhibited by normal pancreatic duct cells. The cAMP stimulated Cl^-/HCO_3^- exchange was inhibited by dihydro-4,4′-diisothiocyanostilbene-2,2′-disulfonic acid (H_2-DIDS), but not by a specific CFTR inhibitor, $CFTR_{inh}$-172. Our data show that SeV vector is a potential CFTR gene transfer agent for human pancreatic duct cells and that expression of CFTR in CF cells is associated with a restoration of Cl^- and HCO_3^- transport at the apical membrane.

J. Cell. Physiol. 214: 442–455, 2008.

Abbreviations: β, buffering capacity; BCECF-AM, 2′,7′-bis-(2-carboxyethyl)-5(6)-carboxyfluorescein-acetoxymethyl ester; CF, cystic fibrosis; CFTR, cystic fibrosis transmembrane conductance regulator; dbcAMP, 2′-O-dibutyryladenosine 3′,5′-cyclic monophosphate; DMSO, dimethyl sulphoxide; DRA, downregulated in adenoma; H_2-DIDS, dihydro-4,4′-diisothiocyanostilbene-2,2′-disulfonic acid; IBMX, 3-isobutyl-1-methylxanthine; J_B, base flux; LacZ, β-galactosidase; MOI, multiplicity of infection; NBC, Na^+/HCO_3^- cotransporter; NHE, Na^+/H^+ exchanger; NMDG, N-methyl-D-glucamine; PAT-1, putative anion transporter-1; pH_i, intracellular pH; PKA, protein kinase A; R_T, transepithelial resistance; SDS, sodium dodecyl sulphate; SeV, Sendai virus; wt, wild-type.

Contract grant sponsor: The Wellome Trust;
Contract grant numbers: 069470 (to ZR), 022618 (to PH);
Contract grant sponsor: Hungarian Academy of Sciences;
Contract grant numbers: BO 00218/06 (to ZR), BO 00276/04 (to PH);
Contract grant sponsor: Hungarian Scientific Research Fund;
Contract grant number: PF63951 (to ZR);
Contract grant sponsor: Hungarian Medical Research Council;
Contract grant number: 517/2006 (to JL);
Contract grant sponsor: FCT, Portugal;
Contract grant number: SFRH/BD/17475/2004 (to ACDP);
Contract grant sponsor: The Physiological Society (UK).

*Correspondence to: Dr. Michael A. Gray, Institute for Cell and Molecular Biosciences, School of Biomedical Sciences, University of Newcastle upon Tyne, Medical School, Framlington Place, Newcastle upon Tyne, NE2 4HH, United Kingdom.
E-mail: m.a.gray@ncl.ac.uk

Received 8 January 2007; Accepted 12 June 2007

DOI: 10.1002/jcp.21220

Cystic fibrosis (CF) is one of the most common autosomal recessive diseases in Caucasian people and is caused by absence or dysfunction of CF transmembrane conductance regulator (CFTR), a cAMP/protein kinase A (PKA) regulated Cl^- channel that is expressed on the apical membrane of epithelial cells (Rowntree and Harris, 2003). Sixty two percent of CF patients are pancreatic insufficient at birth, and a proportion (about 21%) of patients who are born with a functional pancreas will later become pancreatic insufficient (Waters et al., 1990). Pancreatic insufficiency is treated with digestive enzyme replacement therapy, but many CF patients have a poor nutritional status making them potentially more susceptible to lung infections (Dodge and Turck, 2006).

CFTR is highly expressed in the ductal system of the pancreas, which secretes a HCO_3^- rich fluid. This alkaline fluid washes digestive enzymes (secreted by acinar cells) into the duodenum and also neutralizes acid chyme entering the duodenum from the stomach (Argent et al., 2006). Pancreatic HCO_3^- secretion is markedly reduced in CF patients (Choi et al., 2001) and this defect probably leads to cyst formation and gland fibrosis in two ways. First, reduced fluidity within the duct lumen initiates precipitation of digestive enzymes and eventual blockage of the ducts (Scheele et al., 1996). Increased luminal pressure above the blockage would then cause cyst formation and leakage of digestive enzymes into the parenchyma of the gland. Second, reduced alkalinity in the duct lumen causes destruction of acinar cells due to the failure of apical membrane recycling following enzyme secretion (Scheele et al., 1996). As well as causing the pancreatic pathology in CF, mutations in CFTR are also associated with increased susceptibility to acute and chronic pancreatitis in the population (Rowntree and Harris, 2003).

Gene therapy offers the best hope for a cure of CF, but to date research in this area has largely focused on the lung with vector delivery via the airways (Griesenbach et al., 2006; Rosenecker et al., 2006). Treatment of the pancreatic defect will require either systemic gene therapy, with targeting of the vector carrying CFTR gene to the ductal epithelium, or retrograde injection of the vector into the pancreatic duct. The aim of this study was to assess the utility of a novel recombinant Sendai virus (SeV) vector construct, which has been previously shown to efficiently infect to the airway epithelium (Yonemitsu et al., 2000), as a vector for introducing CFTR into human pancreatic duct cells in vitro. SeV vector is a new class of cytoplasmic RNA vector that is free from genotoxicity and infects and multiplies in a wide variety of mammalian cells and tissues, including the airway epithelium (Bitzer et al., 2003; Griesenbach et al., 2005). In addition, this vector directs high-level transgene expression and its expression can be regulated at different levels making it possible to avoid cell toxicity due to over-expression during gene therapy (Tokusumi et al., 2002).

We used CFPAC-1 cells, a human pancreatic ductal adenocarcinoma cell line that is homozygous for the common F508del CFTR mutation, as a model of the CF pancreatic duct (Schoumacher et al., 1990). Stable transfection methods have been used successfully in the past to correct the CFTR defect in CFPAC-1 cells (Greeley et al., 2001). Because CFPAC-1 cells can be grown as functionally polarized monolayers (Rakonczay et al. 2006), we have been able to assess the effect of SeV vector-mediated CFTR transduction on the functional polarity of the pancreatic duct epithelium and on the activity of the key membrane transporters involved in HCO_3^- secretion. Our work was prompted by the fact that DNA-based therapies are currently being explored as treatment strategies for other pancreatic diseases, such as pancreatic cancer (for a review see Tamada et al. 2005). Moreover, pancreatic sufficiency (as judged by the absence of steatorrhoea) can be maintained with only 10% of normal pancreatic function (DiMagno et al., 1973), so a gene therapy protocol that provided even a small improvement in pancreatic function might be beneficial to CF patients.

Materials and Methods

Materials and solutions

All laboratory chemicals were purchased from Sigma (Poole, Dorset, UK). 2′,7′-bis-(2-carboxyethyl)-5(6)-carboxyfluorescein-acetoxymethyl ester (BCECF-AM) and dihydro-4,4′-diisothiocyanostilbene-2,2′-disulfonic acid (H_2-DIDS) were from Molecular Probes, Inc. (Eugene, OR). The selective CFTR inhibitor $CFTR_{inh}$-172 (Ma et al., 2002) was kindly provided by Prof. A. S. Verkman (University of California, San Francisco, CA, USA). Stock solutions of BCECF-AM (2 mM) and $CFTR_{inh}$-172 inhibitor (10 mM) were prepared in dimethyl sulphoxide (DMSO). 5-bromo-4-chloro-3-indolyl-β-D-galactopyranoside (X-gal, 50 mg/ml) was dissolved in dimethylformamide. Nigericin (10 mM) and forskolin (50 mM) were dissolved in ethanol and stored at −20°C. Polyester Transwells were supplied by Corning-Costar (Buckinghamshire, UK). The standard HEPES-buffered solution contained (mM): 130 NaCl, 5 KCl, 1 $MgCl_2$, 1 $CaCl_2$, 10 Na-HEPES, 10 D-glucose (pH 7.4 with HCl). In the Na^+-free HEPES solution NaCl was replaced by 140 mM N-methyl-D-glucamine (NMDG)-Cl and the Na-HEPES was replaced by equimolar HEPES-acid. In the Na^+-free HEPES solution containing 20 mM NH_4Cl, the concentration of NMDG-Cl was reduced to maintain osmolarity. The standard HCO_3^--buffered solution contained (mM): 115 NaCl, 5 KCl 1 $MgCl_2$, 1 $CaCl_2$, 25 Na-HCO_3, 10 D-glucose. In the K^+-free HCO_3^--buffered solution KCl was replaced by equimolar NaCl. The high-K^+ HCO_3^--buffered solution contained (mM): 5 NaCl, 115 KCl, 1 $MgCl_2$, 1 $CaCl_2$, 25 Na-HCO_3, 10 D-glucose. The Cl^--free HCO_3^- solution contained (mM): 115 Na-gluconate, 2.5 K_2SO_4, 6 Ca-gluconate, 1 Mg-gluconate, 25 Na-HCO_3, 10 D-glucose. All solutions containing HCO_3^- were continuously equilibrated with 5% CO_2—95% O_2 to maintain pH at 7.4.

Culturing of CFPAC-1 cells

CFPAC-1 cells (passage number 50–60) were obtained from Prof. R. A. Frizzell (University of Pittsburgh, Pittsburgh, PA, USA) and were grown in Iscove's modified Dulbecco's medium supplemented with 10% foetal calf serum, 2 mM glutamine, 100 units/ml penicillin, and 0.1 mg/ml streptomycin and were cultured as described previously (Schoumacher et al., 1990). The medium was changed every 1–2 days. Cells were maintained at 37°C in a humidified atmosphere containing 5% CO_2. Cell monolayers were prepared by seeding at high density (300,000–350,000 cells/cm^2) onto polyester permeable supports (12 mm diameter, 0.4 μm pore size Transwells). Cell confluence was checked by microscopy and determination of transepithelial electrical resistance (R_T) using an EVOM-G voltohmmeter (World Precision Instruments, Sarasota, FL).

Measurement of intracellular pH (pH_i) and determination of buffering capacity (β)

Intracellular pH (pH_i) was estimated as described previously (Thomas et al., 1979; Hegyi et al., 2004; Rakonczay et al., 2006). Briefly, after loading the cells with 2 μM BCECF-AM, the Transwells were transferred to a perfusion chamber mounted on an inverted Nikon Diaphot microscope (Nikon UK, Kingston upon Thames, UK). Experiments were performed on a group of 10–15 cells at 37°C. Apical and basal bath volumes were 0.5 and 1 ml and the perfusion rates were 3 and 6 ml/min, respectively. pH_i was measured using a Life Sciences microfluorimeter system (Life Sciences Resources, Cambridge, UK).The intrinsic buffering capacity (β_i) of CFPAC-1 cells was estimated according to the NH_4^+ prepulse technique (Weintraub and Machen, 1989; Rakonczay et al., 2006). The total buffering capacity (β_{total}) was calculated as $\beta_{total} = \beta_i + \beta_{HCO_3^-}$, where $\beta_{HCO_3^-}$ is the buffering capacity of

the HCO_3^-/CO_2 system. $\beta_{HCO_3^-} = 2.3 \times [HCO_3^-]_i$. $[HCO_3^-]_i$ is the intracellular concentration of HCO_3^-.

Net change in pH_i (ΔpH_i) and calculation of base flux

The net change in pH_i (ΔpH_i) was measured by determining the pH_i immediately before and at the peak level after the changes of solutions by averaging the values of 80 data points. The initial rates of change of pH_i (over 30–50 sec) resulting from solution changes were used to calculate transmembrane base flux (J_B). J_B = change of $pH_i/\Delta t \times \beta_{total}$. The β_{total} value used in the calculation of J_Bs was obtained by using the average pH_i value over a 30 sec period immediately before changing solutions. We denote base influx as J_B and base efflux as $-J_B$.

Construction of recombinant Sendai virus (SeV) vector

The genome order of the full length SeV used in this study was as follows: a leader (ld) sequence at the 3′-end followed by the following viral genes; nucleocapsid (NP), phospho (P), matrix (M), fusion (F), hemagglutinin-neuraminidase (HN), and large proteins (L). Finally, a small trailer (tr) sequence was placed at the 5′-end. We utilized the wild-type (wt) SeV vector (SeV(+)MF) (Tokusumi et al., 2002), in which a NotI restriction site for insertion of the gene of interest is located between the M and F genes. SeV(+)MF carrying the human CFTR gene (SeV-CFTR) was constructed as previously described (Kato et al., 1996). In brief, human CFTR (accession no. M28668) cDNA was amplified with a pair of NotI-tagged primers that contained SeV-specific transcriptional regulatory signal sequences, 5′-ACTTGCGGCCGCCAAAGTT-CAATGCAGAGGTCGCCTCTGGAAAAGGCCAGC-3′ and 5′-ATCCGCGGCCGCGATGAACTTTCACCCTAAGTTTTT-CTTACTACGGCTAAAGCCTTGTATCTTGCACCTCTTC-TTC-3′. The amplified fragment was introduced into the NotI restriction site of the parental pSeV(+)MF, thereby incorporating the cDNA of SeV-CFTR. Note that a number of silent nucleotide changes were introduced into the CFTR cDNA to ensure efficient SeV vector-mediated CFTR expression (Ferrari et al., 2007). The cDNA of the wt SeV vector carrying the LacZ gene (SeV-LacZ) was constructed as previously described using the amplified fragment of LacZ (Shiotani et al., 2001). pSeV-CFTR and pSeV-LacZ were transfected into LLC-MK2 cells after infection of the cells with vaccinia virus vTF7-3 (Fuerst et al., 1986), which expresses T7 polymerase. The T7-driven recombinant SeV-CFTR and SeV-LacZ RNA genomes were encapsulated by NP, P, and L proteins, which were derived from their respective cotransfected plasmids. Forty hours later, the transfected cells were injected into 10-day-old embryonated chicken eggs to amplify the recovered virus (Kato et al., 1996). The SeV vector titer was determined by a hemagglutination assay using chicken red blood cells, and the virus was stored at −70°C until use.

Infection with recombinant Sendai virus (SeV)

For pH_i measurements, or LacZ staining, confluent CFPAC-1 cells grown on Transwells were infected with SeV-CFTR or SeV-LacZ (nuclear localized) 3 days after seeding. Preliminary experiments showed that the cells were much more efficiently infected from the apical compared to the basolateral side. Therefore, after washing the cells with phosphate-buffered saline (PBS), 6×10^5 (0.6 μl) or 3×10^6 (3 μl) plaque forming units (multiplicity of infection, MOI = 3 or 15) of SeV vector was applied to the apical side of the cells in serum-free Iscove's modified Dulbecco's medium (30–32.4 μl) for 1 h. The basolateral side of the cells was incubated in serum-free Iscove's modified Dulbecco's medium (800 μl) only. Thereafter, serum containing Iscove's modified Dulbecco's medium was added to the upper (470 μl) and lower (700 μl) compartments of the Transwells. Twenty-four hours later the cells were rinsed with PBS and fed with fresh virus-free, serum-containing, Iscove's modified Dulbecco's medium. Control (i.e., uninfected) CFPAC-1 cells were subjected to a similar protocol, but the virus aliquots were substituted with serum-free Iscove's modified Dulbecco's medium. Experiments were performed 48–96 h after infection.

For CFTR expression or PKA analysis confluent CFPAC-1 cells, grown in 25 cm^2 tissue culture flasks, were washed with PBS and incubated with serum-free Iscove's modified Dulbecco's medium (825 μl, control), SeV-CFTR or SeV-LacZ in serum-free Iscove's modified Dulbecco's medium (MOI = 3 or 15) for 1 h. Thereafter, 9.2 ml of serum-containing Iscove's modified Dulbecco's medium was added to the flasks. Twenty-four hours later the cells were rinsed with PBS and were fed with fresh virus-free serum-containing Iscove's modified Dulbecco's medium. The cells were trypsinised, pelleted, and frozen on dry ice 48 h after infection.

β-Galactosidase staining

β-Galactosidase activity was detected by in situ staining (Yonemitsu et al., 2000). CFPAC-1 cells grown on Transwells or plastic were washed with PBS and fixed at 4°C in a PBS solution containing 2% formaldehyde, 0.2% glutaraldehyde, 2 mM $MgCl_2$, and 5 mM EGTA for 10 min. The cells were then rinsed with washing buffer (0.01% sodium deoxycholate, 0.02% NP-40 and 2 mM $MgCl_2$ in PBS) and incubated with a chromophore solution (0.1% 5-bromo-4-chloro-3-indolyl-β-D-galactopyranoside, 5 mM potassium ferrocyanide, and 5 mM potassium ferricyanide in washing buffer) at 37°C for 1–2 h. The number of infected (blue) and uninfected cells was counted microscopically and averaged in 5–6 randomly selected 400× viewing fields.

Expression of DRA, PAT-1, AE2, pNBC1, NHE2, NHE3 mRNAs

Isolation of mRNA and reverse transcription (RT). To study the expression of transporter mRNAs in uninfected, SeV-LacZ or SeV-CFTR infected CFPAC-1 cells grown in 25 cm^2 tissue culture flasks, total RNA was isolated using the GenElute™ Mammalian Total RNA Miniprep Kit (Sigma). The RNA concentration was determined by measuring the optical density at 260 nm. RNA integrity was verified by electrophoresis on 1% agarose gel. Total RNA (1 μg) was used for cDNA synthesis by oligodT priming (M-MLV Reverse Transcriptase, RNase H Minus, Point Mutant, Promega, Madison, WI).

Semi-quantitative polymerase chain reaction (PCR). First-strand cDNA was amplified with PCR primers designed, by Primer3 software (Whitehead Institute for Biomedical Research, Cambridge, MA), to be specific for selected transporters (Table 1). PCR was performed using *Taq* polymerase (Promega). Following an initial denaturation at 95°C for 2 min and 30–35 cycles of amplification, samples were incubated at 72°C for a further 5 min. The PCR products were resolved on agarose gels. As an internal concentration reference for the PCR experiments, we performed 19 cycles of amplification with primers for the acidic ribosomal phosphoprotein (XS13) (Wallrapp et al., 1997). Total RNA extracts from normal human pancreas (Stratagene, La Jolla, CA) and HPAF cells were used as positive control for selected primers of electrolyte transporters.

Real-time PCR. For quantitative analysis of gene expression of DRA, PAT-1, AE2, NHE2, and NHE3, real-time PCR was performed.

TABLE 1. Sequences of Primers Used for Semi-Quantitative RT-PCR

			Expected product size (bp)
AE2	Fwd:	5′-CCTCGGTGCAGTTCTTTCTC-3′	373
	Rev:	5′-TTCATGAGGTCTAGGTCGGC-3′	
DRA	Fwd:	5′-GTTCAGGAGAGCACAGGAGG-3′	281
	Rev	5′-TGAAATGCCACACTAGCTGC-3′	
PAT-1	Fwd:	5′-AGGTAGATGTCGTGGGCAAC-3′	264
	Rev:	5′-CCAGGCTCCGAGACATAGAG-3′	
pNBC1	Fwd:	5′-ACA CCT CTT CCA TGG CTC TG-3′	191
	Rev:	5′-ACC TCG GTT TGG ACT TGT TG-3′	
XS13	Fwd:	5′-CGT GCT AAG TTG GTT GCT TT-3′	500
	Rev:	5′-GCAGCTGATCAAGACTGGA-3′	

Real time PCR primers and FAM-labeled MGB target-specific fluorescence probe were purchased from Applied Biosystems (Foster City, CA) for DRA (Hs00230798_m1), PAT-1 (Hs00370470_m1), AE2 (Hs00161738_m1), NHE2 (Hs00268166_m1), NHE3 (Hs00188200_m1), and human acidic ribosomal phosphoprotein P0 (RPLPO, Hs99999902_m1). RPLPO, was used as positive control. The template cDNAs was amplified by the Universal Mastermix (Applied Biosystems) containing AMP-erase. For detection of fluorescence signal during the PCR cycles, the ABI Prism Sequence Detection System 7700 (Applied Biosystems) was employed with the default setting (50°C for 2 min, 95°C for 10 min, 45 cycle: 95°C for 15 s, 60°C for 1 min). Each experiment was repeated two times with 2 replicates. Changes in levels of gene expression were estimated based on the real-time PCR data by calculating the relative expression values (reference/control sample) for the target RNA in each sample and normalizing them by dividing with the relative value of RPLPO from the same sample (Livak and Schmittgen, 2001).

Western blots

CFTR. Total protein extracts from CFPAC-1 and CAPAN-1 cells, as well as from baby hamster kidney (BHK) cells stably expressing wt or F508del-CFTR (Chang et al., 1993) (as controls) were analyzed for CFTR protein expression by Western blotting as described previously (Farinha et al., 2004a,b).

PKA catalytic subunit. PKA catalytic subunit (PKAcat) was detected from the immunoprecipitated pellet used for the PKA activity assay (see below). SDS–PAGE was performed using the Novex (Invitrogen Ltd., Paisley, UK) system on 4–12% Bis-Tris polyacrylamide gels and the proteins were transferred to nitrocellulose membranes. Following blocking in TBS-Tween (0.5% Tween-20) plus 5% milk powder for 30 min, membranes were incubated with anti-PKAcat (C20) antibody for 90 min (1:1,000 dilution, Santa Cruz (sc-903), Santa Cruz, CA) and a secondary anti-rabbit antibody (1:5,000 dilution, Sigma) for 45 min. Enhanced chemiluminescent reagent (Amersham, Little Chalfont, U.K.) was used for visualization.

PKA activity assay

Homogenization of CFPAC-1 cells was achieved by mechanical lysis (Polytron) in three volumes of ice-cold buffer (10 mM Tris, 20 mM NaH_2PO_4, 1 mM EDTA, pH 7.8 containing a fresh protease inhibitor cocktail (Boehringer complete tablet). Whole cell lysates were used as input material for immunoprecipitation. Prior to precipitation, dimethyl pimelimidate linking of PKAcat antibody to protein A sepharose beads was performed according to the method of Harlow and Lane (1988). A 7 μl slurry of antibody-crosslinked protein-A beads was added to 20 μg of whole cell lysate. Samples were then shake-incubated for 60 min at 4°C. The samples were pelleted in a desktop centrifuge, followed by 3 × 1 ml washes with standard assay buffer (50 mM HEPES, pH 7.0, 50 mM NaF, 1.0 mM EGTA, 1.0 mM EDTA, 0.2% Tween-20, 10% glycerol) containing 1 M NaCl and 3 × 1ml washes into standard assay buffer. Precipitation pellets were re-suspended in 20 μl of assay buffer and assayed/probed as described. PKA activity was determined by measuring the incorporation of γ-^{32}P from [γ-^{32}P]ATP (Perkin-Elmer) into the S660 residue of a known amount of purified CFTR-NBD1 fragment (bacterially expressed and purified to homogeneity). Assays were carried out at 30°C for 10 min and terminated by spotting a 15 μl aliquot onto a 1 cm^2 piece of P81 phosphocellulose paper and washing 3 × 5 min in 1% phosphoric acid. Incorporation of γ-^{32}P was quantified using a Packard Instant Imager (Muimo et al., 2000). PKA peptide inhibitor (Calbiochem, Nottingham, U.K.) was used at a working concentration of 100 nM to specify the phosphotransfer activity of PKA.

Iodide efflux assay

Iodide efflux was performed using the protocol described for CFTR-transfected BHK cells (Hughes et al., 2004). After the iodide release had reached a steady state (6 min), the intracellular cAMP level was raised by agonists (10 μM forskolin, 100 μM 3-isobutyl-1-methylxanthine, IBMX, and 100 μM 2′-O-dibutyryladenosine 3′,5′-cyclic monophosphate, dbcAMP) and collection of the efflux medium was resumed for an additional 10 min. In some experiments the cells were administered 10 μM $CFTR_{inh}$-172 or DMSO after removing the iodide loading buffer. The amount of iodide in each sample was determined with an iodide-selective electrode (Thermo Electron Corporation, Fife, Scotland).

Statistical analyses

To avoid errors arising from the variation in the rate and magnitude of HCO_3^- uptake between different set of monolayers, we performed the respective measurements on the same day from one set of cell cultures and in random order and where possible, internal control experiments were carried out. Statistical analyses were determined using either the Student's paired or unpaired *t*-test or the analysis of variance as appropriate. $P < 0.05$ was accepted as statistically significant.

Results

Efficiency of SeV vector-mediated gene transfer

To estimate the efficiency of gene transfer, SeV-LacZ was added to either the basolateral or apical membrane of polarized CFPAC-1 monolayers for 1 h. (n = 6). LacZ activity was measured between 48 and 96 h after infection. Initial experiments showed that very little gene transfer occurred following basolateral exposure to SeV-LacZ. However, following application of SeV-LacZ to the apical membrane at MOI = 3, strong, homogenous LacZ activity was observed in 32 ± 2% of cells. At the higher MOI = 15, 68 ± 3% of the cells were stained. Thus, transduction with SeV vector was more efficient via the apical membrane of CFPAC-1 cells and the proportion of cells infected was clearly dose-related. The former observation suggests that retrograde injection of SeV-CFTR into the pancreatic duct would be required to treat CF patients with this vector.

Effect of SeV vector-mediated transduction on the expression of CFTR, H^+, and HCO_3^- transporters

Figure 1 shows that CFPAC-1 and SeV-LacZ infected cells exhibited very little CFTR protein expression as judged by Western blotting. In these cells only immature CFTR (i.e., core-glycosylated or band B) could be detected, as a very faint band. Similar results were obtained with BHK cells stably expressing F508del-CFTR, although band B staining was much stronger. However, both immature and mature (i.e., fully-glycosylated, processed, or band C) forms of CFTR were detected in SeV-CFTR transduced CFPAC-1 cells, and in the positive controls (CAPAN-1 cells and BHK cells stably expressing wt CFTR).

Functional expression of CFTR was assessed by the iodide efflux assay (Fig. 2). Increases in intracellular cAMP had no effect on iodide efflux in SeV-LacZ (MOI = 3) (n = 8) (Fig. 2A) or in SeV-CFTR (MOI = 15) cells (n = 4, results not shown). In contrast, cAMP stimulated iodide efflux in four out of five experiments (80%) with SeV-CFTR (MOI = 3) cells (Fig. 2B). Finally, Figure 2B also shows that the effect of cAMP on iodide efflux was completely blocked by 10 μM $CFTR_{inh}$-172 (n = 4).

As well as CFTR, a number of other transporters are essential for HCO_3^- secretion by the duct cell (Steward et al., 2005; Argent et al., 2006). These include Na^+/HCO_3^- cotransporters (pNBC1) and Na^+/H^+ exchangers (NHE1) on the basolateral membrane that transport HCO_3^- into the cell and SLC26 family anion exchangers (PAT-1, DRA) that, together with CFTR, secrete HCO_3^- across the apical membrane (Steward et al., 2005; Argent et al., 2006). In addition, AE2 and NHE3 are probably expressed in the basolateral and apical membranes, respectively, although their role in ductal HCO_3^- transport remains to be clarified (Steward

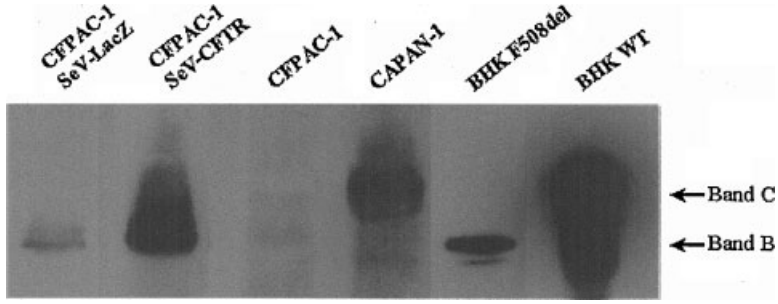

Fig. 1. CFTR protein in SeV infected CFPAC-1 cells (MOI = 15). Representative Western blots of total protein extracts from cells grown in 25 cm^2 flasks using anti-CFTR M3A7 antibody after SDS–PAGE electrophoresis on a 7.5% (w/v) polyacrylamide gel. To prevent over exposure of the film different amounts of protein were loaded as follows: 30 μg for the BHK cells, 50 μg for the CFPAC-1 SeV-CFTR cells, and 100 μg for the remainder of the cell lines. Note the marked increase in CFTR protein expression in SeV-CFTR infected CFPAC-1 cells (50 μg protein per lane) compared to the untransduced and vector only cells (100 μg protein per lane). Both immature, core-glycosylated (band B, 160 kDa) and processed, that is, fully-glycosylated (band C, 170–180 kDa) forms of CFTR were detected in CAPAN-1 and CFPAC-1 SeV-CFTR cells, and in the control BHK wt cells. Uninfected and SeV-LacZ transduced cells exhibited very little CFTR expression (only band B).

et al., 2005; Argent et al., 2006). We examined whether CFPAC-1 cells expressed these transporters and whether infection with SeV vector affected the expression level.

Figure 3A shows that PAT-1, AE2, and pNBC1 were constitutively expressed in uninfected and SeV vector transduced CFPAC-1 cells as determined by semi-quantitative PCR. However, we did not detect mRNA for DRA, NHE2, and NHE3. CFTR transduction had no obvious effect on the level of the mRNA's for PAT-1, AE2, pNBC1 (Fig. 3A), and NHE2 (data not shown). Again, mRNA for DRA and NHE3 was not detectable after CFTR expression. The control house-keeping gene XS13, which encodes a ribosomal phosphoprotein, showed similar expression levels in all the cell samples (Fig. 3A). Note that in the normal pancreas (lane P in Fig. 3A), PAT-1 and pNBC1 were expressed at relatively low levels, and AE2 was not detectable. However, duct cells form only ~10% by volume of the normal gland, so the extracted RNA will be largely derived from acinar cells (Argent et al., 2006).

We also performed some experiments using real-time PCR (Fig. 3B). Again, no statistical difference was found in the expression levels of PAT-1 and AE2 amongst the different cell groups (Fig. 3B). As before, we were unable to detect DRA, NHE2, and NHE3 expression in any of the cells lines using real-time PCR. Taken together, these data indicate that with the exception of CFTR, CFPAC-1 cells express the key transporters required for HCO_3^- secretion, namely pNBC1 and PAT-1. Importantly, in terms of gene therapy, SeV vector infection at both MOI = 3 and MOI = 15 (either with or without CFTR expression), did not affect the expression of these key transporters.

Effect of SeV vector-mediated transduction on the integrity of CFPAC-1 cell monolayer

Transepithelial resistance (R_T). R_T can be used as an indicator of the structural integrity of an epithelial sheet, because electrical resistance is largely determined by the "leakiness" of the tight junctions. CFPAC-1 cells grown on polyester Transwells became confluent 2–3 days after seeding, as judged by visual observation. R_T increased steadily over 4–5 days up to a maximum of $199 \pm 10\ \Omega\,cm^2$ in the untransduced cells. R_T was significantly higher in the SeV-LacZ (MOI = 3: $400 \pm 15\ \Omega\,cm^2$, MOI = 15: $314 \pm 13\ \Omega\,cm^2$) and in the SeV-CFTR (MOI = 3: $243 \pm 5\ \Omega\,cm^2$, MOI = 15: $268 \pm 9\ \Omega\,cm^2$) infected groups compared to the untransduced cells (n = 9–69). These data show that transduction with SeV vector did not disrupt the structural integrity of the CFPAC-1 epithelium; if anything the epithelium became slightly "tighter" after exposure to the virus.

Functional polarity of CFPAC-1 cells. As HCO_3^- is a component of a buffer system, pH_i and β_i are crucial parameters in a HCO_3^--secreting epithelial cell. The resting pH_i of CFPAC-1 cells bathed in the standard HEPES solution was 7.11 ± 0.08 (n = 6) and was not significantly different in SeV-CFTR (MOI = 3) transduced cells (7.09 ± 0.10, n = 6). However, the resting pH_i value of SeV-LacZ cells (MOI = 15) was significantly increased (7.26 ± 0.01) compared to the SeV-CFTR cells (7.20 ± 0.02) in the standard HCO_3^-/CO_2 solution (n = 12). We have previously reported that the intrinsic β_i is quite variable in different CFPAC-1 monolayers (see Fig. 1 in Rakonczay et al., 2006). In a previous study, we found that uninfected CFPAC-1 cells had a β_i of 34 ± 8 mM/pH over the pH_i range 7.0–7.2. The respective β_i values for SeV-CFTR and SeV-LacZ (MOI = 15) transduced cells (n = 9–11) at this pH_i range were 46 ± 7 and 46 ± 6 mM/pH. These β_i values are not statistically different. Taken together, our results indicate that SeV vector infection has no obvious effect on pH_i regulatory mechanisms or β_i in CFPAC-1 cells.

We have previously shown that the apical and basolateral membranes of CFPAC-1 cell monolayers exhibit marked differences in their relative CO_2 and HCO_3^- permeabilities (Rakonczay et al., 2006). Exposing the basolateral side to a solution containing HCO_3^-/CO_2 causes pH_i to alkalinize rapidly, suggesting that HCO_3^- permeates the basolateral membrane rather faster than CO_2 (Rakonczay et al., 2006), consistent with presence of base loaders (principally a $NaHCO_3$ cotransporter) on the basolateral membrane of the duct cell. In contrast, exposing the apical membrane to HCO_3^-/CO_2 causes pH_i to acidify rapidly, consistent with faster diffusion of CO_2 from lumen to cell compared with HCO_3^- (Rakonczay et al., 2006). That the apical membrane of pancreatic duct cells resists back diffusion of HCO_3^- from the lumen is likely to be of physiological importance, since it will favor retention of secreted HCO_3^- in the duct lumen. We therefore checked whether the functional polarity of CFPAC-1 cells was disrupted by SeV vector transduction by exposing the apical and basolateral membranes of SeV-LacZ and SeV-CFTR-transduced cells to HCO_3^-/CO_2.

Figure 4A shows a continuous pH_i recording from a SeV-LacZ (MOI = 15) infected monolayer (n = 12). Initially, the apical and basolateral membranes were perfused with the standard HEPES solution and then the apical solution was

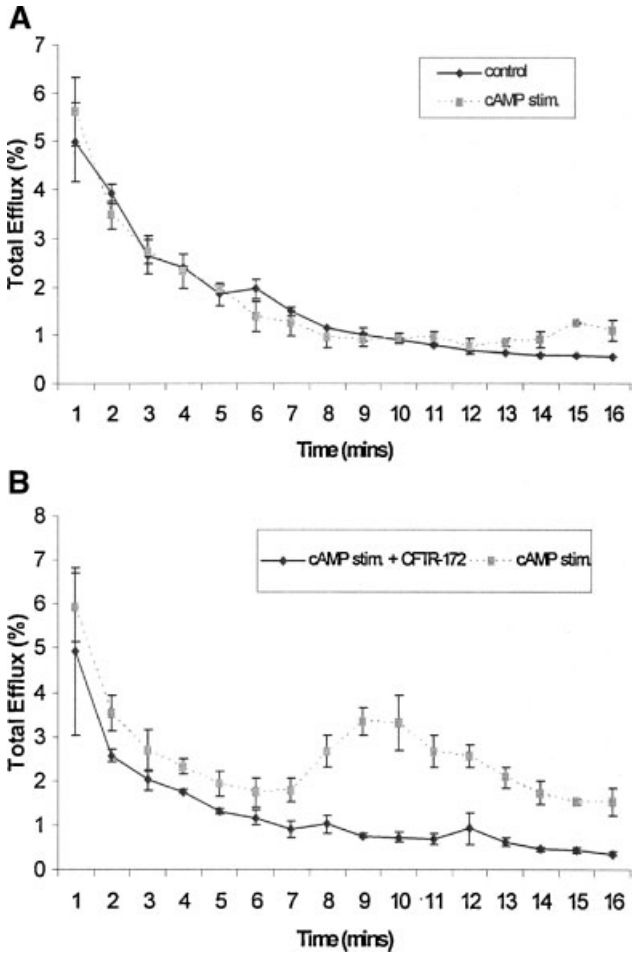

Fig. 2. Functional expression of CFTR in CFPAC-1 cells determined using iodide efflux. A: Iodide efflux from SeV-LacZ cells was not increased by exposure to cAMP (n = 8 experiments). B: In contrast, cAMP-stimulated iodide efflux from SeV-CFTR (MOI = 3) in 4/5 experiments. Data shown are from the four positive experiments. CFTR-172 (10 μM) abolished the stimulatory effect of cAMP (n = 4 experiments). Cells were exposed to a cAMP cocktail (10 μM forskolin, 100 μM 3-isobutyl-1-methylxanthine, IBMX, and 100 μM 2′-O-dibutyryladenosine 3′,5′-cyclic monophosphate, dbcAMP) from the 7th till the 16th min. Data points are mean ± SE.

switched to HCO_3^-/CO_2 (Fig. 4A). This caused the expected rapid acidification of pH_i (Rakonczay et al., 2006), most likely due to CO_2 diffusion into the cells. In 24 similar experiments the ΔpH_i and $-J_B$ following apical HCO_3^-/CO_2 addition were -0.20 ± 0.01 and -23.7 ± 0.9 mM B/min, respectively. After the rapid acidification, pH_i remained stable at the new level (Fig. 4A). Finally, switching the basolateral solution to HCO_3^-/CO_2 caused a rapid alkalinization of pH_i (Fig. 4A), most likely due to rapid HCO_3^- uptake into the cells (Rakonczay et al., 2006). The associated ΔpH_i and J_B were 0.37 ± 0.01 and 17.14 ± 0.74 mM B/min, respectively.

Figure 4B shows a similar experiment performed on SeV-CFTR (MOI = 15) transduced cells (n = 12). The fall in pH_i following apical HCO_3^-/CO_2 addition was not significantly different from that observed in the SeV-LacZ cells (compare Fig. 4A and B). However, after the rapid acidification, pH_i continued to rise slowly in about 50% of the experiments (by 0.034 ± 0.006 during 4 min, n = 8) with SeV-CFTR transduced cells (Fig. 4B). CFTR does exhibit a finite permeability to HCO_3^- (Gray et al., 1990; Linsdell et al., 1997), so this slow alkalinization might reflect back flux of HCO_3^- from the luminal compartment through CFTR. Switching the basolateral solution to HCO_3^-/CO_2 caused pH_i to alkalinize in the high titer SeV-CFTR (MOI = 15) cells (Fig. 4B). However, comparison of Fig. 4B with Fig. 4A, suggests that both the rate (J_B was 10.37 ± 0.69 mM B/min) and the degree of the alkalinization (ΔpH_i was 0.27 ± 0.01) of SeV-CFTR cells were significantly reduced compared to SeV-LacZ cells (see J_B and ΔpH_i values in the previous paragraph). In contrast, in the low titer SeV-CFTR (MOI = 3) cells, switching the basolateral solution to HCO_3^-/CO_2 caused pH_i changes similar to those observed in SeV-LacZ cells (data not shown).

These data are consistent with hyperexpression of CFTR in the high titer MOI = 15 cells either decreasing the rate at which HCO_3^- enters across the basolateral membrane or increasing the rate of HCO_3^- efflux across the apical membrane. Nevertheless, cells transduced with SeV vector, even at a high vector concentration, clearly retain the typical differences in apical and basolateral CO_2 and HCO_3^- permeabilities that we have previously described in untransduced CFPAC-1 cells (Rakonczay et al., 2006).

Effect of SeV vector-mediated transduction and CFTR expression on apical Cl^-/HCO_3^- exchange activity. Anion exchange activity can be detected in both the basolateral and apical membranes of pancreatic duct cells (Steward et al., 2005; Argent et al., 2006). The physiological role of the basolateral anion exchangers (probably AE2) is uncertain, as with a normal transmembrane Cl^- gradient they would be expected to cause HCO_3^- efflux and to oppose secretion (Steward et al., 2005; Argent et al., 2006). In contrast, it is well established that secretion of HCO_3^- across the apical membrane of pancreatic duct cells involves both CFTR and SLC26 family Cl^-/HCO_3^- exchangers, although the quantitative importance of each pathway is controversial (Steward et al., 2005; Argent et al., 2006). Furthermore, it has been shown that phosphorylation of CFTR, as occurs during stimulation of HCO_3^- secretion, activates SLC26 anion exchangers (Lee et al., 1999b; Shcheynikov et al., 2006). Our PCR data indicate that PAT 1 (SLC26A6) is the important SLC26 exchanger in CFPAC-1 cells (see Fig. 2A). Given the role of anion exchangers in pancreatic duct cell function, we decided to investigate whether SeV vector transduction and CFTR expression had any effect on their activity.

Basolateral membrane. Figure 5A (left part) shows an experiment in which pH_i was continuously recorded from a SeV-LacZ infected CFPAC-1 monolayer. Removal of Cl^- from the basolateral HCO_3^-/CO_2 solution caused a clear increase in pH_i, indicating that the cells have an anion exchanger on their basolateral membrane. However, when the same experiment was performed on a SeV-CFTR infected monolayer; the alkalinization caused by Cl^- removal was much smaller (Fig. 5A right part).

Figure 5B,C show summary data for the increase in pH_i and J_B caused by basolateral Cl^- removal in SeV-LacZ and SeV-CFTR cells infected at MOI = 3 and 15. Note that in the SeV-CFTR cells (both MOI = 3 and 15) the effects of basolateral Cl^- removal on pH_i and J (B) were significantly reduced (Fig. 5B,C). Also, increasing intracellular cAMP, by exposing the cells to a cocktail of forskolin (10 μM), IBMX (100 μM), and dbcAMP (100 μM), had no significant effect on the ΔpH_i and J_B observed after Cl^- removal in either the SeV-LacZ or the SeV-CFTR (MOI = 3 and 15) cell groups (Fig. 5B,C). These data indicate that transduction of CFPAC-1 cells with CFTR inhibits basolateral Cl^-/HCO_3^- exchange (probably mediated by AE2) and that cAMP has no effect on the activity of this exchanger. However, we cannot exclude the fact that the reduced pH_i change following Cl^- removal, in the absence or presence of

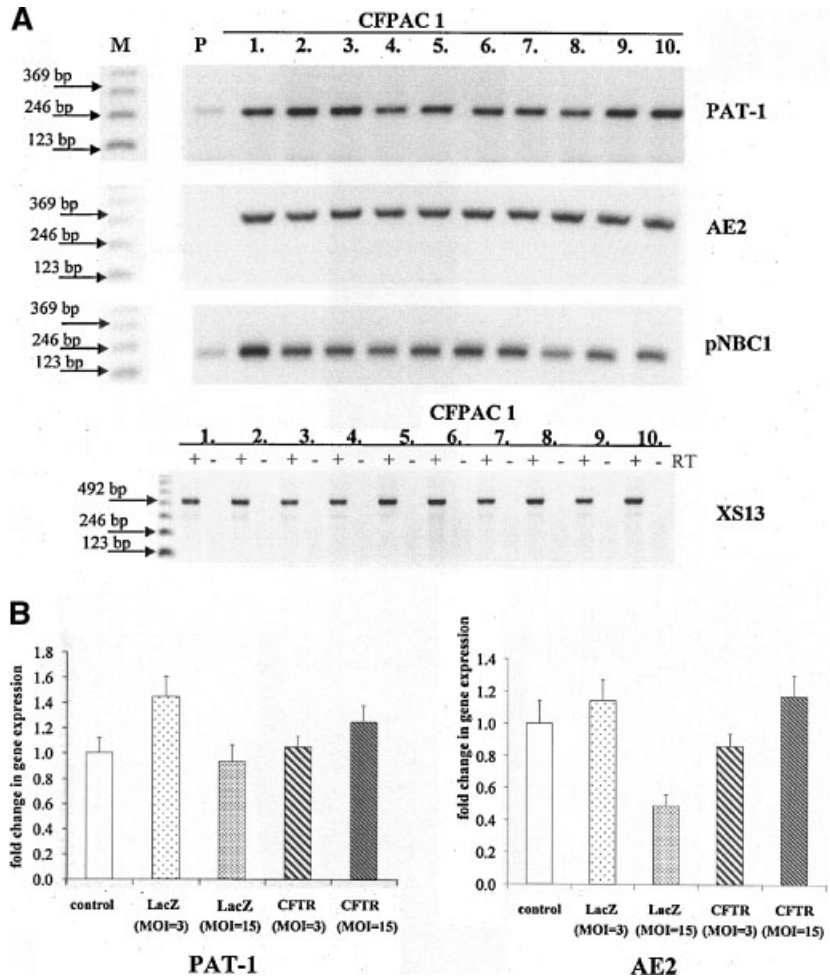

Fig. 3. Expression of HCO_3^- transporters in CFPAC-1 cells. A: Semi-quantitative RT-PCR. Agarose gels stained with ethidium bromide show PCR products for PAT-1, AE2, pNBC1 (upper part) and the positive control ribosomal phosphoprotein gene, XS13 (lower part). Uninfected CFPAC-1 cells (lanes 1,2), Sev-LacZ cells (MOI = 3, lanes 3,4; MOI = 15, lanes 5,6) and SeV-CFTR cells (MOI = 3, lanes 7,8; MOI = 15, lanes 9,10). Lane M is the molecular weight ladder and lane P is normal human pancreas. RT ± indicates the presence/absence of reverse transcriptase in the XS13 experiment. B: Real-time RT-PCR data for PAT-1 and AE2 expression.

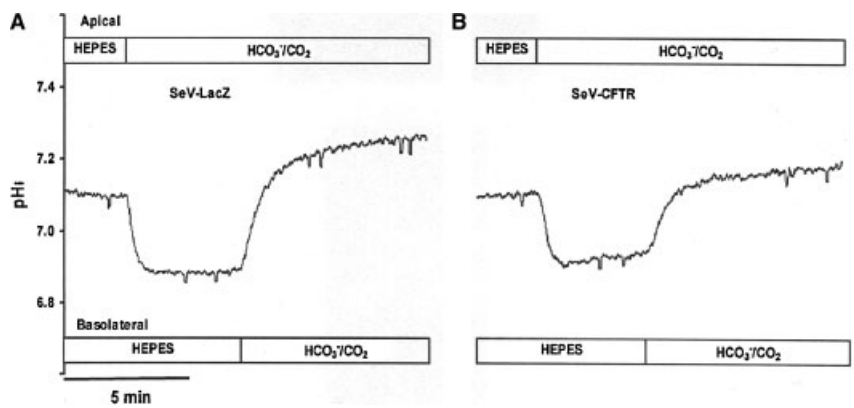

Fig. 4. Functional polarity of CFPAC-1 monolayers. A: Continuous pH_i recording from a SeV-LacZ (MOI = 15) cell monolayer. Horizontal bars indicate the composition of the solutions bathing the apical and basolateral membranes. Both sides of the monolayer were initially perfused with a HCO_3^--free, HEPES-buffered solution and then the apical and basolateral solutions were sequentially changed to standard HCO_3^-/CO_2 as indicated by the horizontal bars. B: Similar experiment on a SeV-CFTR (MOI = 15) cell monolayer. Note that the alkalinization following basolateral addition of HCO_3^-/CO_2 is reduced in the CFTR expressing cells.

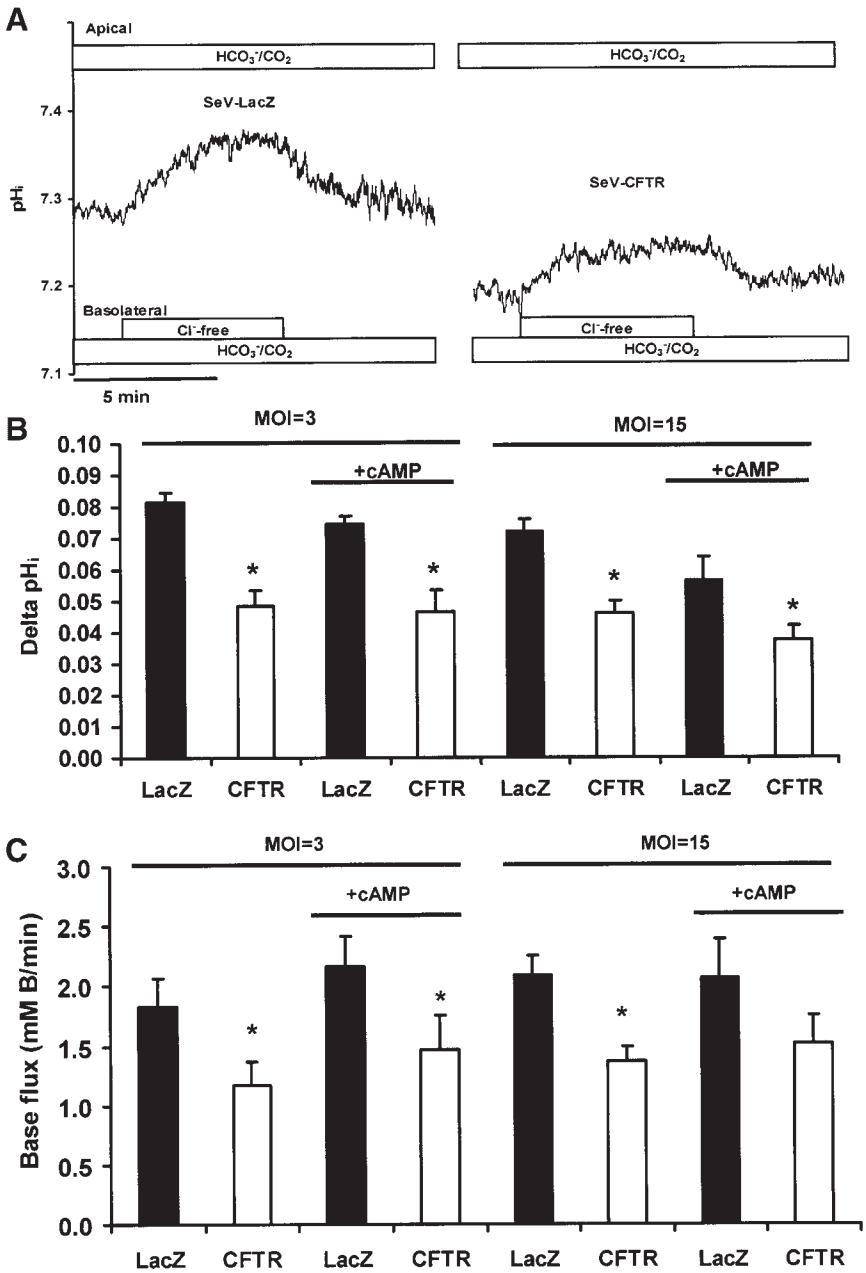

Fig. 5. Basolateral Cl^-/HCO_3^- exchange in CFPAC-1 monolayers (A). Continuous pH_i recordings from SeV-LacZ (left part) and SeV-CFTR (MOI = 15) (right part) infected cells. Horizontal bars indicate the composition of the solutions bathing the apical and basolateral membranes. Removal of Cl^- from the basolateral solution caused pH_i to alkalinize in both cell types, but the effect is larger in the SeV-LacZ cells (left part). B: Summary data for ΔpH_i following basolateral Cl^- removal (n = 6–9) in SeV-LacZ (closed columns) and SeV-CFTR (open columns) transduced cells with and without cAMP stimulation. C: Summary data for the J_B changes following basolateral Cl^- removal. Column notation is the same as (B). * Indicates significant difference ($P < 0.05$) versus the respective control group.

cAMP stimulation could simply reflect faster exit of HCO_3^- across the apical membrane, either through the apical anion exchanger or CFTR. Nonetheless physiologically, inhibition of the basolateral AE2 by CFTR expression would tend to favor HCO_3^- secretion and would be beneficial to CF patients.

Apical membrane. In uninfected CFPAC-1 cells and in SeV-LacZ infected cells, removal of Cl^- from the apical membrane of the monolayers had no effect on pH_i, either in the absence or presence of cAMP (data not shown). Thus, Cl^-/HCO_3^- exchange activity was not detectable in the apical membrane of cells that did not express CFTR.

In contrast, Cl^- removal from the apical membrane of low titer SeV-CFTR MOI = 3 cells caused a clear alkalinization of pH_i (Fig. 6A). Thus, expression of CFTR revealed an anion exchange activity in the apical membrane of CFPAC-1 cells. Figure 6A also shows that stimulating the SeV-CFTR MOI = 3 monolayer with cAMP increased both the rate and magnitude of the pH_i alkalinization following Cl^- removal.

Figure 6B shows a similar experiment performed on SeV-CFTR MOI = 15 cells. Removal of apical Cl^- caused a large alkalinization of pH_i in the high titer cells. However, exposing

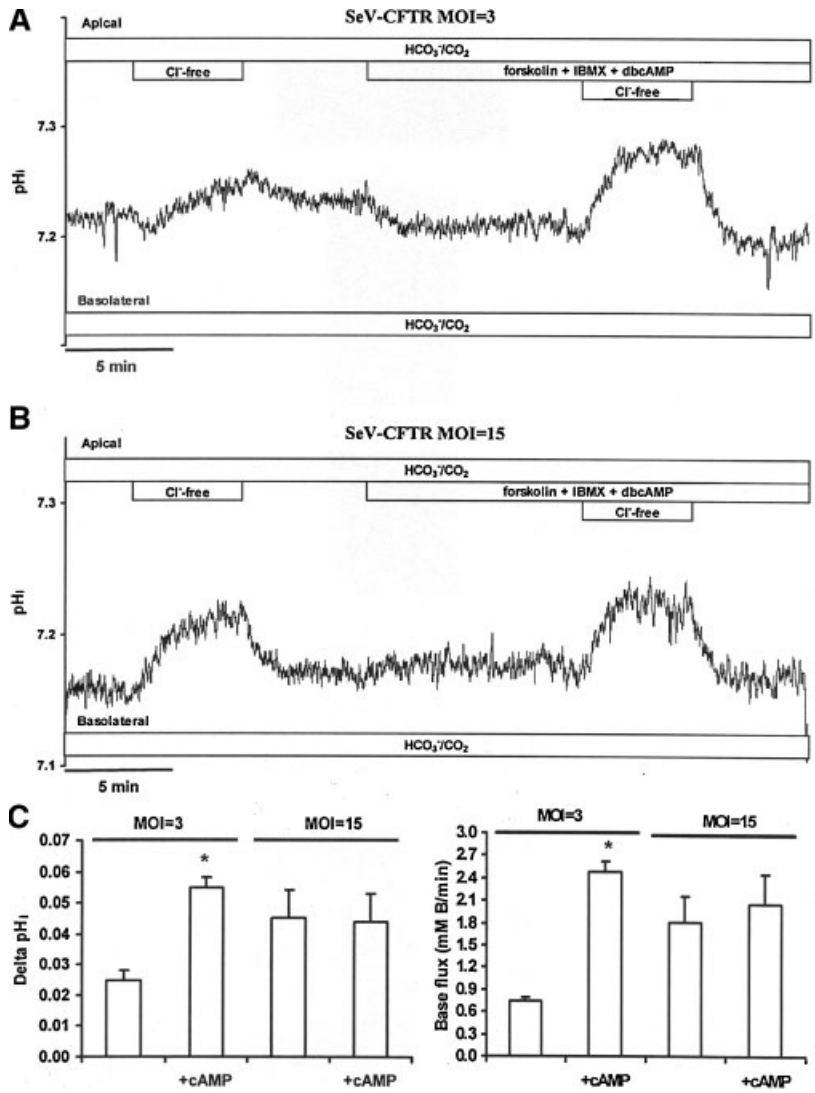

Fig. 6. Apical Cl^-/HCO_3^- exchange activity in SeV-CFTR CFPAC-1 monolayers. A: Continuous pH_i recording from a low titer, SeV-CFTR (MOI = 3), monolayer. Horizontal bars indicate the composition of the solutions bathing the apical and basolateral membranes. Cl^-/HCO_3^- exchange activity was assessed by removing Cl^- from the apical solution, first in the absence and then in the presence of the cAMP cocktail. Note the clear stimulation of Cl^-/HCO_3^- exchange activity in the presence of cAMP. B: Similar experiment performed with a high titer, SeV-CFTR (MOI = 15) monolayer. Note that cAMP did not stimulate Cl^-/HCO_3^- exchange activity. C: Summary data showing the effects of Cl^- removal on pH_i and J_B; n = 31 for MOI = 3 cells and n = 6 for MOI = 15 cells. * Indicates significant difference ($P < 0.05$) versus the respective unstimulated control group.

the SeV-CFTR MOI = 15 cells to cAMP did not increase the degree of alkalinization in response to Cl^- withdrawal (Fig. 6B).

Figure 6C is a summary of the ΔpH_i and J_B values obtained in this series of experiments. Unstimulated CFTR MOI = 3 cells exhibited a low, but clearly detectable, level of apical anion exchange. Furthermore, in these cells cAMP significantly increased ΔpH_i and J_B after apical Cl^- removal by 2.2- and 3.4-fold, respectively ($P < 0.05$ for both parameters, n = 31). In contrast, unstimulated CFTR MOI = 15 cells exhibited a much higher level of anion exchange than the unstimulated MOI = 3 cells (Fig. 6C), and the ΔpH_i and J_B values were unaffected by cAMP (n = 6). We conclude that transducing CFPAC-1 cells with CFTR at MOI = 3 are consistent with an apical Cl^-/HCO_3^- exchange activity. In contrast, cells transduced with CFTR at the higher virus titer of MOI = 15 have a constitutively active apical Cl^-/HCO_3^- exchanger that cannot be further stimulated by cAMP.

cAMP-stimulated anion exchange activity in the MOI = 3 SeV-CFTR cells was completely blocked by 500 μM H_2-DIDS; J_B was -0.10 ± 0.26 mM B/min and ΔpH_i was -0.022 ± 0.011 when apical Cl^- was removed in the presence of the inhibitor (control values were 2.45 ± 0.40 mM B/min and 0.051 ± 0.007, respectively, n = 5). To test the electrogenicity of the cAMP stimulated anion exchange activity, SeV-CFTR cells were perfused with basolateral K^+-free or high-K^+ HCO_3^-/CO_2 solution 10 min before the removal of apical Cl^-. Apical Cl^- withdrawal in the absence of basolateral K^+ did not significantly alter J_B (1.48 ± 0.22 mM B/min) and ΔpH_i (0.066 ± 0.009) versus standard conditions (J_B: 1.54 ± 0.29 mM B/min, ΔpH_i: 0.05 ± 0.008, n = 7). In addition, apical Cl^-

withdrawal in the presence of basolateral high-K^+ HCO_3^-/CO_2 solution resulted in no alteration of J_B (3.12 ± 0.49 mM B/min), but a significant increase of ΔpH_i (0.12 ± 0.01) compared to the control (2.24 ± 0.45 mM B/min and 0.06 ± 0.008, respectively, $n = 9$). Overall, it seems that the cAMP stimulated apical Cl^-/HCO_3^- exchange activity is electroneutral.

Finally, $CFTR_{inh}$-172 had no effect on either the rate or magnitude of the pH_i alkalinization following activation of apical Cl^-/HCO_3^- exchange in cyclic AMP stimulated SeV-CFTR (MOI = 3) CFPAC-1 cells ($n = 7$, data not shown). Thus, Cl^- transport by CFTR is probably not required to maintain apical Cl^-/HCO_3^- exchange activity.

Effect of SeV vector-mediated CFTR expression on PKA activity and expression of the PKA catalytic subunit

Because apical Cl^-/HCO_3^- exchange in the MOI = 15 SeV-CFTR transduced cells was constitutively active and did not respond to cAMP (Fig. 6B,C), we were concerned that the higher virus titer may have affected the cAMP signaling system. We therefore measured PKA activity, and the amount of the 42 kDa PKA catalytic subunit (PKAcat), in the MOI = 15 CFPAC-1 cells.

Figure 7A shows that PKA activity was similar in the uninfected, and in the SeV-LacZ and SeV-CFTR cells infected at MOI = 3. About the same level of PKA activity was also observed in SeV-LacZ cells infected at MOI = 15. However, in contrast, PKA activity was almost undetectable in SeV-CFTR cells infected at the higher titer.

We used Western blotting to measure the amount of PKAcat expressed in the various cell types. The results indicated that all cells groups contained about the same amount of PKAcat (Fig. 7B). Taken together, these data suggest that hyperexpression of CFTR inhibits PKA activity, thus, providing an explanation for our failure to detect cAMP stimulation of apical Cl^-/HCO_3^- exchange activity in SeV-CFTR MOI = 15 cells (Fig. 6). Clearly, disabling the cAMP signaling pathway in this way would be a disadvantage in terms of gene therapy and predicts that over-expression of CFTR in pancreatic duct cells of CF patients will need to be avoided.

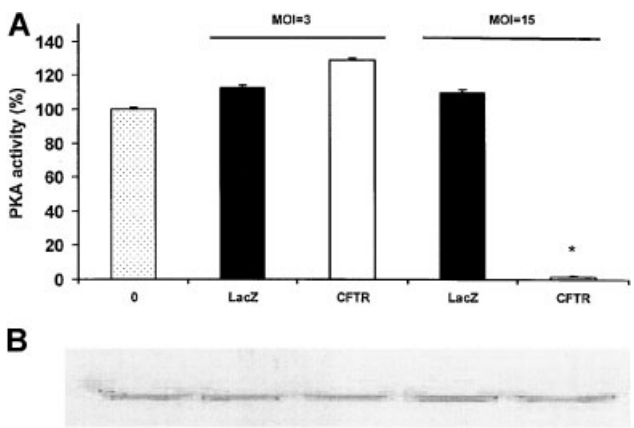

Fig. 7. PKA activity and total catalytic subunit measured in CFPAC-1 cells. A: PKA activity was determined in uninfected (0), SeV-LacZ (LacZ) and SeV-CFTR (CFTR) transduced cells by measuring the incorporation of γ-^{32}P into purified CFTR-NBD1 fragments. Data for low titer (MOI = 3) and high titer (MOI = 15) cells are shown. * Indicates significant difference ($P < 0.05$) versus the uninfected control group. B: Representative Western blots (20 μg protein) for the 42 kD catalytic subunit of PKA. Cell samples are as indicated in (A).

The effect of SeV vector-mediated CFTR expression on apical Na^+/H^+ exchange (NHE) activity

Apical NHE activity has been detected in the main pancreatic duct and may be involved in HCO_3^- scavenging from the duct lumen (Marteau et al., 1995; Steward et al., 2005; Argent et al., 2006). HCO_3^- scavenging is probably a protective mechanism which acidifies the ductal contents, thereby reducing the chances of pro-enzyme activation when flow rates are low during interdigestive periods (Lee et al., 2000; Steward et al., 2005; Argent et al., 2006). We have recently shown that CFPAC-1 cells express an apical NHE activity (Rakonczay et al., 2006).

Figure 8A shows a continuous pH_i recording from a SeV-LacZ (MOI = 15) infected CFPAC-1 monolayer. Exposing the cells to a 20 mM NH_4Cl pulse, administered in the absence of Na^+ on both sides of the monolayer, reduced pH_i to about 6.7. In the continued absence of Na^+, pH_i stabilized at this new value, indicating the absence of any other Na^+-independent pH_i recovery mechanisms such as H^+ pumps (Fig. 8A). Re-addition of Na^+ to the apical membrane caused pH_i to increase, due to activation of the apical NHE. Similar results were obtained when the SeV-LacZ cells were exposed to the NH_4Cl pulse in the presence of the cAMP cocktail (Fig. 8A).

Figure 8B shows a similar experiment performed on a SeV-CFTR (MOI = 15) transduced monolayer. Qualitatively, the results were similar to those obtained with the SeV-LacZ cells. However, the effect of re-adding Na^+ on pH_i and J_B was significantly greater in the SeV-CFTR cells as compared to the SeV-LacZ cells (MOI = 3: 1.71 ± 0.27-fold, $n = 10$; MOI = 15: 2.12 ± 0.44-fold, $P < 0.05$, $n = 5$) (and compare Fig. 8A,B). Finally, exposure of the SeV-CFTR monolayer to the cAMP cocktail had no significant effect on the J_B observed in response to re-addition of Na^+ (Fig. 8B). Similar results were obtained in four other experiments. These data suggest that the NHE expressed in the apical membrane of CFPAC-1 cells is upregulated in the presence of CFTR, but is unaffected by cAMP stimulation.

Discussion

In the present work recombinant SeV vector constructs were assessed as gene transfer agents in polarized monolayer cultures of human CFPAC-1 cells. This cell line is homozygous for the common F508del CFTR mutation, and has no measurable apical Cl^- permeability (Schoumacher et al., 1990). SeV is a single-stranded RNA virus that has been shown to produce efficient gene transfer and expression in airway epithelial cells, both in vitro and in vivo (Yonemitsu et al., 2000; Tokusumi et al., 2002). The virus attaches via both cholesterol and sialic acid receptors bound to gangliosides, present on the luminal surface of the epithelial cells. Our results indicate that CFPAC-1 cells could be efficiently infected by the virus from the apical side, as judged by LacZ staining, and that infection with the SeV-CFTR construct was associated with an increase in both Cl^- transport (via CFTR) as well as the induction of an apical cAMP-regulated Cl^-/HCO_3^- exchange activity. Taken together these results suggest that transduction with SeV vector is capable of correcting the HCO_3^- secretory defect in these human CFPAC-1 cells.

Effect of virus infection on the integrity and functional polarity of CFPAC-1 cells

Transduction by SeV vector (LacZ or CFTR) at both low (3) and high (15) MOI did not produce any detrimental effects on cell growth or electrical resistance, at least up to 96 hr post-

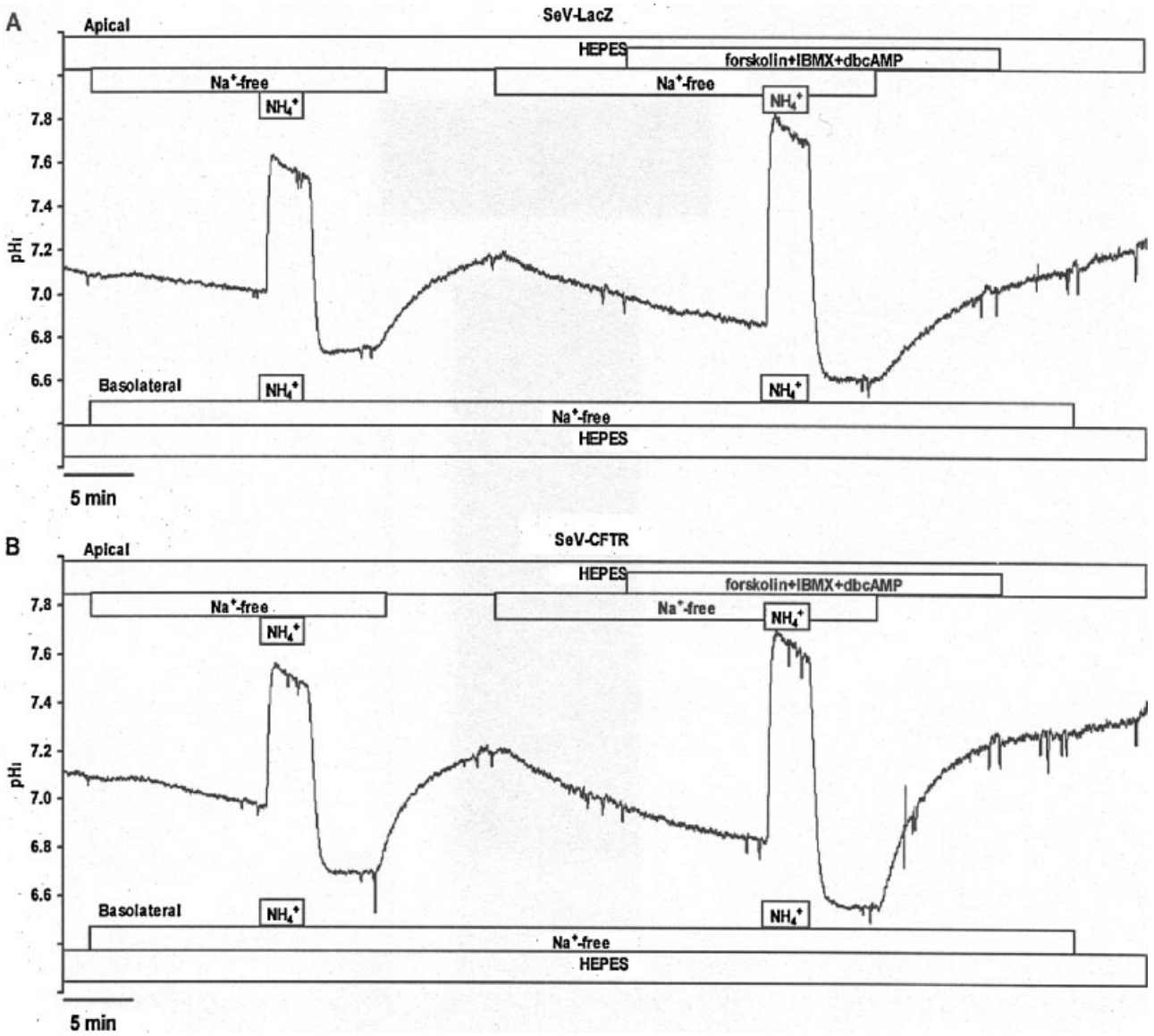

Fig. 8. Apical Na^+/H^+ NHE activity in SeV-transduced CFPAC-1 cells. A: Continuous pH_i recording from a SeV-LacZ (MOI = 15) monolayer. Horizontal bars indicate the composition of solutions bathing the apical and basolateral membranes. During bilateral perfusion with a Na^+-free solution, the cells were acidified by a pulse of NH_4Cl (20 mM). Subsequent re-introduction of Na^+ to the apical side caused pHi and J_B to increase reflecting activation of the apical NHE. The same protocol was repeated in the second half of the experiment, but with the cells exposed to the cAMP cocktail. B: Continuous pHi recording from a SeV-CFTR (MOI = 15) transduced monolayer. Same protocol as in (A). Note that the effect of Na^+ re-addition on ΔpH_i and J_B was greater in the SeV-CFTR transduced cells (n = 5).

infection. This suggests that the virus was well tolerated by the cells and that even at high virus titers the cells were still able to maintain polarity. We have previously shown that CFPAC-1 cells demonstrate a differential permeability to HCO_3^-/CO_2 at the apical and basolateral membranes (Rakonczay et al., 2006). Physiologically, the apical membrane of the duct cell must resist back-flux of HCO_3^- from the lumen as this would work against HCO_3^- secretion. Our results show that CFTR expression did not alter the permeability of the apical membrane to CO_2, but in some monolayers we did observe a small increase in apical HCO_3^- influx following CFTR transduction. This suggests that HCO_3^- influx through transport proteins increases at the apical membrane when CFTR is present, as found by Ishiguro et al. (2000) using isolated guinea-pig ducts.

Effect of SeV on Cl^-/HCO_3^- exchange activity in pancreatic cells

We found that basolateral Cl^-/HCO_3^- exchange activity in CFPAC-1 cells was significantly reduced following CFTR transduction at high MOIs, and was not influenced by cAMP stimulation. Similarly, Greeley et al. (2001) showed that Cl^-/HCO_3^- exchange (as measured by $^{36}Cl^-$ influx) was decreased by about 33% in corrected CFPAC-1 cells. However, in contrast to these data, basolateral anion exchange activity was not significantly different in main pancreatic ducts isolated from wt versus CF mice (Lee et al., 1999a). These differences between cultured human cells and native murine tissue maybe related to the expression levels of CFTR, which are low in

native mouse tissue (Gray et al., 2002). Exactly how CFTR expression inhibits basolateral anion exchange is not clear at the moment, but our real time PCR data indicates that it is not via a reduction in AE2 mRNA levels. One possibility is that an increased Cl^- conductance of the plasma membrane following CFTR expression causes intracellular Cl^- concentration to fall. Thus, when extracellular Cl^- was withdrawn, a reduced outward Cl^- gradient would be available to drive HCO_3^- into the cell.

In contrast to the basolateral membrane, non-infected CFPAC cells as well as LacZ transduced cells displayed no apical Cl^-/HCO_3^- exchange activity under any conditions. Our results clearly show that CFTR expression is associated with the appearance of an apical Cl^-/HCO_3^- exchange activity that can be further enhanced by cAMP stimulation. These results are consistent with Greeley et al. (2001), who reported that total Cl^-/HCO_3^- exchange activity was elevated in non-polarized, stably corrected, CFPAC-1 cells grown on glass coverslips. Similar to our results, this effect was accompanied by enhanced apical Cl^-/HCO_3^- exchanger activity as judged by $^{36}Cl^-$ uptake in polarized monolayers. However, Greeley et al. (2001) found that DRA mRNA was present in the corrected, but not in the non-corrected CFPAC-1 cells, and that PAT-1 expression was enhanced fivefold in the corrected cells, which we did not observe. CFTR has also been shown to activate DRA and PAT-1 in heterologous expression systems (Chernova et al., 2003; Ko et al., 2002, 2004). Lee et al. (1999a) also found that the apical Cl^-/HCO_3^- exchange activity was increased in perfused pancreatic ducts from wt versus CFTR-knockout mice, and that forskolin markedly elevated luminal Cl^-/HCO_3^- exchange activity.

To determine the identity of the apical anion exchanger(s) responsible for the cAMP stimulated Cl^-/HCO_3^- exchange activity, we examined the effect of a high concentration of the disulfonic stilbene H_2-DIDS (500 μM). This compound completely blocked stimulated Cl^-/HCO_3^- exchange. Since the disulfonic stilbene does not inhibit CFTR from the extracellular side (Gray et al., 1993; Akabas, 2000) and Chernova et al. (2003) and Melvin et al. (1999) reported that DRA has a low sensitivity to DIDS when Cl^-/HCO_3^- exchange was measured (although Cl^-/SO_4^{2-} exchange by DRA seems to be DIDS-sensitive, Silberg et al. 1995; Moseley et al., 1999), then neither of these transporters are likely to be involved. There is, however, general agreement that PAT-1 is sensitive to block by DIDS (Wang et al., 2002; Lohi et al., 2003; Petrovic et al., 2003; Alvarez et al., 2005). There is no evidence that SLC26 anion exchangers can be activated directly by cAMP. However, activation of SLC26 anion exchangers by phosphorylated CFTR is well described (Shcheynikov et al., 2006), and this is clearly preserved in our CFPAC-1 cells transduced with SeV-CFTR at MOI = 3. Taken together with our semiquantitative and real time RT-PCR data point to PAT-1 as the SLC26 family member expressed on the apical surface of SeV-CFTR infected CFPAC-1 cells. Furthermore, cAMP stimulated apical Cl^-/HCO_3^- exchange activity in SeV-CFTR CFPAC-1 cells was not influenced by alteration of the membrane potential by variation of extracellular K^+ concentration. The electrogenicity of SLC26 transporters is still a matter of debate (Ko et al., 2002; Mount and Romero, 2004; Alper et al., 2006). Our results seem to be in accord with Alper et al. (2006) who have shown that human PAT-1 mediates electroneutral Cl^-/HCO_3^- exchange.

In order to test whether the Cl^- conductance of CFTR was necessary for cAMP-dependent activation of apical Cl^-/HCO_3^- exchange in SeV-CFTR (MOI = 3) CFPAC-1 cells, we tested the effect of $CFTR_{inh}$-172. This compound completely inhibited CFTR as assessed by the iodide efflux assay, but it had no effect on Cl^-/HCO_3^- exchange in SeV-CFTR transduced cells. Thus, it would appear that there is no strong coupling between CFTR ion transport and anion exchange activity, a conclusion consistent with results in native mouse pancreatic duct (Lee et al., 1999a). However, Simpson et al. (2005), using a different (non-specific) CFTR inhibitor, glybenclamide, showed that this compound did to reduce resting Cl^-/HCO_3^- exchange in mouse intestine. How CFTR expression leads to an upregulation of apical anion exchange activity is still not fully understood, but recent work has shown that SLC26A3, A4, and A6 physically and functionally interact with CFTR (Shcheynikov et al., 2006). Furthermore, phosphorylation of CFTR on its R domain stimulates anion exchange activity which appears to be preserved in our CFTR-transduced cells. Interestingly, CFTR activity appears to be enhanced in pancreatic ducts from SLC26A6 knock-out mice (Wang et al., 2006), suggesting that the exchanger tonically inhibits CFTR. Lack of SLC26A6 led to enhanced spontaneous, but reduced cAMP-stimulated fluid secretion, illustrating the important role the exchanger plays in both basal and stimulated pancreatic HCO_3^- secretion. However, in another SLC26A6 knockout mouse model no differences were observed in fluid or HCO_3^- secretion between wt and knockout animals, a finding explained by a compensatory upregulation in SLC26A3 activity in the knockout animals (Ishiguro et al., 2007).

High versus low expression of CFTR

Hyperexpression of CFTR can alter the molecular physiology of the protein (Mohammad-Panah et al., 1998), and in some cases we observed significant differences in HCO_3^- transport between the MOI = 3 and 15 SeV-CFTR infected cells. For example, basolateral uptake of HCO_3^- was only affected (reduced) in the MOI = 15 SeV-CFTR infected cells and not the MOI = 3 cells. Furthermore, although resting apical Cl^-/HCO_3^- exchange activity was upregulated in both the MOI = 3 and MOI = 15 SeV-CFTR transduced cells, only the MOI = 3 group responded to cAMP stimulation. Since the key regulatory pathway determining CFTR activity involves elevation of cAMP and activation of PKA, we measured the amount of the 42 kDa PKAcat and PKA activity in CFPAC-1 cells. The amount of PKAcat was similar in uninfected and infected cells, however, PKA activity was reduced in the SeV-CFTR MOI = 15 group providing an explanation as to why the apical exchangers cannot be stimulated with cAMP. The reason for this decrease in PKA activity in the MOI = 15 group remains unclear. However, Mohammad-Panah et al. (1998) showed that hyperexpression of wt CFTR in CFPAC-1 cells caused the appearance of a time-independent, non-rectifying Cl^- current that was insensitive to cAMP stimulation, suggesting that the CFTR channels were permanently activated and not susceptible to cAMP regulation. Moreover, high-levels of CFTR expression has been shown to be associated with biosynthetic and growth abnormalities (Schiavi et al., 1996), so there must be a fine line between the beneficial and toxic effects of CFTR.

Apical Na^+/H^+ exchange (NHE)

CFTR expression resulted in a marked upregulation of apical NHE activity in CFPAC-1 cells. Although it is possible that this effect could be due to apical bath Na^+ accessing basolateral NHE1 (given the low paracellular resistance of the CFPAC-1 monolayers), Ahn et al. (2001) observed similar results and found an increased luminal Na^+-dependent pH_i recovery from an acid load in microperfused pancreatic ducts from isolated wt versus F508del mice. This effect probably resulted from reduced levels of NHE3 expression in the knock-out animals (Ahn et al., 2001). However, we must note that we could not detect NHE2 or NHE3 expression by RT-PCR in our CFPAC-1 cells. In contrast to our data, stimulation of the wt mouse ducts with forskolin dose-dependently inhibited luminal Na^+-dependent pH_i recovery. Our failure to detect an inhibitory effect of forskolin on apical NHE in the MOI = 15 SeV-CFTR

group was not surprising since these cells had no detectable PKA activity. However, the MOI = 3 group, which did exhibit PKA activity, behaved similarly. It is possible that human pancreatic duct cells either express a different, cAMP-insensitive, NHE isoform in their apical membrane or that apical NHE is regulated by another mechanism in human cells, for example, by an interaction with Cl^-/HCO_3^- exchangers (Lamprecht et al., 2002).

We conclude that that SeV is an effective CFTR gene transfer vector for human pancreatic duct cells. Moreover, CFTR transfected CF duct cells maintain their normal epithelial polarity and evidence restoration of Cl^- and HCO_3^- transport processes at the apical membrane. As SeV-mediated CFTR gene transfer is much more effective via the apical as compared to the basolateral membrane, efficient gene transfer into the pancreas in vivo will probably require retrograde injection of the vector into the pancreatic duct. Moreover, as 62% of CF patients are born with a non-functional pancreas, gene therapy would need to be initiated in utero in the majority of cases. Thus, the smaller group of patients who are pancreatic sufficient at birth, but who become pancreatic insufficient in later life, might be best helped by gene therapy.

Uncited References

Hug et al., 2003, Lee et al., 1999b, Lee et al., 2000, Linsdell et al., 1997, Loussourn et al., 1996, Marteau et al., 1995, McNicholas et al., 1996, Shcheynikov et al., 2004.

Acknowledgments

We thank Prof. R. A. Frizzell (University of Pittsburgh, Pittsburgh, PA, USA) and Prof. A. S. Verkman (University of California, San Francisco, CA, USA) for kindly providing us with the CFPAC-1 cells and the $CFTR_{inh}$-172 inhibitor, respectively. We would also like to thank T. Tokusumi, H. Bang, and T. Yamamoto (DNAVEC Corporation), for their assistance in the construction of the recombinant SeV. DNAVEC Corporation supplied the SeV.

Literature Cited

Ahn W, Kim KH, Lee JA, Kim JY, Choi JY, Moe OW, Milgram SL, Muallem S, Lee MG. 2001. Regulatory interaction between the cystic fibrosis transmembrane conductance regulator and HCO_3^- salvage mechanisms in model systems and the mouse pancreatic duct. J Biol Chem 276:17236–17243.

Akabas MH. 2000. Cystic fibrosis transmembrane conductance regulator. Structure and function of an epithelial chloride channel. J Biol Chem 275:3729–3732.

Alper SL, Stewart AK, Chernova MN, Zolotarev AS, Clark JS, Vandorpe DH. 2006. Anion exchangers in flux: Functional differences between human and mouse SLC26A6 polypeptides. Novartis Found Symp 273:107–119.

Alvarez BV, Vilas GL, Casey JR. 2005. Metabolon disruption: A mechanism that regulates bicarbonate transport. EMBO J 24:2499–2511.

Argent BE, Gray MA, Steward MC, Case RM. 2006. Cell physiology of pancreatic ducts. In: Johnson LR, editor. Physiology of the Gastrointestinal Tract 4th edition San Diego: Elsevier. pp. 1371–1396.

Bitzer M, Armeanu S, Lauer UM, Neubert WJ. 2003. Sendai virus vectors as an emerging negative-strand RNA viral vector system. J Gene Med 5:543–553.

Chang XB, Tabcharani JA, Hou YX, Jensen TJ, Kartner N, Alon N, Hanrahan JW, Riordan JR. 1993. Protein kinase A (PKA) still activates CFTR chloride channel after mutagenesis of all 10 PKA consensus phosphorylation sites. J Biol Chem 268:11304–11311.

Chernova MN, Jiang L, Shmukler BE, Schweinfest CW, Blanco P, Freedman SD, Stewart AK, Alper SL. 2003. Acute regulation of the SLC26A3 congenital chloride diarrhoea anion exchanger (DRA) expressed in Xenopus oocytes. J Physiol 549:3–19.

Choi JY, Muallem D, Kiselyov K, Lee MG, Thomas PJ, Muallem S. 2001. Aberrant CFTR-dependent HCO_3^- transport in mutations associated with cystic fibrosis. Nature 410:94–97.

DiMagno EP, Go VL, Summerskill WH. 1973. Relations between pancreatic enzyme ouputs and malabsorption in severe pancreatic insufficiency. N Engl J Med 288:813–815.

Dodge JA, Turck D. 2006. Cystic fibrosis: Nutritional consequences and management. Best Pract Res Clin Gastroenterol 2006. 20 531–546.

Farinha CM, Mendes F, Roxo-Rosa M, Penque D, Amaral MD. 2004. A comparison of 14 antibodies for the biochemical detection of the cystic fibrosis transmembrane conductance regulator protein. Mol Cell Probes 18:235–242.

Farinha CM, Penque D, Roxo-Rosa M, Lukacs G, Dormer R, McPherson M, Pereira M, Bot AG, Jorna H, Willemsen R, Dejonge H, Heda GD, Marino CR, Fanen P, Hinzpeter A, Lipecka J, Fritsch J, Gentzsch M, Edelman A, Amaral MD. 2004. Biochemical methods to assess CFTR expression and membrane localization. J Cyst Fibros 3:73–77.

Ferrari S, Griesenbach U, Iida A, Farley R, Wright AM, Zhu J, Munkonge FM, Smith SN, You J, Ban H, Inoue M, Chan M, Singh C, Verdon B, Argent BE, Wainwright B, Jeffery PK, Geddes DM, Porteous DJ, Hyde SC, Gray MA, Hasegawa M, Alton EW. 2007. Sendai virus-mediated CFTR gene transfer to the airway epithelium. Gene Ther [Epub ahead of print] doi 10.1038/sj.gt.3302991.

Fuerst TR, Niles EG, Studier FW, Moss B. 1986. Eukaryotic transient-expression system based on recombinant vaccinia virus that synthesizes bacteriophage T7 RNA polymerase. Proc Natl Acad Sci USA 83:8122–8126.

Gray MA, Pollard CE, Harris A, Coleman L, Greenwell JR, Argent BE. 1990. Anion selectivity and block of the small-conductance chloride channel on pancreatic duct cells. Am J Physiol 259:C752–C761.

Gray MA, Plant S, Argent BE. 1993. cAMP-regulated whole cell chloride currents in pancreatic duct cells. Am J Physiol 264:C591–C602.

Gray MA, Winpenny JP, Verdon B, O'Reilly CM, Argent BE. 2002. Properties and role of calcium-activated chloride channels in pancreatic duct cells. In: Fuller CM, editor. Current topics in Membranes,Vol. 53. Calcium-activated chloride channels. San Diego: Academic Press. pp. 231–256.

Greeley T, Shumaker H, Wang Z, Schweinfest CW, Soleimani M. 2001. Downregulated in adenoma and putative anion transporter are regulated by CFTR in cultured pancreatic duct cells. Am J Physiol 281:G1301–G1308.

Griesenbach U, Inoue M, Hasegawa M, Alton EW. 2005. Sendai virus for gene therapy and vaccination. Curr Opin Mol Ther 7:346–352.

Griesenbach U, Geddes DM, Alton EW. 2006. Gene therapy progress and prospects: Cystic fibrosis. Gene Ther 13:1061–1167.

Harlow E, Lane D. 1988. Antibodies: A Laboratory Manual. Cold Spring Harbor: Cold Spring Harbor Laboratory Press.

Hegyi P, Rakonczay Z, Jr, Gray MA, Argent BE. 2004. Measurement of intracellular pH in pancreatic duct cells: A new method for calibrating the fluorescence data. Pancreas 28:427–434.

Hughes LK, Li H, Sheppard DN. 2004. Use of an iodide-selective electrode to measure CFTR Cl^- channel activity http://central.igc.gulbenkian.pt/cftr/vr/d/hughes_iodide_selective_electrode_measure_cftr_cl_activity.pdf.

Ishiguro H, Naruse S, Kitagawa M, Suzuki A, Yamamoto A, Hayakawa T, Case RM, Steward MC. 2000. CO_2 permeability and bicarbonate transport in microperfused interlobular ducts isolated from the guinea-pig pancreas. J Physiol 528:305–315.

Ishiguro H, Namkung W, Yamamoto A, Wang Z, Worrell RT, Xu J, Lee MG, Soleimani M. 2007. Effect of Slc26a6 deletion on apical Cl^-/HCO_3^- exchanger activity and cAMP-stimulated bicarbonate secretion in pancreatic duct. Am J Physiol 292:G447–G455.

Kato A, Sakai Y, Shioda T, Kondo T, Nakanishi M, Nagai Y. 1996. Initiation of Sendai virus multiplication from transfected cDNA or RNA with negative or positive sense. Genes Cells 1:569–579.

Ko SB, Shcheynikov N, Choi JY, Luo X, Ishibashi K, Thomas PJ, Kim JY, Kim KH, Lee MG, Naruse S, Muallem S. 2002. A molecular mechanism for aberrant CFTR-dependent HCO_3^- transport in cystic fibrosis. EMBO J 21:5662–5672.

Ko SB, Zeng W, Dorwart MR, Luo X, Kim KH, Millen L, Goto H, Naruse S, Soyombo A, Thomas PJ, Muallem S. 2004. Gating of CFTR by the STAS domain of SLC26 transporters. Nat Cell Biol 6:343–350.

Lamprecht G, Heil A, Baisch S, Lin-Wu E, Yun CC, Kalbacher H, Gregor M, Seidler U. 2002. The down regulated in adenoma (dra) gene product binds to the second PDZ domain of the NHE3 kinase A regulatory protein (E3KARP), potentially linking intestinal Cl^-/HCO_3^- exchange to Na^+/H^+ exchange. Biochemistry 41:12336–12342.

Lee MG, Choi JY, Luo X, Strickland E, Thomas PJ, Muallem S. 1999a. Cystic fibrosis transmembrane conductance regulator regulates luminal Cl^-/HCO_3^- exchange in mouse submandibular and pancreatic ducts. J Biol Chem 274:14670–14677.

Lee MG, Wigley WC, Zeng W, Noel LE, Marino CR, Thomas PJ, Muallem S. 1999b. Regulation of Cl^-/HCO_3^- exchange by cystic fibrosis transmembrane conductance regulator expressed in NIH 3T3 and HEK 293 cells. J Biol Chem 274:3414–3421.

Lee MG, Ahn W, Choi JY, Luo X, Seo JT, Schultheis PJ, Shull GE, Kim KH, Muallem S. 2000. Na^+-dependent transporters mediate HCO_3^- salvage across the luminal membrane of the main pancreatic duct. J Clin Invest 105:1651–1658.

Linsdell P, Tabcharani JA, Rommens JM, Hou YX, Chang XB, Tsui LC, Riordan JR, Hanrahan JW. 1997. Permeability of wild-type and mutant cystic fibrosis transmembrane conductance regulator chloride channels to polyatomic anions. J Gen Physiol 110:355–364.

Livak KJ, Schmittgen TD. 2001. Analysis of relative gene expression data using real-time quantitative PCR and the 2(-Delta Delta C(T)). Methods 25:402–408.

Lohi H, Lamprecht G, Markovich D, Heil A, Kujala M, Seidler U, Kere J. 2003. Isoforms of SLC26A6 mediate anion transport and have functional PDZ interaction domains. Am J Physiol 284:C769–C779.

Ma T, Thiagarajah JR, Yang H, Sonawane ND, Folli C, Galietta LJ, Verkman AS. 2002. Thiazolidinone CFTR inhibitor identified by high-throughput screening blocks cholera toxin-induced intestinal fluid secretion. J Clin Invest 110:1651–1658.

Marteau C, Silviani V, Ducroc R, Crotte C, Gerolami A. 1995. Evidence for apical Na^+/H^+ exchanger in bovine main pancreatic duct. Dig Dis Sci 40:2336–2340.

Melvin JE, Park K, Richardson L, Schultheis PJ, Shull GE. 1999. Mouse down-regulated in adenoma (DRA) is an intestinal Cl^-/HCO_3^- exchanger and is up-regulated in colon of mice lacking the NHE3 Na^+/H^+ exchanger. J Biol Chem 274:22855–22861.

Mohammad-Panah R, Demolombe S, Riochet D, Leblais V, Loussouarn G, Pollard H, Baro I, Escande D. 1998. Hyperexpression of recombinant CFTR in heterologous cells alters its physiological properties. Am J Physiol 274:C310–C318.

Moseley RH, Hoglund P, Wu GD, Silberg DG, Haila S, de la Chapelle A, Holmberg C, Kere J. 1999. Downregulated in adenoma gene encodes a chloride transporter defective in congenital chloride diarrhea. Am J Physiol 276:G185–G192.

Mount DB, Romero MF. 2004. The SLC26 gene family of multifunctional anion exchangers. Pflugers Arch 447:710–721.

Muimo R, Hornickova Z, Riemen CE, Gerke V, Matthews H, Mehta A. 2000. Histidine phosphorylation of annexin I in airway epithelia. J Biol Chem 275:36632–36636.

Petrovic S, Ma L, Wang Z, Soleimani M. 2003. Identification of an apical Cl^-/HCO_3^- exchanger in rat kidney proximal tubule. Am J Physiol 285:C608–C617.

Rakonczay Z, Jr, Fearn A, Hegyi P, Boros I, Gray MA, Argent BE. 2006. Characterisation of H^+ and HCO_3^- transporters in CFPAC-1 human pancreatic duct cells. World J Gastroenterol 12:885–895.

Rosenecker J, Huth S, Rudolph C. 2006. Gene therapy for cystic fibrosis lung disease: Current status and future perspectives. Curr Opin Mol Ther 8:439–445.

Rowntree RK, Harris A. 2003. The phenotypic consequences of CFTR mutations. Ann Hum Genet 67:471–485.

Scheele GA, Fukuoka SI, Kern HF, Freedman SD. 1996. Pancreatic dysfunction in cystic fibrosis occurs as a result of impairments in luminal pH, apical trafficking of zymogen granule membranes, and solubilization of secretory enzymes. Pancreas 12:1–9.

Schiavi SC, Abdelkader N, Reber S, Pennington S, Narayana R, McPherson JM, Smith AE, Hoppe H IV, Cheng SH. 1996. Biosynthetic and growth abnormalities are associated with high-level expression of CFTR in heterologous cells. Am J Physiol 270:C341–351.

Schoumacher RA, Ram J, Iannuzzi MC, Bradbury NA, Wallace RW, Tom Hon C, Kelly DR, Schmid SM, Gelder FB, Rado TA, Frizzell RA. 1990. A cystic fibrosis pancreatic adenocarcinoma cell line. Proc Natl Acad Sci USA 87:4012–4016.

Shcheynikov N, Ko SB, Zeng W, Choi JY, Dorwart MR, Thomas PJ, Muallem S. 2006. Regulatory interaction between CFTR and the SLC26 transporters. Novartis Found Symp 273:177–186.

Shiotani A, Fukumura M, Maeda M, Hou X, Inoue M, Kanamori T, Komaba S, Washizawa K, Fujikawa S, Yamamoto T, Kadono C, Watabe K, Fukuda H, Saito K, Sakai Y, Nagai Y, Kanzaki J, Hasegawa M. 2001. Skeletal muscle regeneration after insulin-like growth factor I gene transfer by recombinant Sendai virus vector. Gene Ther 8:1043–1050.

Silberg DG, Wang W, Moseley RH, Traber PG. 1995. The down regulated in adenoma (dra) gene encodes an intestine-specific membrane sulfate transport protein. J Biol Chem 270:11897–11902.

Simpson JE, Gawenis LR, Walker NM, Boyle KT, Clarke LL. 2005. Chloride conductance of CFTR facilitates basal Cl^-/HCO_3^- exchange in the villous epithelium of intact murine duodenum. Am J Physiol 288:G1241–G1251.

Steward MC, Ishiguro H, Case RM. 2005. Mechanisms of bicarbonate secretion in the pancreatic duct. Annu Rev Physiol 67:377–409.

Tamada K, Wang XP, Brunicardi FC. 2005. Molecular targeting of pancreatic disorders. World J Surg 29:325–333.

Thomas JA, Buchsbaum RN, Zimniak A, Racker E. 1979. Intracellular pH measurements in Ehrlich ascites tumor cells utilizing spectroscopic probes generated in situ. Biochemistry 18:2210–2218.

Tokusumi T, Iida A, Hirata T, Kato A, Nagai Y, Hasegawa M. 2002. Recombinant Sendai viruses expressing different levels of a foreign reporter gene. Virus Res 86:33–38.

Wallrapp C, Muller-Pillasch F, Solinas-Toldo S, Lichter P, Friess H, Buchler M, Fink T, Adler G, Gress TM. 1997. Characterization of a high copy number amplification at 6q24 in pancreatic cancer identifies c-myb as a candidate oncogene. Cancer Res 57:3135–3139.

Wang Z, Petrovic S, Mann E, Soleimani M. 2002. Identification of an apical Cl^-/HCO_3^- exchanger in the small intestine. Am J Physiol 282:G573–G579.

Wang Y, Soyombo AA, Shcheynikov N, Zeng W, Dorwart M, Marino CR, Thomas PJ, Muallem S. 2006. Slc26a6 regulates CFTR activity in vivo to determine pancreatic duct HCO_3^- secretion: Relevance to cystic fibrosis. EMBO J 25:5049–5057.

Waters DL, Dorney SFA, Gaskin KJ, Gruca MA, O'Halloran M, Wilcken B. 1990. Pancreatic function in infants identified as having cystic-fibrosis in a neonatal screening program. N Engl J Med 322:303–308.

Weintraub WH, Machen TE. 1989. pH regulation in hepatoma cells: Roles for Na-H exchange, Cl-HCO_3 exchange, and Na-HCO3 cotransport. Am J Physiol 257:G317–G327.

Yonemitsu Y, Kitson C, Ferrari S, Farley R, Griesenbach U, Judd D, Steel R, Scheid P, Zhu J, Jeffery PK, Kato A, Hasan MK, Nagai Y, Masaki I, Fukumura M, Hasegawa M, Geddes DM, Alton EW. 2000. Efficient gene transfer to airway epithelium using recombinant Sendai virus. Nat Biotechnol 18:970–973.